ABSTRACT

GURARSLAN, RANA. Characterization of Polymers with the Kerr Effect. (Under the direction of Dr. Alan E. Tonelli).

Advanced synthetic techniques have been recently developed in to tailor the architectures of polymers. While polymer chemists are discovering new ways to control polymerizations to design specific polymer micro- and macrostructures, techniques to characterize these elaborate polymer architectures/macrostructures have not similarly advanced.[1]

Polymer macrostructures, *i.e.*, the positions or locations of constituent microstructures along their chains, are essentially the complete molecular architectures of their chains. A complete characterization of polymer macrostructures should be detailed enough to identify, count/quantify, and locate all microstructures along the polymer chains[2]. This is necessary to establish a relevant structure-property relation and to predict their processability.

Currently the best characterization method is the observation of polymer solutions with high field, high resolution ^{13}C-NMR spectroscopy. It is possible to characterize microstructures as long as monomer tetrads using new methodologies, such as heteronuclear 2D-NMR. However, because of its local sensitivity it is impossible to determine the exact locations or the distribution of these microstructural elements along or among the polymer backbones due to NMRs [3,4,5].

Here we suggest a non-traditional method for characterizing polymer macrostructures, *i.e.*, coupling of NMR spectroscopy, sensitive to short-range microstructures, with the Kerr effect, a macroscopic experimental probe which is sensitive enough to distinguish polymer

macrostructures[6]. The Kerr effect of polymer solutes is the birefringence contributed to their dilute solutions when subjected to strong electric fields[7]. We focused on examining the sensitivity of the Kerr effect and molar Kerr constants, $_mK$s, of dilute polymer solutions to their microstructures and determine if the same microstructures located at different positions in polymers are reflected in distinct $_mK$s.

In the first and second study, styrene (S)/*para*-Br-styrene (*p*-BrS) tri-blocks $pBrS_{90}$-S_{120}-$pBrS_{90}$ (I) and S_{60}-$pBrS_{180}$-S_{60} (II) were analyzed and distinguished by the signs of their Kerr constants, B. A series of random and gradient S/*p*-BrS copolymers synthesized by RAFT polymerization were characterized. While NMR spectra could reveal only the local structures of copolymers, a comparison of observed and calculated $_mK$s of dilute copolymer solutes indicated both the difference between the copolymers and an additional gradient in stereosequence that parallels their comonomer gradient in the gradient S/*p*-BrS copolymers.

We investigated the surface stability of S/pBrS copolymer thin films on silica surface by observing their dewetting mechanisms. Two random S/pBrS copolymers, both with 50:50 S:pBrS composition, synthesized by RAFT and the other by free-radical initiated polymerization, were annealed above their glass transition temperature (Tg). While the random S/pBrS film prepared by uncontrolled free-radical polymerization did dewet from silica surface, RAFT film was stable. This verified our Kerr effect observations and revealed the importance of polymer stereosequence on thermal stability of polymer thin films.

Later, we synthesized S/pBrS copolymers with random, gradient, diblock comonomer sequences using ATRP and measure their $_mK$s. These were compared to those already measured RAFT synthesized random and gradient S/pBrS copolymers. The experimental

results confirmed that ATRP produce atactic stereosequence as expected in contrast with our previously performed RAFT polymerizations.

Precise and random, regioregular or irregular, and atactic and isotactic ethylene/vinyl acetate E/VAc copolymers and regularly alternating styrene/butadiene multi-block copolymers which were kindly sent to us from other collaborators were measured. The Kerr effect observations of these appeared to be sensitive to their carefully synthesized macrostructures. Single concentration measurements on precise, regioregular, isotactic and atactic E-VAcs yielded, respectively, large negative and moderate positive B. On the other hand, their ^{13}C-NMR spectra are identical.

In the last study, the potential heterogeneity of polymer micro-/macrostructures and the ability of the Kerr effect to distinguish diluted samples of atactic S/p-BrS copolymers (50:50, 20:80, 80:20 S: pBrS) with homogeneous and heterogeneous populations of micro- and macrostructures were demonstrated.

Characterizing Polymers with the Kerr Effect

by
Rana Gurarslan

A dissertation submitted to the Graduate Faculty of
North Carolina State University
in partial fulfillment of the
requirements for the degree of
Doctor of Philosophy

Fiber and Polymer Science

Raleigh, North Carolina

2015

APPROVED BY:

_____	_____
Alan E. Tonelli Committee Chair	Jan Genzer
_____	_____
Michael Dickey	Christopher Gorman

DEDICATION

This dissertation is dedicated to my deeply loved family;

my daughter Bahar Gurarslan, my husband Alper Gurarslan

and my parents Rabia and Nevzat Erol.

BIOGRAPHY

Rana Gurarslan was born on February 15, 1985 in Aydin, Turkey. Aydin is a lovely small city located on Turkish Aegean Coast. She graduated from Science and Mathematics Class of Adnan Menderes Anatolian High School of Aydin in 2002 and was accepted into the Textile Engineering Program at Usak University.

After receiving her Bachelor of Science degree in 2007, she went to Uludag University, Institute of Science, and Department of Textile Technology to pursue her Master's Degree where she studied environmentally friendly ozone pretreatment for water- energy saving dyeing processes of garments and graduated in 2010.

She decided to pursue a doctoral degree in order to gain a fundamental scientific understanding of polymers. Thus, in August 2011, she joined the Fiber and Polymer Science Program in North Carolina State University. Under the excellent mentorship of Dr. Alan Tonelli, she focused her research on characterizing polymer micro and macrostructures as well as understanding structure–property relationship of polymers.

ACKNOWLEDGMENTS

First and foremost, I would like to express my great appreciation and gratitude to my advisor Dr. Alan Tonelli for the chance had given to me to gain a better scientific understanding in Polymer Science. His kindness and patience in guiding me forward through my graduate study will undoubtedly on my mind for the rest of my mind.

I would like to thank my committee members, Drs. Jan Genzer, Michael Dickey and Christopher Gorman.

I would like to thank Dr. Hanna Gracz for her help and expertise on NMR.

I would like to acknowledge Dr. Xiaojing Cai for training and helping me for dewetting experiments, Rohan Patil for teaching how to conduct polymerization reactions and performing GPC, Dr. Casey Galvin for the training of ellipsometer and the Kerr Effect Instrument. Many thanks to the all lab-mates in Dr. Genzer's group for their friendship and kind help no matter how busy they were.

I also would like to thank to my friends, Jialong Shen, Yavuz Caydamli, Shansan Li and Drs. Abhay Joijode and Ganesh Narayanan in Dr. Tonelli's group for being around me like a family.

I must express my deepest thanks to my husband Alper Gurarslan who encouraged and supported me to pursue my dream on an advanced graduate degree. I owe this to him.

Finally, I am deeply grateful to my parents who have taught me to carefully observe the world with a philosophical perspective and taught me never give up in life. They have always believed in me. I hope I made them proud.

This work was financially supported by the National Science Foundation (DMR-Polymers Program, grant # 0966478) for financial support and to the Army Research Office for a DURIP equipment grant (grant #53583 CH-RIP) to construct our Kerr effect instrument. The assistance provided by our home Departments and Universities is also appreciated.

TABLE OF CONTENTS

LIST OF TABLES

LIST OF FIGURES

CHAPTER 1

Introduction and Literature Review

1.1 Introduction

Polymer 'Macrostructure' is the complete full scale structure or detailed architecture of a polymer[8]. This includes the types and amounts of short-range microstructures, as well as their locations or positions along the polymer chain. For example, the primary structures of proteins, *i.e.* the sequence of amino acid residues along their chains, constitutes their macrostructures. The distinct macrostructures drawn below contain the same microstructures, monomer diad stereosequences (left) and comonomer sequences (right), but have equivalent local triad microstructures, *i.e.* the same numbers of **mm, mr, rr** stereosequences and **AAA, AAB, ABA, ABB, BAB, BBB** comonomer sequences.

While NMR and other spectroscopic probes with short-range sensitivities to polymer microstructures may be able to determine, respectively, the number of m,r and mm,mr=rm, rr monomer diads and triads and AAA, BBB, AAB=BAA, BBA = ABB, ABA, BAB commoner triad sequences, they cannot distinguish the distinct macrostructures shown in the top and bottom structures in Figure 1.1[4,5]. To locate the microstructures identified by NMR requires an experimental probe sensitive to the complete architecture of polymers. The Kerr effect of polymer solutions, the birefringence produced by strong electric fields and contributed by their

(a) Monomer Diad Stereosequences	(b) Comonomer Sequences
…mmmmmmrmrmrmrmrrrrrrm…	**…AAAABABBBBABAA…**
vs	vs
…mrmmmrrrmrrmmrrmmmrrm…	**…ABAAAABBBBABAB…**

Figure 1.1 (a) Two distinct homopolymer stereosequences, where m and r denote meso and racemic monomer diads, respectively. (b) Two distinct comonomer sequences.

polymer solutes, has been demonstrated to be an experimental probe that may be sensitive enough to determine the complete structures of polymer chains, *i*.e., their macrostructures.

In this introductory chapter the theoretical and experimental background of the electro-optical Kerr effect is given. The literature review covers some demonstrations of Kerr effect studies performed on dilute solutions of flexible polymers. The potential of the Kerr effect to characterize polymer macrostructures is summarized in the motivation section.

1.2 The Kerr effect

The electro-optic Kerr effect is the birefringence induced in materials by the application of strong direct or alternating electric fields [9]. When an optically isotropic material is subjected to a strong electric field, its constituent molecules rotate until their dipole moments align along the electric field direction, and are brought into a preferred direction as illustrated in Figure 1.2. Consequently, the substance becomes anisotropic, with distinct refractive indices in the directions parallel and perpendicular to the applied electric field direction[10].

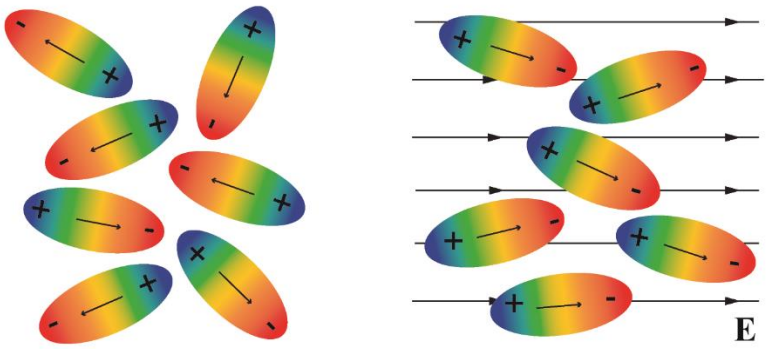

Figure 1. 2 Molecular orientation under electric field, E. Over all molecular dipole moment is parallel to the long axis of the ellipsoidal molecular polarizability tensor.

The history of the Kerr effect phenomenon dates back to 1875 when John Kerr, a Scottish physician, observed the rotation of the plane of polarization of light passing through an optical medium when a strong electric field was applied. The intensity of the exiting light was different depending on the direction of the applied electric field[7]. Anisotropic materials transmit plane polarized light at various speeds, depending upon the direction of the plane polarized light relative to the orientation of the substituent molecules. The difference in refractive indices parallel and perpendicular to the applied electric field causes retardation between the components of the exiting light, as shown in Figure 1.3. Hence, initially plane polarized light is transformed into elliptically polarized light. The ellipticity, *i.e.*, the rotation of the plane of polarization of the exiting light, determines the electric birefringence of the sample [9]. John Kerr's experiments on many substances yielded an empirical law which is known as Kerr's Law. Eq. 1.1, describes the relationship between the applied electric field E and the birefringence Δn induced in a substance when light of wavelength λ travels through it.

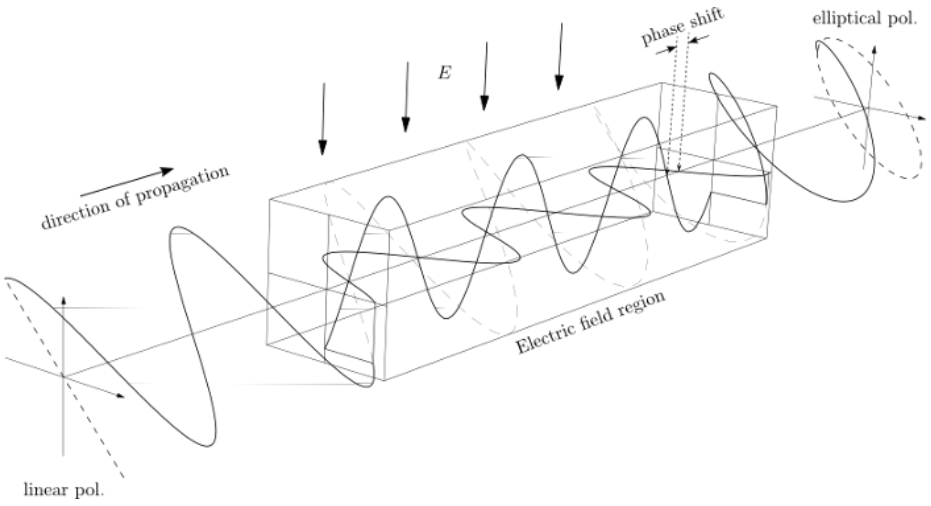

Figure 1. 3 The Kerr effect on linearly polarized light, producing elliptically polarized light. Figure is taken from Ref.11

Kerr's Law shows that the induced birefringence of each substance is characterized by a constant B, the Kerr constant, with the dimensions of [length x (electric field)^2]$^{-1}$, mV^{-2} (SI units).

$$\mathbf{B} = \frac{\Delta \mathbf{n}}{\lambda \mathbf{E}^2} \tag{1.1}$$

Significant contributions to Kerr effect studies were made by Le Fevre and his group between 1955 and 1971, establishing the technique as a method to probe stereochemistry. They reported Kerr constants and optical parameters of more than a thousand compounds to obtain information on their molecular geometries for the first time [12].

According to Le Fevre[13, 14], the experimental Kerr constant, B, can be expressed as a relative retardation, δ, between two light waves emerging from the sample under an electric field. So, B can be expressed by

$$\boldsymbol{\delta = 2\pi l \Delta n/\lambda = 2\pi l B E^2} \quad (1.2)$$

The molecular origin of B arising from Δn can be summarized as follows. When the substance is subjected to an electric field E an induced dipole moment, m is produced in the molecule.

$$\boldsymbol{m = \alpha . E} \quad (1.3)$$

The polarizability tensor α, determines the response, m, of a system subjected to the external electrical field as a result of the electronic charge distribution around the molecular bonds, as shown in Eq.1.3. The electric field orients molecules in the direction of non-zero polarizability, with the dipole moment parallel to it in order to stay in the lower energy state. This dipolar orientation makes the beam of light travel faster in the direction of maximum polarizability and the substance becomes birefringent. Thus, as seen in Eq. 1.4 the Kerr effect is very sensitive to any difference between components of the optical polarizability tensor, α.

$$\begin{bmatrix} \boldsymbol{mx} \\ \boldsymbol{my} \\ \boldsymbol{mz} \end{bmatrix} = \begin{bmatrix} \alpha_{xx} & \alpha_{yx} & \alpha_{zx} \\ \alpha_{xy} & \alpha_{yy} & \alpha_{zz} \\ \alpha_{xz} & \alpha_{yz} & \alpha_{zy} \end{bmatrix} \begin{bmatrix} \boldsymbol{Ex} \\ \boldsymbol{Ey} \\ \boldsymbol{Ez} \end{bmatrix} \quad (1.4)$$

For molecules with a permanent dipole moment, μ, their orientation in the electric field is largely controlled by μ, since μ is larger than the dipole moment, m, induced by E. Having μ parallel or perpendicular to the direction of maximum polarizability determines the sign of the Kerr effect. Molecules align with their permanent dipole moment μ in the direction of the external field, so if the largest polarizability is parallel to μ, light travelling vertically (See Figure 1.3) will move faster, and consequently $B > 0$, or positive. If the largest polarizability is perpendicular to μ, then $B < 0$, or negative [10]. In solutions, both solvent (B_1) and solute (B_2) molecules contribute to the magnitude of the solution Kerr constant (B_{12}). Volume fractions ϕ

are used as the unit of concentration in Eq. 1.5 [15]. ΔB is the difference between the Kerr constants of the solution and the pure solvent.

$$\mathbf{B12 = B1\phi1 + B2\phi2 = B1 - B1\phi2 + B2\phi2},$$

so

$$\mathbf{B2 = \Delta B/\phi2 + B1} \tag{1.5}$$

When determining the experimental Kerr constant of a solute, several measurements are performed on solutions having different concentrations and an extrapolation to zero concentration is required to avoid intermolecular interactions between solute molecules.

In order to avoid the dependence of the Kerr constant for a given substance on the number of molecules per unit volume, the birefringence induced by electric filed is expressed as the molar Kerr constant, ${}_mK$. For solutes in solution at infinite dilution, Le Fevre and his group derived ${}_mK$ from Eq.(1.6)

$$\mathbf{{}_mK = (6N\lambda nB)/[(\rho(n+2)^2(\varepsilon+2)^2]} \tag{1.6}$$

where m, N_A, λ, n, B, ρ, ϵ are the molar concentration of the solution, Avogadro's constant, the wavelength of the light, the refractive index, the Kerr constant, density and dielectric constant, respectively[13].

A more recent expression was given by Riande and Saiz[10] for polymers at infinite dilution with m molar concentration of repeat units [Eq. (1.7)] and gives the Kerr constant per repeating unit of the chain, ${}_mK/x$, where x is the number of repeat units; v *is* the molar volume of the solute.

$$\mathbf{{}_mK = \frac{54\lambda n_1}{(n^2+2)^2(\epsilon^2+2)^2}\left[\lim_{m\to 0}\left(\frac{\Delta B}{m}\right) + vB_1\right]} \tag{1.7}$$

The molar Kerr constant of a polymer measured in its dilute solution is a macroscopic property of the entire chain, like its mean-square end-to-end distance ($<r^2>$) or radius of gyration ($<s^2>$) and dipole moment ($<\mu^2>$). Because the molar Kerr constants of polymers depend on the magnitudes and orientations of their overall dipole moment vectors and anisotropic polarizability tensors, identical or similar microstructural features located at different positions along the macromolecular chain can produce different overall ${}_mK$s. Thus, the Kerr effect may be potentially used as a method to characterize complete polymer macrostructures by identifying and locating constituent microstructures [2, 9, 10].

1.2.1 Theory of the Electro optic Kerr effect of Flexible Polymers

The molar Kerr constants of low molecular weight substances vary over more than four orders of magnitudes and can be positive or negative[13]. This sensitivity has led to many studies both experimentally[13-16] and theoretically by Stuart-Peterlin[17], Buckingham[18], Gotlip[19], and Dows[20], with the aim of understanding the chain flexibility and structural and conformational properties of long chain molecules. The most realistic statistical mechanical treatment of ${}_mK$ was developed by Nagai and Ishikawa[21], and Flory and coworkers[22] demonstrated how to average ${}_mK$ over all conformations of a polymer chain.

A qualitative description of their theory can be summarized as follows. When polymer molecules interact with a static electric field, the field orientates their backbone bonds in the direction of minimum energy. However they cannot orientate independently, since they are connected. Therefore, the theoretical calculation of ${}_mK$ requires an evaluation of the overall polymer dipole moment and optical anisotropy averaged over all possible conformations of

the chain. Thus, the geometry of the chain, the relative energy of the conformations available to the polymer, *i.e.,* the rotational states along the backbone, the dipole moments, and the polarizability anisotropies of the repeat units must be known in order to perform the calculations [21-25].

Theoretically the molar Kerr constant for flexible polymers is calculated from the equation (1.8) developed by Nagai and Ishikawa[21].

$$ {}_{m}K = (2\pi NA/135)[(<\mu T \alpha \mu>)/k^2T^2 + (<\alpha^R \acute{\alpha}^C>)/kT] \qquad (1.8) $$

α and μ are the anisotropic polarizability tensor and dipole moments respectively. They comprise a sum of bond contributions that is averaged (< >) over all possible chain conformations. R and C indicate row and column representation and the prime signifies static polarizability. Intermolecular interactions between polymer chains or between chains and solvent molecules are neglected and bond valence angles are assumed to be constant.

Flory *et al.*[22] showed how to calculate the average of any configurationally dependent property of a polymer. The method is based on the following two key assumptions. First, the rotational isomeric state approximation (RIS), where it is assumed that each rotatable bond has a discrete number of states, usually trans and gauche± conformations, and only nearest neighbor interactions are important in determining their energies and probabilities. Second, the bond additivity approximation (BAA), where it is assumed that the electrical property to be calculated, for instance α, is a tensorial sum of non-interacting contributions from constitutive groups, segments, or bonds of the polymer. Though it is known that bond dipoles are not additive and BAA has been shown to be incorrect in the gas phase, it is

speculated that this is not the case for polymers dissolved in isotropically polarizable nonpolar solvents. Even if there are some doubts about the reliability of BAA for all polymer solvent systems, it is at least applicable for comparison of chemical structures [10].

Assuming the RIS and BAA models are correct, any conformational average of a property g, $\langle g(\tau) \rangle$, over all internal degrees of freedom τ is given by equation (1.9),

$$\langle \mathbf{g(\tau)} \rangle = \mathbf{Z^{-1}\ J^{*}}\ G_1^n\ \mathbf{J} \tag{1.9}$$

where Z is the partition function, J* and J are row and column vectors. G_i is the generator matrix containing information on bond geometry, rotational states and their energies, and electrical parameters of the i^{th} backbone bond of the polymer. G_1^n denotes a serial product of generator matrices for each backbone bond in the chain (1 to n). Further information concerning the calculations of ${}_mKs$ can be found in Flory's book "Statistical Mechanics of Chain Molecules"[22].

1.2.2 Kerr Effect Measurements

Kerr effect experiments are performed to measure the state of polarization of a light beam emerging from a sample exposed to a strong electric field. Figure 1.4 is presented to show the main components of the experiment and the pathway of the laser light in the Kerr Effect instrument.

The ellipticity, *i.e.*, the rotation of the light exiting the Kerr cell, determines the Kerr constant, B. Depending upon the substance examined, various types of Kerr systems can be built by modifying the kind of electric field and recording systems used. Pulsed ac electric fields with a different setup are used for biological systems in ionic solutions[26]; while dc field

setups are used for flexible synthetic polymers and low molecular weight compounds observed in non-conducting solutions.

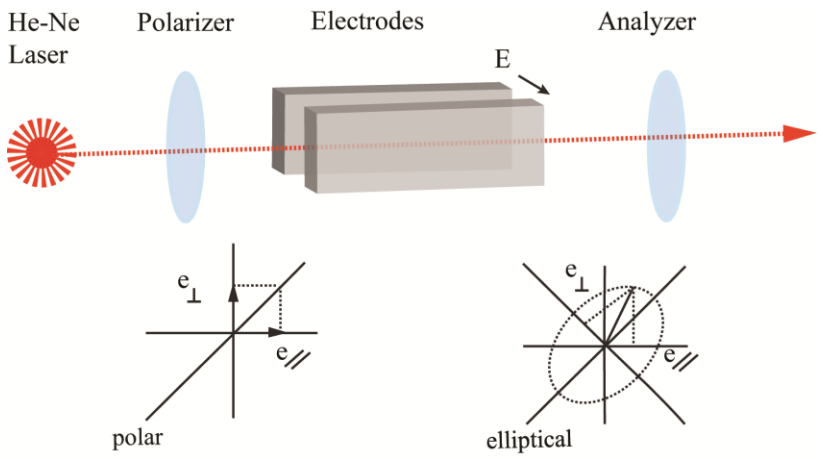

Figure 1.4 Experimental set up of electro-optical Kerr effect. (Adapted from Ref. 9)

An instrument quantifying the change in birefringence in solutions and molten polymers is mainly composed of the followings: [10]

→ A light source producing a monochromatic beam with stable intensity

→ A polarizer providing stable polarization and giving a good extinction ratio with the analyzer

→ A light detector composed of a photomultiplier, which measures the intensity of light emerging from the analyzer

→ A compensating unit determining the state of polarization of the emerging light. This is done with a quarter wave plate, which is a sheet of birefringent material mounted in a rotatable

stage and introduces a λ/4 phase shift to the emerging elliptically polarized light and transforms it to plane polarized light

→ An analyzer which rotates the exiting light until it gives complete extinction. The angle between initial and final beams is proportional to the birefringence produced.

The sample cell contains two conducting plates that serve as electrodes to apply the electric field to the sample, two low birefringent windows to let the light travel through the sample, two insulated spacers, and filling caps made of a chemically stable material. Its geometric dimensions affect the Kerr constant and the accuracy of the measurement (See Figure 1.5). The relation between phases is expressed by eq. 1.10 where δ ,*B*, *E*, and *l* are the phase shift, Kerr constant, electric field, and spatial coordinate direction of light beam propagation, *i.e.*, the cell length *l*, respectively. The phase shift between two components of the emerging light is proportional to cell dimensions.

$$\boldsymbol{\delta = 2\pi \int_0^l BE^2 l} \tag{1.10}$$

As seen from eq. (1.10), longer electrodes produce stronger signals. However, the cell length is usually kept as short as possible in order to minimize the required amount of sample and the alignment difficulties, while still obtaining reasonable signals. Dimensions of the cell gap should be designed to be big enough to avoid electrical discharges between the electrodes and small enough to get strong electric fields produced by a given voltage and to minimize the required sample amount[10].

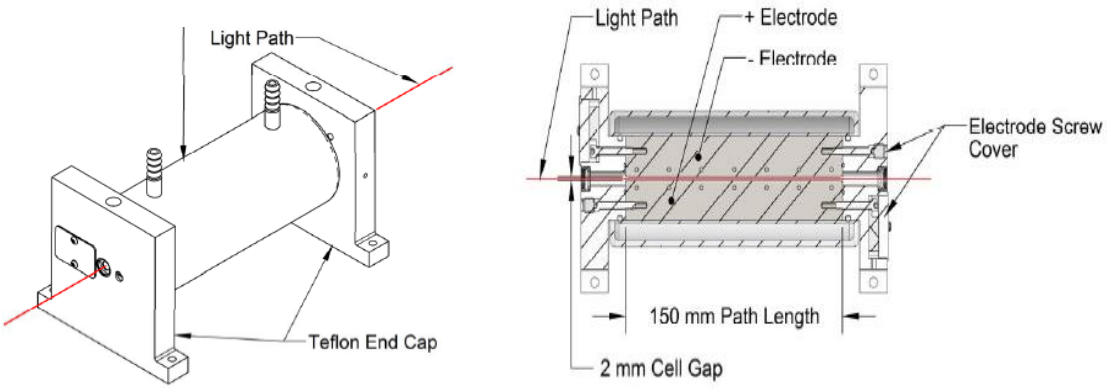

Figure 1. 5 Schematic view of the Kerr cell. Pictures are takened from Kerr constant measuremnt system user manual prepared by Hinds Instruments Inc.

The precision of the measurement can be improved by modifying the polarization states of the He-Ne laser beam and the detection system and minimizing residual birefringence in all of the components in the optical path[27]. A new system permitting state-of-the-art Kerr constant measurements was reported by Hinds Instruments, Inc. and is shown in Figure 1.6. In this instrument, a photoelestic modulator (PEM) produces a phase retardation which is a precise sinusoidal function of time at a frequency of several tens of kilohertz to provide high sensitivity and speed for birefringence measurements.

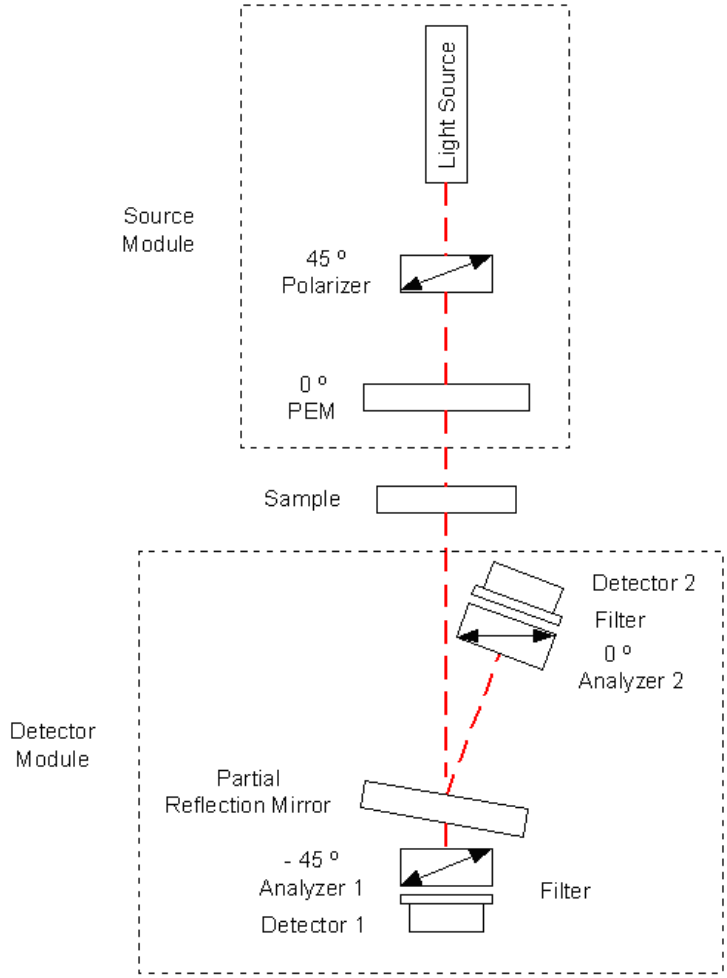

Figure 1.6 The main components of the state of the art Kerr effect instrument built by Hinds Instruments Inc. Figure is taken from the instrument user manual.

1.3 Nuclear Magnetic Resonance of Polymers

1.3.1 Introduction

NMR is a local spectroscopic probe which gives a one-to-one relationship between the strengths of signals and the number of atoms producing those signals *via* a correctly acquired and processed NMR spectrum. ^{1}H- and ^{13}C-NMR spectroscopies are utilized as standard

techniques to characterize and determine the chemical species and types of molecular connections present in polymeric materials. Solution NMR is used routinely to monitor polymerization reactions and to check the purity of polymers, to identify unknown materials, and to study polymer microstructures, dynamics, and interactions [3,4].

Characterization of polymer microstructure is achieved by establishing resonance assignments *via* a variety of methods, including the use of model compounds, the γ-gauche effect, and calculation of expected chemical shifts from empirical rules, which allow a comparison of the estimated to observed spectra that can lead to resonance assignments[5]. Many different techniques and methodologies of pulsed 1D- and 2D-NMR are available and still being developed as more complex spectra are observed for more complex organic structures.

1.3.2 Nuclear Spin and the NMR phenomena

NMR is a kind of absorption spectroscopy related to radio frequency induced transitions between different levels of magnetic energy of nuclei under an external magnetic field. All nuclei carry mass and charge. In addition, some isotopes, with odd numbers of protons and neutrons, like ^{13}C, ^{1}H, ^{19}F, ^{14}N, ^{17}O, ^{31}P, and ^{33}S, carry non-spherical charge distribution, which cause their nuclear magnetic moments, μ, to have spin quantum number $I = 1/2$ and to spin with intrinsic spin quantum numbers, $m = I, 1\text{-}1, 1\text{-}2, -I$, *i.e.*, m = ±1/2, on the nuclear axis with an angular momentum associated with its magnetic moment[4] (Figure 1.7). Magnetic nuclei can adopt distinct orientations in a magnetic field depending on the spin quantum number m. If $I = ½$, then there are two orientations available; to align with the external magnetic field (m=1/2), B_o, or against the field (m= -1/2) (Figure 1.8).

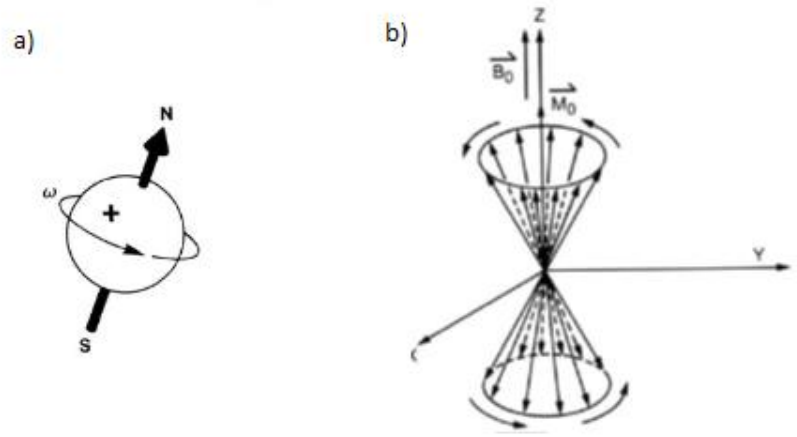

Figure 1. 7 a) The charged nucleus (e.g. ^{1}H) rotating with angular frequency $\omega=2\pi\nu$ creates a magnetic field B. b) Orientation and precession of nuclear spins (I= ½) at thermal equilibrium in a magnetic field B_o. Figure is taken from reference 28.

The alignment with the field is more populated than against the field, since nuclei prefer to stay in a lower energy state. Basically the nuclear magnetic resonance phenomenon is using excess energy in the form of electromagnetic radiation, Radio Frequency (RF), to flip or orient those nuclei aligned with the field in the opposite direction against the field. Eventually the nuclei jump into and attain a higher energy level, which are functions of the nuclear magnetic moment, μ, and the strength of the external magnetic field, B_o.

When the RF energy is removed, the energized nuclei dissipate the excess energy by relaxing back to the lower energy state *via* two processes; spin-lattice or longitudinal relaxation, which involves transfer of energy from the nuclei to the molecular lattice and spin-spin or transverse relaxation without any energy transfer to the lattice, which involves direct interactions between different nuclear spins.

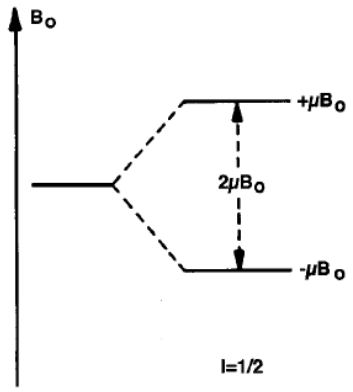

Figure 1.8 Possible energy levels of a nucleus with spin ½ in an applied magnetic field.

A relaxation process, called resonance, is dictated by the electron cloud around the nuclei. Since the nuclei in different parts of a molecule have unique electronic environments, depending on the nature of bonding and other surrounding groups, different absorption frequencies and fields are required to flip the nuclear spins. Thus, a fluctuation in the magnetic field is associated with a resonance. As magnetic fields can generate electric currents, the resonance induces a voltage in the radio frequency coil that is amplified, recorded and converted into absorption peaks *via* a Fourier Transformation, as they appear in an NMR spectrum, as illustrated in Figure 1.9.

Interpretation of an NMR spectrum can be done by analyzing the number of resonance peaks, which indicate the symmetry of the molecule; the integral that gives the relative ratio of non-equivalent types of nuclei, and chemical shifts or resonance frequencies, which reflect the electronic/structural environments of the nuclei. Resonance signals and shapes are related to the longitudinal and transverse relaxation times, T_1 and, T_2.

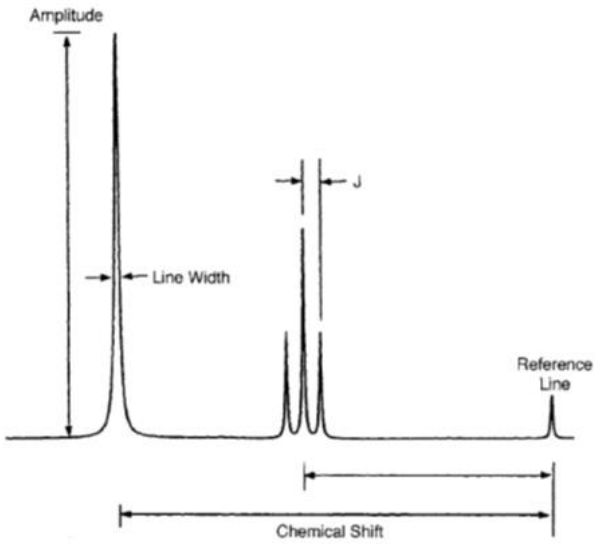

Figure 1.9 A demonstrative NMR spectrum[28].

Two neighboring nuclei influence each other's effective magnetic field. This influence shows up in the NMR spectrum if the distance between non-equivalent nuclei is less than or equal to three bond lengths. This effect is called spin-spin coupling or J coupling. The quantitative structural values of the J-coupling constant and cross-relaxation rates provide information about local conformations, distances, bond angles, and local mobility[4].

1.4 Literature Review

The Kerr effect has been used for stereochemical and conformational analyses of flexible polymers with the assistance of some other methods of structural analyses, such as x-ray, NMR, and conformational dependent properties, such as dipole moments and mean squared optical anisotropies. A general procedure used is to extract an unknown characteristic

(molecular structure) from the provided known information (experimental observation) through a critical comparison between theoretical and experimental values of the molar Kerr constant.

One of the earliest conformational analysis of low and high molecular weight compounds in solution was provided by Le Fevre's group when they measured Kerr constant of a series of different polymers including polystyrenes, polyvinyl acetates, polyethylene glycols, poly (vinyl chlorides), and poly (vinyl bromides) [29, 30]. Le Fevre also reported Kerr effect studies on chain flexibility, which was supported by X-ray studies. For instance, after a comprehensive study of the molar Kerr constants, dipole moments, and anisotropic polarizabilities of a series of poly (methyl methacrylates) and polymethacrylates[31], they were able to conclude that large poly (methyl methacrylate) chains may adopt curved helical configurations, while shorter segments are stiff because of strong impediments to internal rotations within the polymer chain.

Le fevre[29] also presented empirical relations between the degree of polymerization and observed Kerr constant of various small molecules. Their comprehensive experimental and theoretical Kerr effect studies were successful in interpreting the conformations of low molecular weight compounds. However, a discrepancy between theory and observed results came about for long flexible polymer chains[23]. Those inconsistencies were overcome and the Kerr effect started to be a useful tool for studying chain flexibility after a realistic theory was developed by Nagai and Ishikawa[21]. This yielded the relation connecting the electric birefringence produced at infinite dilution in solution to the overall molecular dipole moments and polarizability tensors of flexible polymers. The molar Kerr constant, $_mK$, was established

and more precise chemical structures and geometric and energetic parameters of the polymers were used to carry out the theoretical calculations of $_mK$s [21, 22, 24].

A good example of this is the Kerr effect studies of polyethylene glycols (PEG) started by Aroney[32], where dipole moments and molar Kerr constants of six different PEGs [H-(O-CH_2-CH_2)$_x$-H, with x = 4.1, 6.4, 18, 34, 78, and 153, in benzene solutions were measured. It was concluded for x up to 5, gauche and trans conformations of the -O-CH_2-, and -CH,-O- bonds are equally probable, but for x above 7, gauche- or cis- arrangements occur more frequently than the trans conformation. Thus, helically coiled portions are produced in long PEG chains. This conclusion was supported by X-ray studies on PEG. On the other hand their experimental values indicated that $_mK/x$ continues to decrease in magnitude with no sign of saturation for **x** as high as 153 repeat units, or 461 backbone bonds. However, $_mK$s should saturate, or reach an asymptote as x gets bigger, according to Ishikawa and Nagai[23].

The disagreement between the theoretical calculations and the experimental results reported by Aroney[32] was attributed to excluded volume effects. However, questions concerning the molecular weight dependence of, $_mK/x$ and the applicability of RIS theory and bond additivity assumption to the calculation of PEG $_mK$s remained unanswered.

In 1977, Tonelli[33] reported $_mK$ values calculated for the homopolymers polypropylene (PP), poly(viny1 chloride) (PVC), polystyrene (PS), poly(p-methylstyrene) (PPMS), and poly(p-chlorostyrene) (PPCS) and the (PP-PVC, PS-PPCS, and PPMS-PPCS) copolymers as functions of their stereoregularities and sequence distributions. Those calculations confirmed the expected sensitivity of polymer Kerr effects to their conformation, configurations, and/or sequence distributions of polar homo- and copolymers. The calculated $_mK$ values showed a

noticeable dependence on stereoregularity of the homopolymers PVC and PPCS and copolymer sequence distribution of the copolymers. These results preceded a series of pioneering experimental Kerr effect studies. They can serve as typical examples of the application of ${}_mK$ to macromolecular characterization, where ${}_mK$s were measured on dilute solutions of a variety of polymers and oligomers and were compared to their calculated values.

One of those studies was reported by Kelly et al.[34] on PEGs, where questions concerning the molecular weight dependence of ${}_mK/x$, the applicability of RIS theory, and the bond additivity assumption used in the calculation of ${}_mK$ values were raised again. A reasonable answer was sought *via* the comparison of the observed ${}_mK$s of poly(oxyethlenes) (POE) $CH_3(\text{-O-}CH_2\text{-}CH_2\text{-})_x\text{O-}CH_3$] with x = 1, 2, 3, 4, and 91(hydroxyl termination) in carbon tetrachloride solutions to the ${}_mK$s calculated using more precisely determined conformational characteristics, bond dipole moments, and bond polarizability tensors[35,36] of the POE chains. Their result agree with Nagai and Ishikawa[23] as calculated and measured ${}_mK$s reached asymptotes with increasing chain length, but showed a large disagreement in magnitudes with the results of Aroney[32].

Later, Khanarian *et al.*[37] repeated Aroney *et al.*[32] and Kelly *et al.*'s[34] studies with more extensive measurements to see whether or not $({}_mK/x)$s reach an asymptotic value. They reported the ${}_mK$s and $\langle\mu^2\rangle$s of poly (oxyethy1ene glycols) [(POEG) $H\text{-}(O\text{-}CH_2\text{-}CH_2)_x\text{-}OH$ (x = 2-317)] and poly (oxyethy1ene dimethyl ethers) [(POEDE) $CH_3\text{-}(O\text{-}CH_2\text{-}CH_2)_xO\text{-}CH_3$ (x = 1-4)] in the isotropically polarizable solvents carbon tetrachloride, cyclohexane, and dioxane. Calculated ${}_mK$s based on the rotational isomeric state model of Mark and Flory[35] and energy parameters of Abe and Mark[38] reached an asymptotic value, unlike the data of Aroney *et al.*[32]

and agreed with the experimental results, unlike that reported by Kelly *et al.*[34]. They emphasized the importance of correct extrapolation of the observed Kerr constant of POEG to infinite dilution in order to eliminate solute-solute interactions since there is a fairly strong nonlinear dependence of the Kerr constant on the solution concentration. They pointed out that observing more dilute concentrations gives more reliable experimental results and performing the Kerr effect experiments in a higher concentration range (5-10% w/w) can lead to smaller observed $_mK$s than those calculated and reported by Kelly *et al.*[34].

Furthermore they reported no excluded volume effect on $_mK$ based on the closely similar $_mK$s of POEG observed in CCl_4, cyclohexane, and dioxane solutions.

Another experimental detail noted by Khanarian *et al.*[37] is the importance of the isotropy of the solvent. Anisotropic solvents can cause specific solvation around the backbone of the polymer and yield much larger $_mK$s as seen in the experimental results of Aroney *et al.*[32]. This demonstration suggested the sensitivity of the Kerr effect to interactions of polymers with surrounding small molecules, *i.e.*, solvent or other polymers. Tonelli[2] suggested potential application of the Kerr effect to study molecular interactions in solution like non-covalent complexion of small molecules in solution.

Khanarian and Tonelli[39] reported another study of the Kerr effect, where theoretical $_mK$s were examined by comparison with the experimental results for a well characterized series of α,ω-dibromoalkanes [Br-(CH_2)n-Br, with n = 3-20] measured in cyclohexane. Experiments yielded $_mK$s of -4.5 to 160 ($10^{-12}cm^7SC^{-2}mol^{-1)}$ for n = 3-20, and demonstrated the sensitivity of $_mK$s to the addition of carbon atoms to the chain and the highly anisotropic and polar character of the C-Br bonds . It was concluded, that with increasing number of intervening

-CH_2-CH_2- bonds, the relative positions and orientations of the terminal α-Br-CH_2- and ω-CH_2-Br bonds lose their conformational correlation. This provided evidence that ($_mK/x$) should saturate and reach a plateau with increasing chain length x.

Moreover, a quantitative agreement between experimental results and theoretical calculations was achieved if it was assumed the gauche conformations permitted to the first and last -CH_2-CH_2- bonds were ± (80-90°), rather than the usual perfectly staggered values of ±120° (trans = 0°). It was stated that the steric repulsion between bulky Br atoms and CH_2 groups separated by three bonds should be reduced when the intervening bond is in the ±80-90° conformation rather than the perfectly staggered ±120° conformations.

They concluded the theoretical method composed of the RIS model with nearest neighbor interactions and the optical valence scheme of bond polarizability additivity was useful for predicting the conformations of more complex polymers.

Khanarian and Tonelli[40] reported a Kerr effect study on the fluorinated polymers; poly fluoromethylene -$(CHF)_x$-, poly vinyldene fluoride -$(CF_2$-$CH_2)_x$-, and poly trifluoroethylene -$(CHF$-$CF_2)_x$-. As shown in Table1.1, the experimental measurements of $_mK$s and theoretical calculations of mean square dipole moments demonstrate the sensitivity of $_mK$s to the degree and type of fluorination.

Table 1.1 Experimental $_mK$ and dipole moments of Fluoropolymers per Repeat unit *x*[42].

	$(_mK/x)^a$	$(\langle\mu^2\rangle/x)^b$
-(CHF-CF_2)x-	-9.1	0.86
-(CHF)x-	~0	0.31
-(CF_2-CF_2)x-	14	2.38

a *$10^{-12}$$cm^7$ SC^{-2} mol^{-1}. b *10^{-36} cm^2 SC^2 mol^{-1}.

Khanarian et. al.[41] also reported the observed and calculated molar Kerr constants and dipole moments of atactic poly(vinyl chloride) (PVC) and its oligomeric model compounds, m- and r-2,4-dichloropentanes (DCP) and mm-, mr-, and rr-2,4,6-trichloroheptanes (TCH) measured in CCl_4 and p-dioxane. The sensitivity of observed $_mK$s to the stereoregularity was demonstrated again. They reported a positive $_mK$ for rr-TCH, while mm-TCH showed a small negative $_mK$. Observed $_mK$s were used to modify the RIS model previously developed for PVC by Williams, Pickels and Flory[42,43]. Calculated $_mK$s and $\langle\mu^2\rangle$ for PVC were also found to be sensitive to its tacticity, especially in both stereoregular regions for $_mK$s and in the syndiotactic region for $\langle\mu^2\rangle$s.

The literature shows that predicted conformational characteristics can be tested with the assistance of experimental Kerr effect studies. For instance, when two different RIS models derived by Saiz *et al.* (RIS-S)[44] and by Tonelli (RIS-T)[45] for poly (vinyl bromide) (PVB) significantly disagreed, they were tested by Tonelli and Khanarian[46] *via* electric birefringence and previous dipole moment experiments. The molar Kerr constants and dipole moments of the PVB oligomers m- and r- 2,4-dibromopentane (DBP) and mm-, mr-, and rr-

tribromoheptane (TBH) and DBP and TBH isomer mixtures of r:m = 58:42 and rr:mr:mm = 38:48:14, as determined by ^{13}C NMR, were measured in carbon tetrachloride and calculated using both RIS models. While measured dipole moments agreed with both conformational descriptions, measured $_{m}K$s agreed only with the RIS-T conformational model, and once more, the high sensitivity of observed $_{m}K$s to conformational and configurational characteristics of flexible polymers was exemplified.

The series of copolymers characterized with the Kerr effect was expanded by Tonelli and Valenciano[47] and the potential of the method as a characterization technique was examined with a study on a series of ethylene-vinyl chloride (E-V) copolymers all with the same chain length produced by the reductive dechlorination of PVC with tri-n-butyltinhydride. First, stereosequences and comonomer composition and sequence distributions of the copolymers were determined by ^{13}C NMR. Second, $_{m}K$ calculations were performed for two different models of Monte Carlo generated sets of polymer chains. In the first model E and V units were randomly added one at a time with adjacent V units (VV diads) incorporated with the stereoregularity of the parent atactic-PVC and the second model was generated according to the known chemical composition, triad comonomer sequence distribution, and the stereosequence of its VV diads as observed from ^{13}C NMR analyses. Finally the comparison of calculated $_{m}K$s to those observed in p-dioxane solutions were performed, and much better agreement with the $_{m}K$s calculated for the second model was obtained.

In conclusion, while the sensitivity of the Kerr effect to comonomer sequence distribution, and the stereosequence of E-V copolymers were confirmed by NMR, coupling of

these two techniques helped to improve the accuracy of the macrostructural characterization of the E-V copolymers.

Another halogenated vinyl copolymer system was thoroughly characterized by comparison of Kerr effect observations and calculations. A series of random styrene/p-Br-styrene (S/p-BrS) copolymers produced by bromination of atactic polystyrene was reported by Khanarian *et al.*[48]. They reported $_{m}K$ calculations averaged for 15 chains of S/p-BrS copolymers with 200 repeat units for each copolymer composition that were generated via Monte Carlo Methods. A random comonomer distribution with different tacticities was assumed.

The results obtained and shown in Figure 1.10 reflect the remarkable sensitivity of $_{m}K/x$ to the copolymer tacticity or stereoregularity as calculated $_{m}Ks$ covered a 3 orders of magnitude range and also changed sign. Both experimental and calculated $_{m}Ks$ showed sensitivity to comonomer composition. A close agreement between $_{m}Ks$ of random S/p-BrS copolymers assuming a random distribution of 45% m- and 55% r-diads with measured values suggested a similar stereosequence for the parent a-PS used to obtain the S/p-BrS copolymers by bromination.

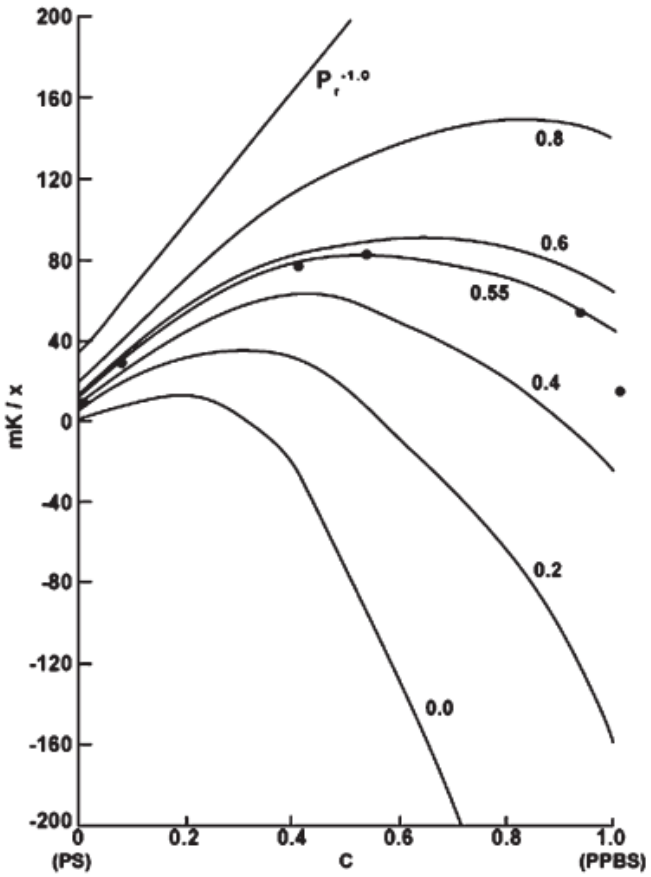

Figure 1.10 Comparison of mKs observed and calculated for S/p-BrS-I copolymers. x, Pr, and C are the number of repeat units (200), fraction of r-diads, and fractional content of p-BrS units.[49]

Later, Sato *et al.*[49] reported the precise tacticity of a-PS after performing ^{13}C NMR studies on the stereoisomeric tetrad and pentad model compounds of a-PS, and also found a random stereosequence characterized by 45% m- and 55% r-diads. Clearly, to synthesize multiple model compounds and record their ^{13}C-NMR spectra in order to achieve a complete characterization of polymer microstructures is much more time consuming than the Kerr effect method.

While traditional characterization methods are inadequate to prove the success of newly developed synthetic techniques for tailoring complex polymer architectures, characterizing polymer macrostructures with the Kerr effect can be a useful alternative method. As an example, Semler *et al.*[50] demonstrated how the Kerr effect can serve to determine the co-monomer distribution in random and blocky S/p-BrS copolymers that were synthesized *via* adjustment of the solvent quality during the bromination of atactic polystyrene (PS). The degree of bromination and the chemical composition of S/p-BrS were analyzed by elemental analysis and NMR. However NMR, including ^{13}C NMR, did not reveal any key differences in the comonomer sequences of the expected blocky and random copolymers. This was due to the fact that the p-substituted bromine atoms have no effect on the conformational characteristics of PS and their stereosequences are the same as the atactic PS used to obtain them, so their ^{13}C- and ^{1}H-NMR spectra are not sensitive to their comonomer sequences. Their glass transition temperatures, T_g, were also insensitive to their comonomer sequences, since they have identical conformational charcteristics[51].

With insight from previous Kerr effect studies of S/p-BrS copolymers[33,48], Kerr effect analyses were conducted in order to obtain more information about comonomer sequencing in these presumably random and blocky samples. For each comonomer composition, Semler *et al.* observed smaller Kerr constants for samples brominated under poor solvent conditions relative to the polymers brominated in good solvents[50]. Moreover, the Kerr constants increased with increasing p-BrS content in the copolymers. These trends, which are in qualitative agreement with the predictions of the earlier theoretical work of Tonelli and

coworkers, confirm that Kerr effect observations provide a means for monitoring both the chemical composition and comonomer sequence distribution in copolymers.

Additionally they calculated Kerr constants using the rotational isomeric state model of Yoon *et al*[52] and the matrix multiplication methods of Flory[22] for a few selected periodic sequences having the same degree of bromination (≈60%) and degree of polymerization (=300) as the PS they brominated. The observed and calculated $_{m}$Ks in Table 1.2 show a decreasing trend in $_{m}$K as the sizes of p-BrS blocks are increasing. This comparison provided clear evidence of the arrangements and average block lengths of the p-BrS units within the copolymers.

Further experimental verification was obtained via the investigation of interfacial properties of thin films of these S/p-BrS copolymers, which depend very sensitively upon their detailed comonomer sequence distributions. According to their thin film annealing studies, Semler et al.50 observed thin films of S/p-BrS prepared by brominating parent PS below the Θ-temperature to dewet more slowly than thin films of S/p-BrS prepared by bromination above the Θ-temperature. Thus the degree of blockiness affected the interfacial behavior of the copolymer, with increasingly blocky samples adhering more strongly. The use of Kerr effect measurements made it possible to establish the macrostructure–property relation [comonomer sequence distribution-interfacial response (thin film dewetting)] of these copolymers even though other characterization techniques were not able to.

Table 1.2 Normalized S/p-BrS mKs Measured[50] and Calculated for Different Blocky Comonomer Sequence Distributions using the [a]RIS model of Yoon et al.[52].

Monomer sequence	Distribution method	${}_mK_{blocky}/{}_mK_{random}$
$(PS_2\text{-}b\text{-}P\text{-}BrS_3)_{60}$	RIS	0.773±0.14
$(PS_4\text{-}b\text{-}P\text{-}BrS_6)_{30}$	RIS	0.621± 0.14
$(PS_{10}\text{-}b\text{-}P\text{-}BrS_{15})_{12}$	RIS	0.363± 0.15
$(PS_{20}\text{-}b\text{-}P\text{-}BrS_{30})_6$	RIS	0.216± 0.15
$PBr_{0.63S}\text{-}CUD_{33}$	exp	0.533± 0.03[a]
$PBr_{0.58}S\text{-}CDD33$	exp	0.304± 0.03[a]

[a]CUD and CDD: Parent Styrene was Brominated in Chloroundecane (Θ= 32.8 ° C) and Chlorododecane (Θ= 58.6° C) at 33° C.

1.5 Motivation and Highlights

The molar Kerr constant, ${}_mK$, is a "macroscopic" property characteristic of a polymer's entire chain architecture, and depends on any structural element that modifies its overall polarizability tensor and the magnitude and/or orientation of its overall dipole moment vector. Thus, the positions/locations of microstructural elements along the polymer chain (middle vs. end) may yield a wide range of ${}_mK$ values either positive or negative in sign, as observed in the ${}_mK$s of small molecules.

Kerr effect studies of flexible polymers presented in the literature demonstrated the unique sensitivity of the ${}_mK$ to the local microstructures including the tacticities of homo and copolymers and comonomer sequence of the latter. The method is very promising for fully characterizing polymer microstructures where at least one of their monomer repeat units is

polar or at least reasonably and anisotropically polarizable. Because, the $_{m}$Ks expected for polymers with given or known microstructures can be estimated if their conformational characteristics are known, a comparison of observed and calculated, $_{m}$Ks can be used to confirm or derive their conformational preferences, as represented in their Rotational Isomeric States (RIS) models. Thus, it seems likely that the Kerr effect can contribute to advancements in micro- and particularly macrostructural characterization of polymers beyond those possible with currently available techniques.

REFERENCES

1. https://www.nsf.gov/mps/dmr/NSF_Polymer_Workshop.pdf.; Interdisciplinary Globally-Leading Polymer Science and Engineering, NSF Polymers Workshop (2007)

2. Tonelli, A. E.; *Macromolecules*; *42*, 3830 (2009)

3. Cheng, H. et al.; In NMR Spectroscopy of Polymers: Innovative Strategies for Complex Macromolecules; *ACS Symposium Series*; American Chemical Society: Washington, DC (2011)

4. Bovey, F.A., Mirau, P. A.; "NMR of Polymers"; Academic Press (1996)

5. Tonelli, A. E.; NMR Spectroscopy and Polymer Microstructure: The conformational Connection; VCH, New York, N.Y. (1989)

6. Le Fèvre, R.J.W.; "Molecular Refractivity and Polarizability" in *"Advances in Physical Organic Chemistry"; Vol. 3, V. Gold, Ed. Academic Press, New York, N. Y.* (1965)

7. Kerr J.; *Phil. Mag*.; *50*, 337 (1875)

8. Flory, P. J; "Principles of Polymer Chemistry"; Ithaca, Cornell University Press. (1953)

9. Coelho, R.; "Physics of Dielectrics for the Engineer"; *Elsevier*. (1979)

10. Riande, E., Saiz, E.; "Dipole Moments and Birefringence of Polymers"; Prentice Hall: Englewood Cliffs, NJ, Chapter 6 and 7 (1992)

11. http://vlf.stanford.edu/research/electric-field-remote-sensing#carlsonKerr (10/17/2014)

12. Aroney M.J., Buckingham A.D.; *Historical Records of Australian Science;* 7 (3) 273-297 (1987)

13. Le Fèvre, C. G., Le Fèvre, R. J. W; *Rev. Pure Appl. Chem; 5*, 26. (1955)

14. Le Fèvre, C. G., Le Fèvre, R. J. W; *J. Chem. Soc.;* 3549. (1956)

15. Le Fèvre, R. J. W. and collaborators; *J. Chem. Soc. (Resumed)*; Issue 0, 1468 (1958); 1814, 2890 (1960); 1880, 3180 (1963)

16. Le Fevre, R. J. W., Orr B. J., and Ritchie, G. L. D., *J. Chem. Soc., Sect. B*; 273. (1966)

17. Stuart, H. A. and Peterlin, A.; *J. Polymer Sci. 5*,551 (1950).

18. Buckingham A. D. and PopIe J. A.; Proc. Phys. Soc. *A68*, 905 (1955)

19. Gotlib Y. Y., Ph.D. Dissertation, Gertsen Leningrad Pedagogical Institute. (1963)

20. Dows; *J. Chem. Phys. 41*, 2656 (1964)

21. Nagai, K., Ishikawa, T.; *J. Chem. Phys. 43*, 4508 (1965)

22. Flory, P. J.; "Statistical Mechanics of Chain Molecules" Wiley-Interscience: New York; Chapter IX. (1969)

23. Nagai, K., Ishikawa; *Polymer Journal, 2*, 263-273 (1971)

24. Tonelli, A. E.; *Macromolecules, 42*, 3830 (2009)

25. Flory, P. J.; Reviews; *Macromolecules*, *7*, (1974)

26. Stoylov, S.P., Stoimenova M.V.; "Molecular and Colloidal Electro-optics"; Surfactant Science ; CRC (2006)

27. Wang B., Oakberg T. C.; *Rev*. *Sci. Instrum*. *70*, 3847-3854 (1999)

28. James T. L.; "Fundamentals of NMR. Nuclear Magnetic Resonance"; *Biophysical Society*; Chapter I. (1998)

29. Le Fevre, R. J. W., Le Fevre, C. G.; J. Chem. Soc. *(Resumed);* Issue 0, 1468(1958)

30. Le Fevre R.J.W., Sundaram K.M.S.; *J. Chem*. *Soc. (Resumed);* Issue 0, 3188 (1963)

31. Le Fevre R.J.W., Sundaram K.M.S.; *J. Chem*. *Soc*. *(Resumed);* Issue 0, 4003 (1962)

32. Aroney M. J., Le Fevre, R.J. W., Parkins G.M.; *J. Chem*. *Soc*. *(Resumed)*; Issue 0, 2890 (1960)

33. Tonelli, A. E.; *Macromolecules;* 10, 153 (1977)

34. Kelly, K. M., Patterson, G. D., Tonelli, A. E.; *Macromolecules; 10*, 859. (1977)

35. Mark, J. E.; Flory, P. J.; *J. Am*. *Chem*. *Soc*.; *87*,1415 (1965)

36. Patterson G. D., Flory P. J.; Trans. *Faraday Soc*.; *68*, 1111 (1972)

37. Khanarian, G.; Tonelli, A. E.; *Macromolecules*; *15*, 145 (1982)

38. Abe, A.; Mark, J.E.; *J. Am*. *Chem*. *Soc*.; *98*, 6468 (1976)

39. Khanarian, G.; Tonelli, A. E. *J. Chem. Phys.*; 75, 5031 (1981)

40. Khanarian, G.; Tonelli, A. E.; Nonlinear Optical Properties of Organic and Polymeric Materials; ACS *Symp. Ser.* 233; American Chemical Society: Washington, DC;Chapter 12 (1983)

41. Khanarian, G.; Schilling, F. C.; Cais, R. E.; Tonelli, A. E.; *Macromolecules*; *1*6, 287 (1983)

42. Williams, A. D.; Flory, P. J.; *J. Am. Chem. Soc.*; 91, 3118 (1969)

43. Pickels, C.J.; Flory, P. J.; *J.Am. Chem. Soc., Faraday Trans. 2*; 69,632 (1973)

44. Saiz, E., Riande, E., Delgadp, M.P., Rienda, J.M.; *Macromolecules*; *15*, 1152 (1982)

45. Tonelli, A.E.; Khanarian, G.; *Macromolecules;* 15, 290. (1982)

46. Tonelli, A. E.; Khanarian, G.; Cais, R. E.; *Macromolecules;* 18, 2324 (1985)

47. Tonelli, A. E.; Valenciano, M.; *Macromolecules*; *19*, 2643 (1986)

48. Khanarian, G.; Cais, R. E.; Kometani, J. M.; Tonelli, A. E.; *Macromolecules*; *15*, 866 (1982)

49. Sato, H.; Tanaka, Y.; Hatada, K.; *Macromol. Rapid Commun*; 3,175 (1982); *J. Polym. Sci., Part B: Polym. Phys Ed.*; 21, 1667-1674 (1983)

50. Semler, J. J.; Jhon, Y. K.; Tonelli, A.; Beevers, M.; Krishnamoorti, R.; Genzer, J.; *Adv. Mater*; *19*, 2877 (2007)

51. Tonelli, A. E.; Jhon, Y. K.; Genzer, J; *Macromolecules*; *43*, 6912–6914 (2010)

52. Yoon, D. Y.; Sundararajan, P. R.; Flory, P. J.; *Macromolecules*; *8*, 77 (1975)

CHAPTER 2

Characterizing Polymer Macrostructures by Identifying and Locating Microstructures along Their Chains with the Kerr Effect

2.1 Abstract

In this brief report we demonstrate that Kerr effect measurements, which determine the excess birefringence contributed by polymer solutes in dilute solutions observed under a strong electric field, are highly sensitive to and capable of determining their microstructures, as well as their locations along the macromolecular backbone. Specifically, using atactic triblock copolymers with the same overall composition of styrene (S) and *p*-bromostyrene (*p-BrS*) units, but with two different block arrangements, *i.e.*, *p-BrS*$_{90}$-b-S$_{120}$-b-*p-BrS*$_{90}$ (I) and S$_{60}$-b-*p-BrS*$_{180}$-b-S$_{60}$ (II), which are indistinguishable by NMR, we detected a dramatic difference in their molar Kerr constants ($_{m}$K), in agreement with those previously estimated. Though similar in magnitude, their Kerr constants differ in sign, with $_{m}$K(II) positive and $_{m}$K(I) negative. In addition, S/*p-BrS* random and gradient copolymers synthesized by reversible addition-fragmentation chain-transfer (RAFT) polymerization exhibit a heretofore unexpected enhanced enchainment of *racemic (r) p-BrS-p-BrS* diads. Comparison of their observed and calculated $_{m}$Ks suggests that the gradient S/*p-BrS* copolymers possess an unanticipated additional gradient in stereosequence that parallels their comonomer gradient, *i.e.*, as the concentration of *p-BrS* units decreases from one end of the copolymer chain to the other, so does the content of *r* diads. This conclusion could only be reached by comparison of observed

and calculated Kerr effects, which access and are sensitive to the global properties of macromolecules, and not NMR, which is only sensitive to local polymer structural environments, but not to their locations on the copolymer chains. Because molar Kerr constants are characteristic of entire polymer chains, and are highly sensitive to their constituent microstructures and their distribution along the chain, they may be used to both identify and locate them, thereby enabling the characterization, for the first time, of their complete macrostructures.

Published in *J. Polym. Sci., PART B: Polym. Phys*. 2013, *51*, 735–741.

2.2 Introduction

The molar Kerr constants $_mK$s of polymer solutes, as obtained from electrical birefringence, *i.e.*, Kerr effect, measurements performed on their dilute solutions, are characteristic of their overall macromolecular conformations and the magnitudes and directions of their resultant overall polarizability tensors and dipole moments. In many instances $_mK$s are more sensitive to polymer microstructures than local, short-range spectroscopic probes, such as NMR.[1] ^{13}C-NMR[2-4] performed in solution, though currently the most sensitive technique for determining polymer microstructures is often not adequate, because of the short-range sensitivity of the resonance frequencies of carbon nuclei to the microstructures they are part of. For example, in a poly (styrene/methylmethacrylate) copolymer there are 20 distinct microstructures (comonomer and stereosequences) at the comonomer triad level,[2,3] and ^{13}C-NMR does not completely distinguish among them with

different resonance frequencies. In contrast, the Kerr effect measured in dilute polymer solutions possesses the potential sensitivity to resolve much longer-range microstructures[1].

The molar Kerr constant of a polymer solute measured in dilute solution represents a macroscopic property characteristic of the entire chain, like its mean-square end-to-end distance ($<r^2>$) or radius of gyration ($<s^2>$) and dipole moment ($<\mu^2>$). While alterations in the microstructures of polymers may typically change their dimensions ($<r^2>$,$<s^2>$) or dipole moments ($<\mu^2>$) by factors of ~2-5, the ${}_mK$s of small molecules (*e.g.* monomers) range over more than four orders of magnitude, and may be either positive or negative.

While a microstructural alteration anywhere along a polymer chain may potentially be evident in its NMR spectrum, because of its inherent short-range sensitivity, the spectral consequence, *i.e.*, chemical shifting of its resonance frequencies, are not sensitive to nor reflect its position or location along the chain. Because the molar Kerr constants of polymers depend on the magnitudes and orientations of their overall dipole moment vectors and anisotropic polarizability tensors, identical or similar microstructural features located at different positions along the macromolecular chain may produce substantially different overall ${}_mK$s, and so may be distinguished and located.

The purpose of this study is two-fold. First we wish to demonstrate that the sensitivity of Kerr effect measurements performed on dilute polymer solutions is sufficient to determine their microstructures. Second we intend to determine if the same microstructures located at different positions along polymer chains (end, middle,…etc.) are reflected in distinct ${}_mK$s, and so may be located. For both purposes, styrene (S)/*para*-bromostyrene (*p-BrS*) copolymers, with specially synthesized micro- and macrostructures, serve as the subjects under

examination. S/*p-BrS* copolymers were chosen for the following important reasons. First, the highly polarizable S and *p-BrS* repeat units possess very different dipole moments[5,6]. Second, for the same stereosequences, the conformational characteristics, or average randomly-coiling conformations, of all S/*p-BrS* copolymers are essentially identical.[5-7] As a consequence, those portions of their ^{13}C-NMR spectra sensitive to microstructure(*i.e.*, the resonance frequencies of their backbone CH and CH_2 and side chain C_1 carbons, are largely independent of both their comonomer compositions and sequences.[2,5,6]

Third, conformations that are dependent solely on copolymer stereosequence, but that are independent of their comonomer compositions and sequences,[7] simplify the calculation of their $_m$Ks. The latter two reasons are important, because the $_m$Ks measured for polymers can only be interpreted, in terms of the types and the locations of their microstructures, by comparison to the $_m$Ks calculated for the same corresponding macrostructural features.

Although here we restrict our Kerr effect studies, their analyses, and discussion to S/*p-BrS* copolymers with different micro- and macrostructures, this should in no way imply that their utility is confined to them. As noted in ref. 1, homo- and copolymers with a wide variety of chemical structures have been successfully examined with the Kerr effect to determine their microstructures, conformations, and their interactions with solvents, even in cases where the difference between the birefringence induced by the applied electric field and contributed by the polymer solute is small. As an example, poly (ethylene oxide) oligomers in benzene exhibit $_m$Ks in the range 80-300% of that shown by the symmetric small molecule CCl_4.[8,9], yet they were readily measured.

2.3 Experimental

ABA and BAB type triblock copolymers comprising S and *p-BrS* units (*i.e.*, S-b-*p-BrS*-b-S and *p-BrS*-b-S-b-*p-BrS*), and S/*p-BrS* copolymers with more intimate comonomer sequences (*i.e.*, random/statistical or gradient) were synthesized by reversible addition-fragmentation chain-transfer (RAFT) polymerization and their $_{m}$Ks were measured and compared to those calculated for copolymers with the same comonomer compositions, but with variable distributions of comonomers and stereosequences. Details of their syntheses and characterization (comonomer compositions and molecular weights) and a more in-depth description of the evaluation of their experimental and calculated $_{m}$Ks will be presented in a subsequent paper. In this brief report we provide comparisons of $_{m}$Ks observed and calculated for S/p-BrS copolymers and demonstrate that the Kerr effect has the potential to both identify and locate microstructures along polymer chains, *i.e.*, to determine their macrostructures.

In 1875 John Kerr[10] first observed that the birefringence, $\mathbf{\Delta n} = \mathbf{n}_{\parallel} - \mathbf{n}_{\perp}$, induced by an applied electric field **E** to both solids and liquids scales as $(\mathbf{B}/\lambda)\mathbf{E}^2$, where λ is the wavelength of light employed to measure the refractive indices, and **B** has since been designated as the Kerr constant. In solutions,[11-15] the Kerr constant $\mathbf{B_{12}}$ is contributed to by the **E** field alignment of both the solvent (1) and solute (2) molecules, with volume fractions $\phi_{1,2}$. Thus, $\mathbf{B_{12} = B_1\phi_1 + B_2\phi_2 = B_1 - B_1\phi_2 + B_2\phi_2}$, and so the Kerr constant of the solute $\mathbf{B_2 = \Delta B/\phi_2 + B_1}$, where $\mathbf{\Delta B}$ is the difference between the Kerr constants of the solution (12) and the solvent (1), with the former extrapolated to infinite dilution. For polymers solutes in solution, the contributions of both solvent and polymer to the electrical birefringence ($\mathbf{B_{12}}$) depend on the magnitudes and

directions of their macroscopic molecular dipole moments, and for polymer solutes these must be appropriately averaged over all rapidly sampled conformations.

Riande and Saiz[16] have summarized the experimental determination and theoretical calculation of molar Kerr constants, $_mK$. For all but the most isotropic (non-polar and minimally polarizable) polymers, the $_mK$ of a polymer solute obtained at infinite dilution in isotropic solvents may be derived experimentally[17,18] from the following relation:

$$_mK = (6N_A\lambda nB)/[\rho(n + 2)^2(\varepsilon + 2)^2],$$

where **n**, **B**, **ρ**, and **ε** are, respectively, the refractive index, Kerr constant, density, and dielectric constant of the polymer solution, all extrapolated to infinite dilution.

Nagai and Ishikawa[19] developed formal expressions relating the overall molecular dipole moments and polarizability tensors of flexible polymers to yield the relation connecting the birefringence they produce at infinite dilution in solution, *i.e.*, $_mK$, in response to their alignment by the electric field **E**.

$$_mK = (2\pi N_A/135)[(<\mu^T\alpha\mu>)/k^2T^2 + (<\alpha^R\acute{\alpha}^C>)/kT].$$

N_A and **k** are the Avogadro and Boltzmann constants, respectively, and **T** is the temperature. μ^T and **μ** are the overall polymer dipole moment vectors expressed as a row and column, respectively. **α** and **ά** are the overall anisotropic optical and static polarizability tensors of the polymer, respectively, with both contributing to **Δα**, the overall difference in polarizabilities of the entire polymer chain in directions parallel and perpendicular to the applied field **E**. Their superscripts **R** and **C** designate row and column forms of their traceless tensors, and < > indicates the appropriate average of both contributions over all conformations available to the polymer chain.

Flory and Jernigan[20-22] subsequently demonstrated how matrix multiplication techniques can be applied to the dipolar $\langle \boldsymbol{\mu}^{\mathbf{T}}\boldsymbol{\alpha}\boldsymbol{\mu} \rangle$ and polarizability $\langle \boldsymbol{\alpha}^{\mathbf{R}}\acute{\boldsymbol{\alpha}}^{\mathbf{C}} \rangle$ terms of the Nagai-Ishikawa[19] expression for ${}_{m}K$ to perform the correct averaging of both over all of a polymer chain's realistic Rotational Isomeric State (RIS)[20] conformations. Critical to its implementation is the assumption of constituent bond dipole moments and polarizability tensors that are both additive and independent of conformation.

This permits a comparison of realistically estimated and experimentally observed molar Kerr constants for polymers, which is critical to the determination of their underlying microstructures.

S/*p-BrS* copolymers were chosen for the following reasons: 1. The dipole moments of S and p-BrS repeat units are quite different[5,6]; 2. For the same stereosequences, the conformational characteristics, or average randomly-coiling conformations, of all S/*p-BrS* copolymers are essentially identical[5-7], so the portions of their ^{13}C-NMR spectra sensitive to microstructure (*i.e.* the resonance frequencies of their backbone CH and CH_2 and side chain C_1 carbons) are independent of both their comonomer compositions and sequences[2,5,6]; and 3. Conformations that are dependent solely on copolymer stereosequences, but that are independent of their comonomer compositions and sequences[7], simplify the calculation of ${}_{m}Ks$. The latter two reasons are important, because the ${}_{m}Ks$ measured for polymers can only be interpreted, both in terms of the types and the locations of microstructures in the chain, by comparison to the ${}_{m}Ks$ calculated for the same corresponding micro- and macrostructural features.

These advantageous features were previously used to examine S/*p-BrS* copolymers obtained by the bromination of atactic PS to yield various random or blocky samples. From comparison of observed and calculated $_m$Ks for random S/*p-BrS* copolymers, we were able to conclude that the original PS sample was nearly ideally atactic.[5]

Bromination of atactic PS in poor, theta, and good solvents produced S/*p-BrS* copolymers whose comonomer sequences were blocky, random/blocky, and random, respectively, and which could only be confirmed from comparison of their observed and estimated Kerr effects.[6]

When calculating $_m$Ks, we considered styrene S/*p-BrS* copolymers with 300 total comonomer units, because this exceeds the chain length where the calculated $_m$Ks/repeat unit become asymptotic. Although SEC/GPC indicated that some of our synthesized S/*p-BrS* samples had fewer than 300 repeat units, $_m$Ks/repeat unit calculated for them did not differ appreciably from those calculated for their longer 300 repeat unit chains. For each distinct comonomer composition, comonomer sequence, and tacticity or stereosequence, a sample of at least 50 copolymer chains was generated using a commercial random number generator and our own FORTRAN algorithms. Each copolymer chain was built one comonomer unit at a time, with account taken of both the type of comonomer added (S or *p-BrS*) and with which stereosequence the addition occurs to form *meso* or *racemic* (*m* or *r*) diads. Further details of the $_m$K calculations for S/*p-BrS* copolymers can be found in references 5-7.

2.4 Results and Discussion

The tri-block copolymers, *p-BrS*$_{90}$-b-S$_{120}$-b-*p-BrS*$_{90}$ (I) and S$_{60}$-b-*p-BrS*$_{180}$-b-S$_{60}$ (II), *cf*. Figure 2.1, were synthesized by RAFT polymerization.[23] Only very small quantities were obtained, preventing the measurement of the electrical birefringence for a complete series of their dilute dioxane solutions. Instead, measurements were restricted to only one or two solutions at concentrations less than 1 wt% for each tri-block. Nevertheless, these preliminary partial Kerr constant measurements indicate that $_{m}$K(II) is positive, while $_{m}$K(I) is negative, though their magnitudes are similar. For example, 0.6 wt% solutions of the tri-blocks I and II were observed to decrease and increase, respectively, the birefringence of their dioxane solutions by 17 and 26%. In other words, triblock (I) has a negative $_{m}$K, whereas that for triblock (II) is positive.

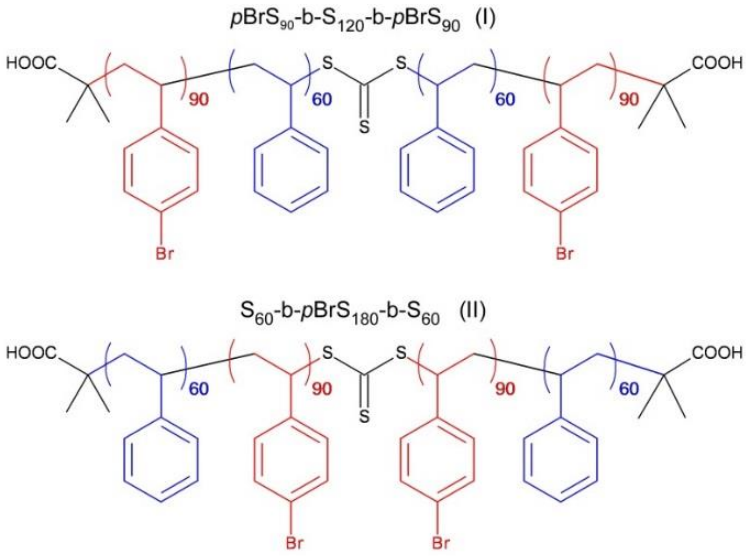

Figure 2.1 Structures of the p-BrS$_{90}$-S$_{120}$-p-BrS$_{90}$ (I) and S$_{60}$-p-BrS$_{180}$-S$_{60}$ (II) tri-block copolymers, synthesized by reversible addition-fragmentation chain transfer polymerization.[2]

This dramatic difference is observed despite both tri-block copolymers having the same overall comonomer composition and number of identical block junctions, which necessarily produce virtually identical ^{13}C-NMR spectra. While a short-range local probe, such as ^{13}C-NMR spectroscopy cannot distinguish between these S/*p-BrS* tri-block copolymers, the Kerr effect can. Because they differ only in the locations of their S and *p-BrS* blocks, comparison of their observed $_{m}$Ks clearly indicates that the Kerr effect may be used not only to identify polymer microstructures, but also to locate them along the macromolecular chain. Although initially unexpected from our calculated molar Kerr constants, we observed similar $_{m}$Ks for the intimate S/*p-BrS* copolymers (*cf*. Figure 2.2) listed in Table 2.1, irrespective of their comonomer sequences. Based on our previous Kerr effect studies of S/p-BrS copolymers obtained by bromination of atactic PS in good and poor solvents, respectively, we had expected that a gradient sequence of comonomers with a similarly atactic stereosequence would produce $_{m}$Ks considerably smaller and larger than those observed for the atactic random/statistical and blocky copolymers.[5, 6]

Figure 2.2 Illustrations of the statistical (stat) and gradient (grad) S/p-BrS copolymer sequences synthesized and investigated by Kerr effect measurements. Correlated comonomer and stereosequence gradients in poly(S-grad-p-BrS) are also shown.

Atactic S/p-BrS copolymers with random and blocky comonomer sequences obtained by bromination of atactic PS were observed to have molar Kerr constants differing by factors of 2–3,[5,6] whereas those of the random and gradient copolymers in Table 2.1 made by RAFT copolymerization are closely similar. It should be mentioned that in the few cases where the Kerr effect of the same sample in Table 2.1 was repeatedly measured, the molar Kerr constants derived from them varied no more than ~10%.

The $_{m}$Ks calculated for S/*p-BrS* copolymers are very sensitive to their stereosequences,[5,6] as well as their comonomer compositions and sequence distributions. Thus, we further assessed the sensitivity of the $_{m}$Ks calculated for gradient copolymers to their stereosequences, because our initial calculations had assumed a random/statistical atactic stereosequence for all of our RAFT synthesized copolymers, independent of their comonomer sequences. However, these resulted in $_{m}$Ks calculated for gradient comonomer sequences that were much smaller than those for random comonomer sequences, unlike those observed in Table 2.1. We found that the $_{m}$Ks calculated for random/statistical and gradient S/*p-BrS* copolymers were closely similar, as observed experimentally, only when the gradient copolymers were assumed to have an associated stereosequence gradient. Only copolymers that were rich in *racemic* (*r*) *p-BrS*─*p-BrS* diads on one chain end and rich in S─S diads, with or without a preference for *meso* (*m*) diads, on the other chain end yielded $_{m}$Ks as large as those of S/*p-BrS* copolymers with random/statistical comonomer sequences and stereosequences, in agreement with the experimental $_{m}$Ks seen in Table 2.1.

Table 2.1 Characteristics and Observed Kerr effects§ of Random/Statistical (S) and Gradient (G) S/p-BrS Copolymers synthesized by reversible addition-fragmentation chain transfer (RAFT) polymerization

Sample name	Mole fraction of *p-BrS* in S/*p-BrS* copolymer	Method of comonomer addition	Comonomer addition rate (mL/min)	Slopes of solution Kerr Constants x 10^{16}, $V^{-2}m$, vs concentration	Relative $_mK$s
Poly (*statistical*-S/*p-BrS*)					
S-50-I	50%	Simultaneous RAFT	NA	2.8	**1.25**
S-50-II	(Targeted feed ratio: 50:50.)	Simultaneous uncontrolled, AIBN	NA	2.7	**1.16**
Poly ("*gradient*"-S/*p-BrS*) RAFT					
G-48-I	48%	Gradient with hand syringe	0.014	2.2	**1.0**
G-47	47%	"	0.025	2.5	**1.16**
G-35	35%	"	0.007	2.7	**1.16**
G-48-II	48%	Gradient with syringe pump	0.014	2.6	**1.25**
G-32	32%	Gradient with syringe pump	0.033	2.3	**1.06**

§Measured in 1,4-dioxane at 25° C.

As a consequence, comparison of experimental and calculated $_mK$s led us to the tentative identification of an unexpected microstructural element/feature introduced during our controlled radical RAFT syntheses of intimate S/*p-BrS* copolymers, *i.e.*, a stereosequence gradient characterized by a changing population of *r* and *m* diads from one chain end to the other, which parallels their gradient commonomer sequence (*cf*. Figure 2). As the population of *p-BrS* units decreases along the chain, the population of *r* diads also appears to decrease. In a forthcoming article, we will further examine the suggestion that in the controlled RAFT synthesis of S/*p-BrS* copolymers with a gradient comonomer sequence a correlated

stereosequence gradient was introduced.[24-26] This is a particularly unexpected, yet important, result, because in the usual uncontrolled free-radical initiated polymerizations of S and *p-BrS*, the resulting homopolymers [PS and P(*p-BrS*)] are found to have nearly ideally random stereosequences characterized by $P_r \approx P_m \approx 0.5$[27-30].

We have begun synthesizing random and gradient S/p-BrS copolymers by atom transfer radical polymerization (ATRP)[31] and will measure their molar Kerr constants. By comparison with those of our RAFT copolymers, we should learn whether in general controlled radical polymerizations produce stereosequences in S/p-BrS copolymers that are other than random or atactic.

Two random S/p-BrS copolymers, both with 50:50 S:p-BrS composition, were synthesized. One polymer was made by RAFT and the other by free-radical initiated polymerizations, and their thin films showed distinct dewetting behaviors. While the RAFT film did not dewet from a silica surface after 2 days of annealing above T_g at 150° C, the random S/*p-BrS* film prepared by uncontrolled free-radical polymerization did. This suggests, as previously observed for random and blocky samples of atactic S/*p-BrS* copolymers [6], that their microstructures differ, and, in the case of these un-controlled and controlled (RAFT) free-radical synthesized 50:50 random copolymers, that difference can only originate from their different stereosequences.

Racemic (*r*) *p-BrS*─*p-BrS* diads substantially populate[7] the extended *trans-trans* backbone conformation, which places both brominated side-chains on opposite sides of the backbone plane, with both up or both down. In contrast, in *meso* (*m*) *p-BrS*─*p-BrS* diads the extended *trans-trans* backbone conformation is not substantially populated, whereas those

conformations that are more heavily populated are not extended with both brominated side-chains either on the same or opposite sides of the backbone plane. Our Kerr effect observations strongly suggest that RAFT synthesized copolymers do and the uncontrolled free-radical copolymers do not have predominantly *r p-BrS—p-BrS* diads, substantially populated by the *trans-trans* backbone conformation. This places both brominated side-chains on opposite sides of the backbone plane in a position to interact with the silicon surface, so possibly, the RAFT random copolymer film should be stickier. Clearly the adherence of S/p-BrS films to silicon substrates depends not only upon their comonomer sequences (blocky stickier than random)[6], but as observed here, also upon their stereosequences, with *r p-BrS—p-BrS* diads apparently stickier than the *m p-BrS—p-BrS* diads.

This micro- and macrostructural detail cannot be obtained from short-range spectroscopic probes, such as ^{13}C-NMR, which is currently the method of choice for characterizing the microstructures of polymers. The severe overlapping of backbone methylene and methine carbon resonances belonging to S and *p-BrS* units seen in Figure 2.3 makes it impossible to identify which comonomer sequences are present and with which stereosequences. In Figure 2.4 the C_1 phenyl ring carbon regions of the same S/*p-BrS* homo- and copolymer spectra are presented. We again see extensive overlapping of resonances belonging to S and *p-BrS* repeat units in the copolymers. Although we cannot determine which stereosequences the S and p-BrS repeat units belong to in the intimate copolymers, examination and comparison of the PS and P(p-BrS) C_1 carbon spectra indicate[27-30] that their RAFT homo- polymerizations have produced comparatively larger quantities of mm and rr-

triad-centered pentad stereosequences, respectively, consistent with the parallel stereo- and comonomer sequence gradients suggested here based on Kerr effect measurements.

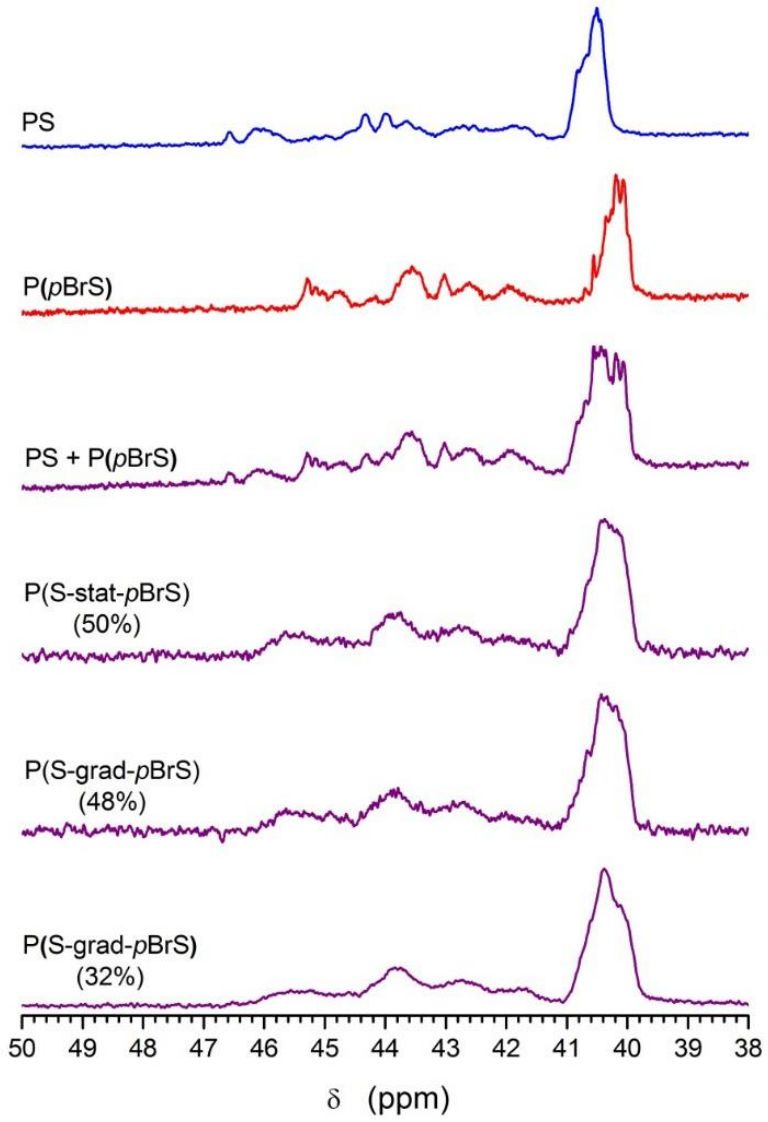

Figure 2.3 The methylene and methine carbon regions of the 13C-NMR spectra of selectedS/p-BrS polymers synthesized by RAFT polymerization and used in this study. Samples P(S-stat-p-BrS) (50%) and P(S-grad-p-BrS) (48 and 32%) correspond to samples S-50-I, G-48-II, and G-32 in Table 2.1.

Although not presented here, the C_1 carbon spectral region of a commercial atactic PS synthesized by uncontrolled free-radical intiation[32] is similar to that seen in Figure 2. 4 for our PS sample obtained by controlled RAFT polymerization.

This suggests that the stereosequence gradient we are proposing for the RAFT S/p-BrS copolymers synthesized with gradient comonomer sequences is largely a result of the preferred enchainment of rr triad stereosequences in p-BrS-rich regions, while in regions rich in S units, little if any preference for triad stereosequences is evident.

In addition, 2D (^{1}H-^{13}C) heteronuclear single quantum correlated spectra[33,34] were also unable to differentiate between the comonomer sequences and stereosequences of our S/p-BrS copolymers.

Thus, our ^{13}C NMR observations of PS and P (*p-BrS*) homopolymers obtained by RAFT polymerization suggest that, while PS is predominantly atactic, P (*p-BrS*) is rich in *rr* triads. This implies that our RAFT synthesized S/*p-BrS* copolymers may also have more *rr* triad stereosequences in their *p-BrS*-rich portions, though their ^{13}C NMR spectra can only be directly used to determine their comonomer compositions. Because the Kerr constants of S/*p-BrS* copolymers provide a measure of the magnitudes and directions of their macromolecular polarizability tensors and dipole moments, comparison of their observed and calculated $_m$Ks can serve to correlate their comonomer sequences with their stereosequences and to locate them along the copolymer chains.

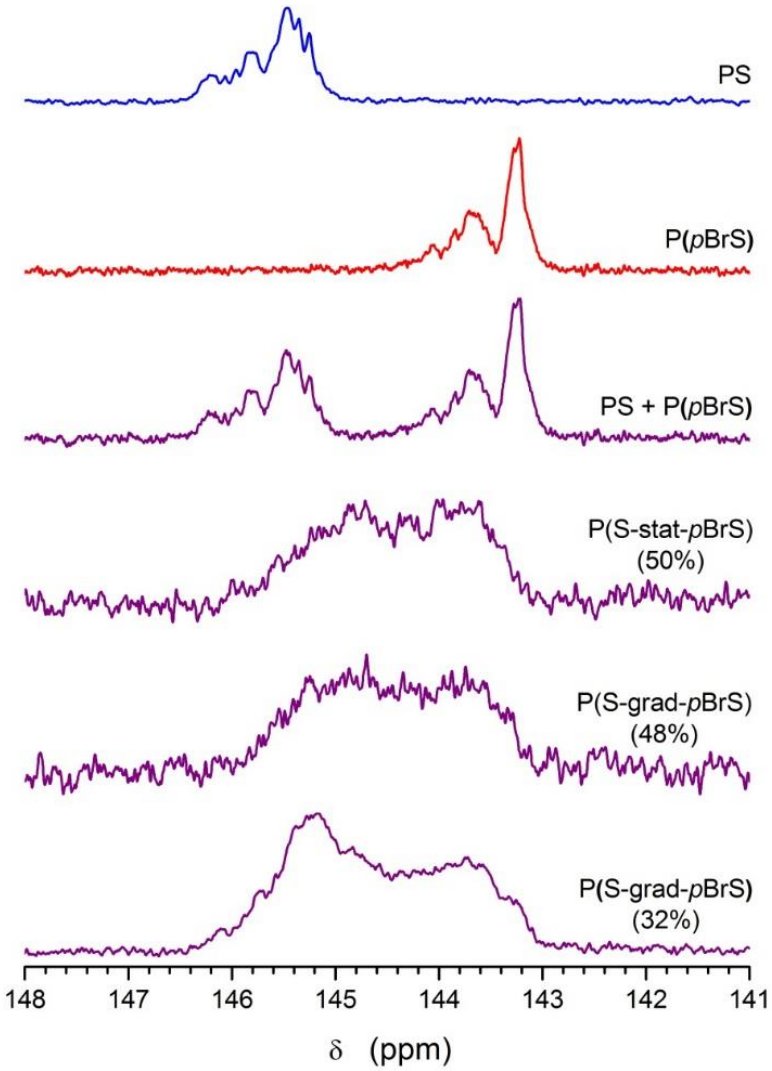

Figure 2.4 The C_1 carbon regions of the ^{13}C-NMR spectra of selected S/p-BrS polymers synthesized by RAFT polymerization and used in this study. Samples P(S-stat-p-BrS) (50%) and P(S-grad-p-BrS) (48 and 32%) correspond to samples S-50-I, G-48-II, and G-32 in Table 1.

It appears that Kerr effect observations of dilute polymer solutions, which provide a measure of the magnitudes and orientations of overall macromolecular polarizability tensors

and dipole moments, can both identify and locate constituent polymer microstructures. While other macromolecular properties of polymers, such as average dimensions ($<r^2>$, $<s^2>$) and dipole moments ($<\mu^2>$), may typically change by factors of 2~5 due to alterations in microstructures, the Kerr effects observed in dilute polymer solutions have a much greater range, and more importantly, they are necessarily dependent on the locations of constituent microstructures. The enhanced sensitivity of this macromolecular property appears sufficient to not only effectively identify microstructures, but also to locate their positions along polymer chains, while inherently locally sensitive spectroscopic probes, such as NMR, cannot. Kerr effect examinations of dilute polymer solutions appear, for the first time, to provide a means to probe and characterize polymer macrostructures.

2.5 Summary and Conclusions

Kerr effect observations of S/*p-BrS* triblock and the more intimate random/statistical and gradient copolymers demonstrate a sensitivity sufficient to not only characterize their constituent microstructures, but also to permit determination of their locations along the macromolecular chain. We may now close the gap, recently noted by the latest NSF Workshop report on Polymers (http://www. nsf. gov/mps/dmr/reports.jsp), between the various newly created chain architectures, currently being produced by the recently developed array of controlled polymerization techniques, and the need to characterize them. Consequently, for the first time the characterization of complete polymer macrostructures appears feasible, and this will undoubtedly lead to significant improvements in structure-property relations developed for polymer materials.

In addition, and as illustrated by observations of the distinct dewetting behaviors of films made from random/statistical S/*p*-*BrS* copolymers synthesized by uncontrolled free-radical and controlled radical (RAFT) means, we hope that this report will raise the awareness of polymer scientists to the importance of characterizing polymer macrostructures. The behaviors of polymer materials are expected to depend not only upon their constituent microstructures, but also to depend upon where along the polymer backbones they are located, as demonstrated here with the Kerr effect.

ACKNOWLEDGEMENTS

We are grateful to the National Science Foundation (DMR-Polymers Program, grant # 0966478) for financial support and to the Army Research Office for a DURIP equipment grant (grant #53583 CH-RIP) to construct our Kerr effect instrument. The assistance provided by our home Departments and Universities is also appreciated.

REFERENCES

1. Tonelli, A. E., *Macromolecules* **2009**, *42*, 3830-40.

2. Tonelli, A. E., "NMR Spectroscopy and Polymer Microstructure: The Conformational Connection" **1989**; VCH: New York.

3. Bovey, F. A.; Mirau, P. A. NMR of Polymers **1996**; Academic Press:New York.

4. Tonelli, A. E.; White, J. L. NMR spectroscopy of Polymers **2007**. In Physical Properties of Polymers Handbook, 2nd ed. **2007**; Chapter 20; Mark, J., Ed.; Springer: New York.

5. Khanarian, G.; Cais, R. E.; Kometani, J. M.; Tonelli, A. E.,*Macromolecules* **1982**, *15*, 866-69.

6. Semler, J. J.; Jhon, Y. K.; Tonelli, A.; Beevers, M.; Krishnamoorti, R.; Genzer, J. *Adv*.*Mater*. **2007**, *19*, 2877-83.

7. Yoon, D. Y.; Sundararajan, P. R.; Flory, P. J. *Macromolecules* **1975**, *8*, 77-83.

8. Kelly, K. M., Patterson, G. D., Tonelli A. E., *Macromolecules* **1977**, *10*, 859

9. Khanarian, G., Tonelli, A. E., *Macromolecules* **1982**,*15*, 145.

10. Kerr, J. *Philos. Mag*. **1875**, 50 (337), 416; **1879**, 8 (85), 229; **1880**, 9,157; **1882**, 13 (153), 248; **1894**, 37, 380; **1894**, 38, 1144.

11. Briegleb, G., Z. *Physik*. *Chem*.**1931**, *B14*, 97.

12. Otterbein, G., *Physik*. *Z*. **1933**, *34*, 645.

13. Sachsse, G., *Physik*. *Z*. **1935**, *36*, 357

14. Friedrich, H., *Physik*. *Z*. **1937**, *38*, 318.

15. Saiz, E., U. W. Suter, U. W., Flory, P. J., *J. Chem*. *Soc.*, *Faraday Trans. 2*. **1977**, *73*, 1538.

16. Riande, E.; Saiz, E. Dipole Moments and Birefringence of Polymers **1992**; Prentice Hall: Englewood Cliffs, NJ, Chapter 7.

17. LeFevre, C. G.; LeFevre, R. J. W. *Rev*. *Pure Appl. Chem*. **1955**, *5*, 26.

18. LeFevre, C. G.; LeFevre, R. J. W. In "Techniques of Organic Chemistry" **1960**; Weissberger, A., Ed.; Interscience: New York, Vol. I, Chapter XXXVI.

19. Nagai, K.,Ishikawa, T., *J. Chem*. *Phys.***1965**, *43*, 4508-15.

20. Flory, P. J.; Jernigan, R. L. *J. Chem*. *Phys.* **1968**, *48*, 3823-24

21. Flory, P. J. "Staistical Mechanics of Chain Molecules" **1969**; Wiley-Interscience: New York; Chapter IX.

22. Flory, P. J. *Macromolecules* **1974**, *7*, 381-92.

23. Mayadunne, R. T. A., Rizzardo, E., Chiefari, J., Chong, Y. K., Moad, G.. Thang, S. H., *Macromolecules* **1999**, *32*, 6977-80.

24. Cherifi, N., Issoulie, A., Khoukh, A., Benaboura, A., Save, M., Derail, C., Billon, L. *Polym*. *Chem*. **2011**, *2*, 1769-77.

25. Lutz, J.F., *Polym*. *Chem*. **2010**, *1*, 55-62.

26. Ishitake, K., Satoh, K., Kamigaito, M., Okamoto, Y., *Polym. Chem*. **2012**, *3*, 1750–1757.

27. Trumbo, D. L., Harwood, H. J., *Polym. Bull.* **1987**, *18*, 27-32.

28. Sato H., Tanaka, Y., Hatada, K, *Makromol. Rapid Commun*. **1982**, *3*, 175-85; *J. Polym. Sci., Polym. Phys.* **1983,** 21, 1667-74.

29. Tonelli, A. E., *Macromolecules* **1983**, *16*, 604-7.

30. Kawamura, T, Toshima, N., *Makromol. Rapid Commun.***1994**, *15*, 479-86.

31. K. Matyjaszewski, *Controlled/Living Radical Polymerization: From Synthesis to Materials*; American Chemical Society: Washington, D.C., 2006; Chapter 9.

32. Ko, T., Harwood, H. J., *Makromol. Rapid Commun*. **1983**, *4*, 463-8.

33. L. E. Kay, P. Keifer, T. Saarinen, J. Am. Chem. Soc. **1992**, 114, 10663–10665.

34. L. Zhang, G. Gellerstedt, Magn. Reson. Chem. **2007**, 45,37–45.

CHAPTER 3

Beyond microstructures: Using the Kerr Effect To Characterize the Macrostructures of Synthetic Polymers

3.1 Abstract

The macrostructures of synthetic polymers are essentially the complete molecular chain architectures, including the types and amounts of constituent short-range microstructures, such as the regio- and stereosequences of the inserted monomers, the amounts and sequences of monomers found in co-, ter-, and tetra-polymers, branching, inadvertent, and otherwise, etc. Currently, the best method for characterizing polymer microstructures uses high field, high resolution 13C-nuclear magnetic resonance (NMR) spectroscopy observed in solution.

However, even ^{13}C-NMR is incapable of determining the locations or positions of resident polymer microstructures, which are required to elucidate their complete macrostructures. The sequences of amino acid residues in proteins, or their primary structures, cannot be characterized by NMR or other short-range spectroscopic methods, but only by decoding the DNA used in their syntheses or, if available, X-ray analysis of their single crystals. Similarly, there are currently no experimental means to determine the sequences or locations of constituent microstructures along the chains of synthetic macromolecules. Thus, we are presently unable to determine their macrostructures. As protein tertiary and quaternary structures and their resulting ultimate functions are determined by their primary sequence of

amino acids, so too are the behaviors and properties of synthetic polymers critically dependent on their macrostructures. We seek to raise the consciousness of both synthetic and physical polymer scientists and engineers to the importance of characterizing polymer macrostructures when attempting to develop structure–property relations. To help achieve this task, we suggest using the electrical birefringence or Kerr effects observed in their dilute solutions. The molar Kerr constants of polymer solutes contributing to the birefringence of their solutions, under the application of a strong electric field, are highly sensitive to both the types and locations of their constituent microstructures. As a consequence, we may begin to characterize the macrostructures of synthetic polymers by means of the Kerr effect. To simplify implementation of the Kerr effect to characterize polymer macrostructures, we suggest that NMR first be used to determine the types and amounts of constituent microstructures present. Subsequent comparison of observed Kerr effects with those predicted for different microstructural locations along the polymer chains can then be used to identify the most likely macrostructures.

Published online in *J. Polym. Sci., Part B: Polym. Phys. 2014*, DOI: 10.1002/polb.23598

3.2 Introduction

The schematic homopolymer stereosequences (left) and comonomer sequences (right) drawn below have equivalent triad microstructures, that is, the same numbers of mm, mr, rr stereosequences and •••, ••○, •○•, •○○, ○•○, ○○○ comonomer sequences, but distinct macrostructures. Solution ^{13}C-nuclear magnetic resonance (NMR), currently the best analytical method, can usually successfully identify and quantify such short-range

microstructural elements.[1, 2] However, due to its relatively short-range, local sensitivity, NMR, including ^{13}C-NMR, cannot determine the exact location of these microstructural elements along the polymer backbone, nor can it reveal if all chains in the observed polymer sample possess the same types and amounts of microstructures or if they are distributed non-uniformly along or among the sample chains.

Stereosequences	**Comonomer Sequences**
…mmmmmmrmrmrmrmrrrrrrm…	**…●●●●○●○○○○○●○●●…**
vs	***vs***
…mrmmmrrrmrrmmrrmmmrrm…	**…●○○○○○●●●●○●○●○…**

This begs the question of whether or not there is an experimental means that can both identify and count/quantify local microstructures and can also locate them along or among polymer chains. If such an experimental technique exists, it must necessarily be sensitive to the entire structures of macromolecular chains. Here, we suggest that the contributions made by polymer solutes to the electrical birefringence observed for their dilute solutions when subjected to strong electric fields, or their Kerr effects, are experimental probes of complete polymer chains that are sensitive enough to distinguish their macrostructures.[3, 4]

The reason we want to determine the macrostructures of polymers, through identification, quantification, and location of their constituent microstructures, is because the macrostructures of polymers dictate their overall behaviors. Structure–property relations developed for polymer materials that are truly useful and relevant must be based on their macrostructures and not simply upon the types and quantities of short-range microstructural

elements they possess. Just as the tertiary and quaternary structures and biological functions of proteins are determined by their primary sequences of amino acids, so too are the behaviors and properties of synthetic polymers critically dependent on their macrostructures.

Along with emphasizing that it is the macrostructures of polymers, that is, the connectivity of their constituent microstructures, which should be the focal point for development of structure–property relations, and more a importantly, we present evidence that the Kerr effect may be used to probe/determine polymer macrostructures. The molar Kerr constant, ${}_mK$ of a polymer solute measured in dilute solution represents a macroscopic property characteristic of the entire chain, like its mean-square end-to-end distance ($\langle r^2 \rangle$) or radius of gyration ($\langle s^2 \rangle$) and dipole moment ($\langle \mu^2 \rangle$). While alterations in the microstructures of polymers may typically change their dimensions ($\langle r^2 \rangle$, $\langle s^2 \rangle$) or dipole moments ($\langle \mu^2 \rangle$) by factors of ~2 to 5, the mKs of small molecules[5] (e.g., monomers) range over more than four orders of magnitude, and may be either positive or negative.

Initially [4, 6, 7] to determine if the Kerr effect may be used to probe/determine polymer macrostructures, we selected and synthesized styrene/p-bromostyrene (S/p-BrS) copolymers with controlled micro- and macro-structures. S/p-BrS copolymers were chosen for the following reasons: (1) The dipole moments of S and p-BrS repeat units are quite different; (2) for the same stereosequences, the conformational characteristics, or average randomly coiling conformations, of all S/p-BrS copolymers are essentially identical.[8] Consequently, portions of their ^{13}C-NMR spectra potentially sensitive to microstructure (i.e., the resonance frequencies of their backbone CH and CH_2 and side chain C_1 carbons) are independent of both their comonomer compositions and sequences, as carefully documented in refs. 4 and 7; and 3

conformations that are dependent solely on copolymer stereosequences, but that are independent of their comonomer compositions and sequences, simplify the calculation of mKs.[3, 4] The latter two reasons are important, because the mKs measured for polymers can only be interpreted, in terms of the types, quantities, and the locations of their microstructures, by comparison with the mKs calculated for the corresponding micro- and macrostructural features.

These advantageous features were previously used to examine S/p-BrS copolymers obtained by the bromination of atactic polystyrene (PS) to yield various random or blocky copolymer samples.[6, 7] From comparison of observed and calculated mKs for random S/p-BrS copolymers, we were able to conclude[6] that the original PS sample was nearly ideally atactic. Bromination of atactic PS in poor, theta, and good solvents produced S/p-BrS copolymers[7] whose comonomer sequences were blocky, random/blocky, and random, respectively, and which could only be confirmed from comparison of their observed and estimated Kerr effects.

More recently,[4] the 60% p-BrS/40% S triblock copolymers S_{60}-b-p-BrS_{180}-b-S_{60} and p-BrS_{90}-b-S_{120}-b-p-BrS_{90} were synthesized and their Kerr constants were observed to have similar magnitudes, but to be, respectively, positive and negative. Also reversible addition-fragmentation chain transfer (RAFT) controlled radical polymerization of random and gradient S/p-BrS were conducted and their Kerr constants were observed. Comparison with the Kerr constants measured for random and blocky S/p-BrS samples[7] made by bromination of PS in poor, theta, and good solvents and those calculated for gradient S/p-BrS copolymers strongly suggested that the gradient copolymers did not have atactic stereosequences.

Rather, we found that calculated and observed mKs for random/statistical and gradient S/p-BrS copolymers produced by RAFT polymerizations were only similar when the gradient copolymers were assumed to have an associated stereosequence gradient, as illustrated in Figure 3.1. Only copolymers that were rich in racemic (r) p-BrS--p-BrS diads on one chain end and rich in S--S diads, with or without a preference for meso (m) diads, on the other chain end yielded mKs as large as those of S/p-BrS copolymers with random/statistical comonomer sequences and stereosequences, in agreement with the experimental $_{m}$Ks.

In this study, we further examined some specifically synthesized S/p-BrS copolymers. We used both uncontrolled and alternative controlled free-radical polymerization (ATRP) to see if their gradient samples showed Kerr effects similar to the gradient samples obtained by RAFT, with largely racemic p-BrS-p-BrS diads.

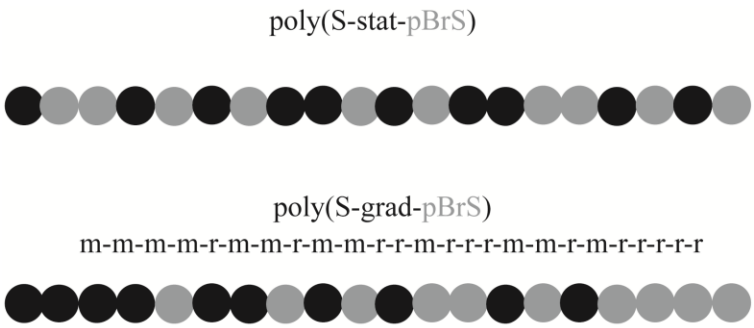

Figure 3.1 Illustrations of the random or statistical (stat) and gradient (grad) S/p-BrS copolymer sequences synthesized and investigated by Kerr effect measurements. Correlated comonomer and stereosequence are also shown in poly(S-grad-p-BrS) (Adapted from ref. 4).

Comparison of the Kerr effect observed for a random 50:50 S/p-BrS copolymer with the Kerr effect of a 50:50 mixture of 80:20 and 20:80 S/p-BrS copolymers was made to learn if the Kerr effect can distinguish between samples with polymer chains that all have the same microstructures from those with a heterogeneous distribution of microstructures, but with the same overall sample average local microstructures. Of course, these samples cannot be distinguished by NMR or other spectroscopies with short-range sensitivity to microstructures.

In addition, we measured the Kerr constants of several copolymer samples with chemical structures very different from S/p-BrS copolymers, which were obtained from two colleagues. Styrene/butadiene multiblock copolymers, with the same overall composition, but with random and regularly alternating block sequences, and ethylene/vinyl acetate (E/ VAc) copolymers with the same overall compositions, but with distinct precise or random placement of comonomer units and distinct stereosequences were provided by the Lee and Bates[9] and Hillmyer and coworkers[10] groups, respectively.

We also measured the Kerr constants of individual very dilute solutions of isotactic (i) and syndiotactic (s) poly(methyl methacrylate) (PMMA) and compared them to that of their mixed solution in two different solvents. At low concentrations, stereoregular PMMAs are known to form soluble complexes in some solvents, but not in others.[11] This was done to determine if interactions between macromolecules could also be successfully probed with the Kerr effect. In each of the above instances, measured Kerr constants were able to distinguish between and help identify the distinct macrostructures of and interactions between these co- and homopolymer samples.

3.3 Polymer Kerr Effects

The Kerr effect[12] is the birefringence produced in materials through application of a strong electric field E. John Kerr showed that $\Delta n = (B/\lambda)E^2$, where $\Delta n = n_{\parallel} - n_{\perp}$, that is, the difference in refractive indices along and perpendicular to the direction of E, λ is the wavelength of light used to measure the birefringence Δn, and B has become known as the Kerr constant. Riande and Saiz[13] have summarized the experimental observation of Kerr constants, and from them, the derivation of molar Kerr constants, mKs. For all but the most isotropic (nonpolar and minimally polarizable) molecules, mKs obtained at infinite dilution may be derived experimentally[14, 15] from the following relation.

$$_{m}K = (6N_A\lambda nB)/[\rho(n + 2)^2(\varepsilon + 2)^2],$$

where n, B, ρ, and ε are the refractive index, Kerr constant, density, and dielectric constant of the solution, respectively, all extrapolated to infinite dilution.The magnitudes and signs of molecular Kerr effects are characteristic of the magnitudes and directions of their resultant overall polarizability tensors, α, and dipole moments, μ. Nagai and Ishikawa[16] have shown that the molar Kerr constant is given molecularly by:

$$_{m}K = (2\pi N_A/135)[(<\mu^T\alpha\mu>)/k^2T^2 + (<\alpha^R\acute{\alpha}^C>)/kT],$$

where < > indicates an average over all conformations of the molecule and is particularly important for flexible macromolecules, which can assume a myriad of conformations. Flory and Jernigan[17, 18] showed how matrix multiplication techniques can accomplish the appropriate conformational averaging, provided a reliable description of a polymer's conformational characteristics is available.

The molar Kerr constant of a polymer solute measured in dilute solution represents a macroscopic property characteristic of the entire chain, like its mean-square end-to-end distance ($<r^2>$) or radius of gyration ($<s^2>$) and dipole moment ($<\mu^2>$). While alterations in the microstructures of polymers may typically change their dimensions ($<r^2>$,$<s^2>$) or dipole moments ($<\mu^2>$) by factors of ~2 to 5, the mKs of small molecules[5] (e.g., monomers) range over more than four orders of magnitude, and may be either positive or negative.

A microstructural alteration anywhere along a polymer chain may potentially be evident in its NMR spectrum. However, because of its inherent short-range sensitivity, the spectral consequence of such a microstructural alteration, that is, chemical shifting of its resonance frequencies,[1, 2] is not sensitive to nor reflects its position or location along the chain. Because the molar Kerr constants of polymers depend on the magnitudes and orientations of their overall dipole moment vectors and anisotropic polarizability tensors, identical or similar microstructural features located at different positions along the macromolecular chain backbone may produce substantially different overall mKs, which can be used to distinguish and locate them. However, they can only be interpreted, in terms of their macrostructures, that is, types and the locations of their contributing microstructures, by comparison to the mKs calculated for the assumed corresponding macrostructural features.

3.4 Results and Discussion

3.4.1 Kerr effects and macrostructures of S/p-BrS copolymers

Although initially unexpected from our calculated molar Kerr constants, and those observed for random and blocky atactic S/p-BrS copolymers made by brominating atactic PS

in solvents of different quality,[7] we observed similar mKs for the intimately enchained S/p-BrS copolymers synthesized by RAFT copolymerization[4] (see Fig. 3.1 above). As listed in Table 3.1, all RAFT S/p-BrS copolymers show closely similar molar Kerr constants, irrespective of their comonomer sequences.

Table 3.1 Comparison of Kerr Constants Measureda for S/p-BrS Copolymers Synthesized by RAFT and ATRP Controlled Radical Polymerizations

Sample name	Mole fraction of *p-BrS* in S/*p-BrS* copolymer	Method of comonomer addition	Comonomer addition rate (mL/min)	Slopes of solution Kerr Constants x 10^{16}, $V^{-2}m$, vs concentration	Relative $_mKs$
Poly (*statistical*-S/*p-BrS*)					
ATRP	**Targeted feed ratio**	**Simultaneous**	**NA**	**2**	**0.9**
S-50-I	50%	Simultaneus	NA	2.8	1.25
S-50-II FRP	Targeted feed ratio: 50:50.)	Simultaneous uncontrolled, AIBN	NA	2.7	1.16
Poly ("*gradient*"-S/*p-BrS*)					
ATRP	**Targeted feed ratio 50:50**	**Gradient with syringe pump**	**0.002**	**1.2**	**0.5**
G-48-I	48%	Gradient with Hand syringe	0.014	2.2	1.0
G-47 RAFT	47%	"	0.025	2.5	1.16
G-35 RAFT	35%	"	0.007	2.7	1.16
G-48-II RAFT	48%	Gradient with syringe pump	0.014	2.6	1.25
G-32 RAFT	32%	"	0.033	2.3	1.06

[a] Measured in 1,4-dioxane (>99% purity) solutions (1–3 wt %) at 293 K.

Based on our previous Kerr effect studies[7] of S/p-BrS copolymers obtained by bromination of atactic PS in good and poor solvents, we had expected that a gradient sequence of comonomers with a similarly atactic stereosequence would produce mKs considerably smaller and somewhat larger, respectively, than those observed for atactic random/statistical and blocky S/p-BrS copolymers.

A comparison of experimental and calculated mKs of random, blocky, and gradient samples of S/p-BrS copolymers obtained by brominations of a-PS and RAFT copolymerizations led us to the tentative identification of an unexpected macrostructural element/feature introduced during our controlled radical RAFT syntheses of intimate S/p-BrS copolymers, that is, a stereosequence gradient characterized by changing population of r and m diads from one chain end to the other, which parallels their gradient comonomer sequence (cf. Fig. 1).

As the population of p-BrS units decreases along the chain, the population of r diads appears to also decrease. This is a particularly important, result, because in the usual uncontrolled free-radical initiated polymerizations of S and p-BrS, the resulting homopolymers [PS and P(p-BrS)] are found to have nearly ideally random stereosequences characterized by $Pr \approx Pm \approx 0.5$.[19-23]

Two random S/p-BrS copolymers, both with 50:50 S:p-BrS compositions, were also synthesized, one by RAFT and the other by conventional free-radical polymerizations. Much like the random and blocky S/p-BrS copolymers produced by bromination in solvents of different quality for PS,[7] their thin films showed distinct dewetting behaviors. While the random RAFT S/p-BrS film did not dewet from a silica surface after 2 days of annealing above

Tg at 150 °C, the random S/p-BrS film prepared from samples synthesized by free-radical polymerization did (See Fig. 3.2).

While the random RAFT S/p-BrS film did not dewet from a silica surface after 2 days of annealing above Tg at 150 °C, the random S/p-BrS film prepared from samples synthesized by free-radical polymerization did (See Fig. 3.2).

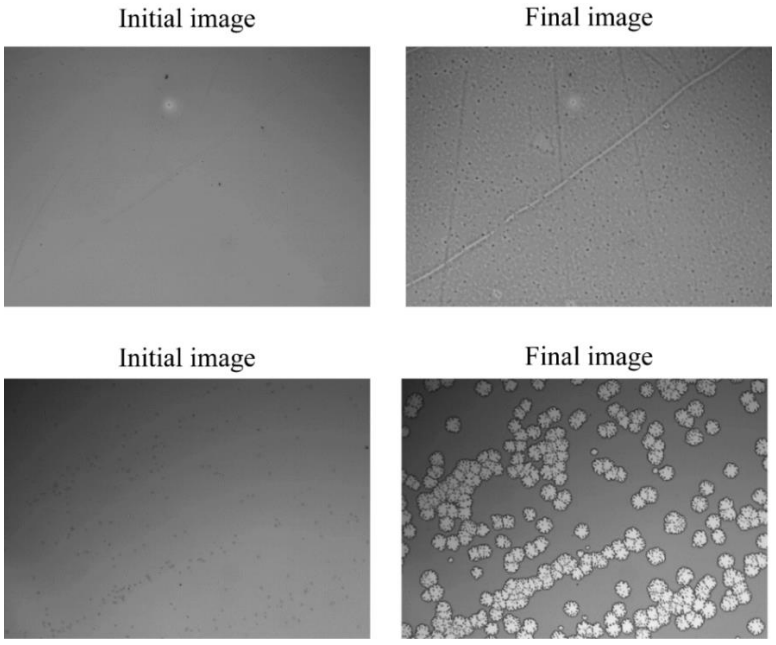

Figure 3.2 Dewetting of random 50:50 S:p-BrS copolymer films made by controlled RAFT (top) and unconctrolled free-radical (bottom) polymerizations.

This suggests that, as previously observed for random and blocky samples of atactic S/p-BrS copolymers,7 the micro- and macrostructures of these samples differ. In the case of the uncontrolled and controlled (RAFT) free-radically synthesized 50:50 random copolymers, this difference can only originate from different locations of their stereosequences.

Racemic (r) p-BrS--p-BrS diads substantially populate[8] the extended trans–trans backbone conformation, which places both brominated side-chain phenyl rings on opposite sides of the extended backbone plane, with both up or both down, as demonstrated in Figure 3.3. In contrast, in meso (m) p-BrS--p-BrS diads the extended trans–trans backbone conformation is not substantially populated, while those conformations that are more heavily populated are not extended with parallel brominated phenyl rings either on the same or opposite sides of the backbone plane.

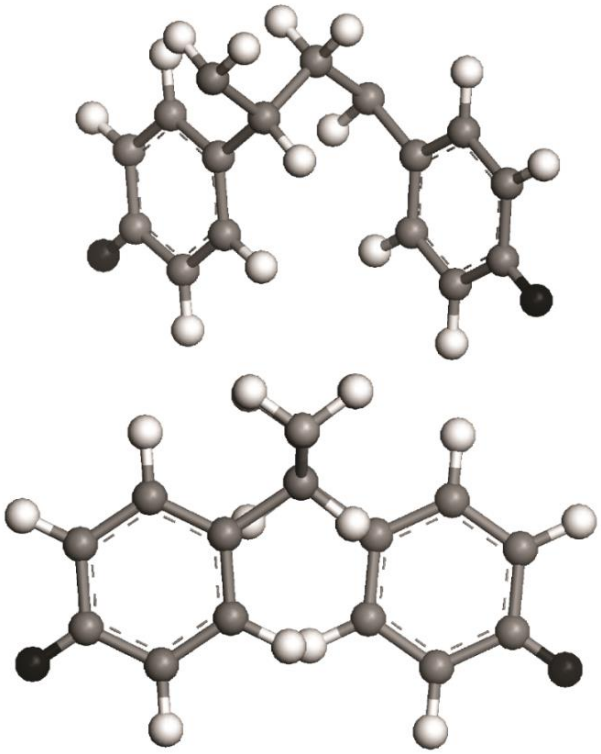

Figure 3.3 Along backbone end-view (bottom) and ~45° from full frontal-view (top) of a r-p-BrS-p-BrS diad.

Our Kerr effect observations strongly suggest that RAFT synthesized copolymers do and the uncontrolled conventionally synthesized free-radical copolymers do not have predominantly racemic p-BrS--p-BrS diads. p-BrS--p-BrS diads, which are substantially populated by the trans–trans backbone conformation, tend to place both brominated phenyl rings on opposite sides of the backbone plane in a position to interact strongly with the silicon surface. So possibly, as observed, the RAFT random copolymer film should be stickier. Clearly, the adherence of S/p-BrS films to silicon substrates depends not only upon their comonomer sequences (blocky stickier than random)[7] but also observed here for random copolymers, also upon their stereosequences, with r p-BrS-p-BrS diads apparently stickier than m p-BrS-p-BrS diads. This micro- and macro-structural detail cannot be obtained from short-range spectroscopic probes, such as ^{13}C-NMR, which is currently the method of choice for characterizing the microstructures of polymers.

To further examine the suggestion that in the controlled RAFT synthesis of S/p-BrS copolymers with a gradient comonomer sequence a correlated stereosequence gradient was introduced,[24-26] we used ATRP[27] to obtain random and gradient samples. ATRP, is known to yield polymers with atactic stereosequences similar to conventional uncontrolled free radical polymerization, with the radical nature of propagation yielding equal m and r addition of monomers.[28, 29] Thus, we assume that both gradient and random/statistical S/p-BrS copolymers obtained by ATRP are atactic. We measured their molar Kerr constants (see Fig. 3.4), and present (in bold) and compare them in Table 3.1 to the Kerr constants measured for the RAFT S/p-BrS copolymers.

Unlike the RAFT samples, the gradient S/p-BrS copolymer obtained by ATRP has a much smaller Kerr constant than the random S/p-BrS copolymer obtained by ATRP, as expected if both have atactic stereosequences (Also see previous discussion of atactic random and blocky S/p-BrS copolymers obtained by bromination of atactic PS in solvents of different quality[7]).

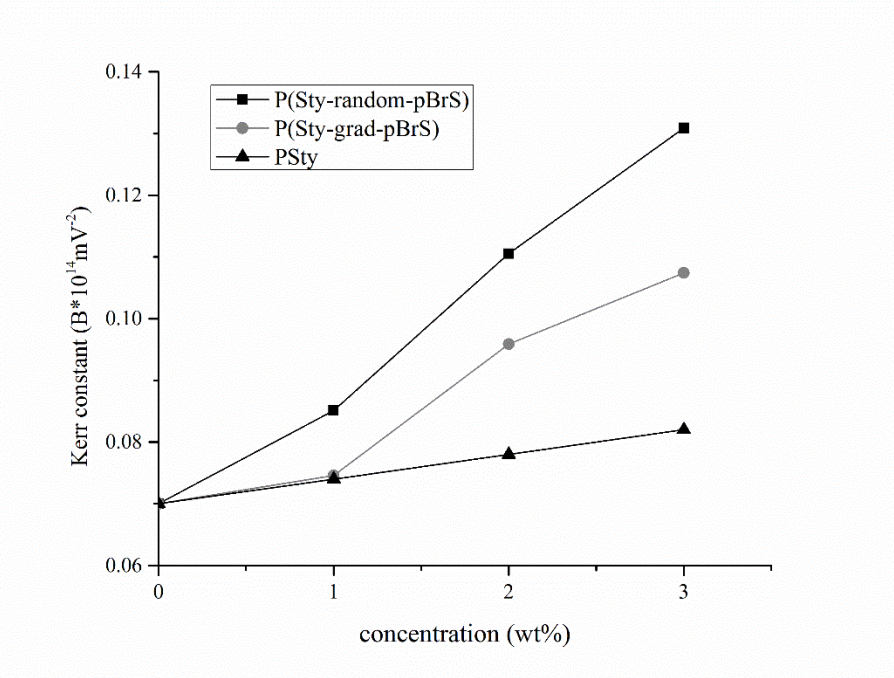

Figure 3.4 Kerr constants of PS (commercial), poly(random-S/p-BrS), and poly("gradient"-S/p-BrS) by ATRP as measured on (1–3 wt %) 1,4-dioxane (>99% purity) solutions at 293 K.

In addition, though not shown here, both ATRP produced 50:50 S: p-BrS films began dewetting from silicon surfaces almost immediately after annealing above their Tg at 150 °C (see Fig. 2 and related discussion). However, the gradient sample remained on the silicon

surface much longer than the random sample. These film dewetting observations are consistent with those seen for atactic random and blocky S/p-BrS samples obtained by bromination in solvents of different qualities for PS.[7] The comparison of both Kerr constants and film dewetting behaviors reinforces the conclusion that in the RAFT and ATRP syntheses of S/p-BrS copolymers enchainment of r p-BrS-p-BrS diads is and is not preferred, respectively, over their m counterpart.

In fact, very recently Ishitake et al.[26] have demonstrated by means of RAFT copolymerization that methacrylic acid (MAA) homo- and co-polymers possessing a stereosequence gradient may be achieved. This was accomplished through copolymerization with bulky esters of MAA, such as triphenylmethyl methacrylate (TrMA), which react more slowly than MAA to produce MAA/TrMA copolymers with a gradient comonomer sequence. The MAA- and TrMA-rich sequences were created by disparate comonomer reactivity ratios and adjustment of the comonomer feeds. The stereosequences in the TrMA- and MAA-rich regions were found to be largely isotactic and atactic, respectively. Furthermore, meso (m) TrMA diads were preferentially formed, resulting in MAA/TrMA copolymers with gradients in both comonomer sequence and stereosequence. According to Ishitake et al.,[26] "…the stereogradient structure is a result of the propagation–depropagation equilibrium, which can convert a less thermodynamically stable growing terminus with a racemic (r) conformation into the more stable meso (m) form." Finally, removal of the triphenylmethyl groups produced MAA homopolymers with a stereosequence gradient that varied from syndiotactic to isotactic (i.e., mm = 11–100%) from one end of the chains to the other.

The fact that Kerr effect measurements are not only sensitive to comonomer stereosequences, but also their locations along the polymer chains suggest the promise of this technique to further probe the mechanistic underpinnings of polymerizations capable of achieving stereocontrol. Because of this capability, we observed that RAFT polymerizations carried out under conditions that led to gradient S/p-BrS copolymers also had a gradient of stereosequences along the chain.

Although invisible to NMR, this Kerr effect observation indicated stereo-control during a controlled radical polymerization without external additives (e.g., Lewis acids). This effect is surprising, and serves as a perfect example of the promise of Kerr effect measurements for elucidating specific characteristics of polymerization mechanisms undetectable by more traditional techniques.

We will further exploit the Kerr effect to probe RAFT gradient copolymerizations. Gradients of various overall comonomer ratios will be prepared to investigate if the stereosequence control is dependent on copolymer feed and/or copolymer composition. Additionally, the percentage of racemic and meso diads present in polymers prepared by radical polymerization is known to depend on polymerization temperature. We will conduct RAFT polymerizations of S and p-BrS at temperatures ranging from room temperature to 110 °C by using initiators and RAFT agents amenable to the chosen temperatures.

To further confirm the ability of Kerr effect measurements to provide information regarding stereosequence control and locations along polymer chains, we will prepare copolymers with well-defined gradients ensured by the slow addition of Lewis acids known to interact with methacryloyl monomers, thereby leading to stereocontrol. By purposely

installing stereosequences at specific locations, we will be able to compare the observed mKs of gradient copolymers of known stereosequences to their calculated values.

We also measured the Kerr constants for 50:50, 20:80, 80:20, and an equal mixture of the 20:80 and 80:20 random atactic S:p-BrS copolymers obtained by conventional free radical polymerization to see if the 50:50 and equal mixture of 20:80, and 80:20 random S:p-BrS copolymers have distinct Kerr constant as the data shown in Figure 3.5 suggests they should. The 50:50 copolymer showed a Kerr constant larger than that of an equal mixture of the 20:80 and 80:20 copolymers in agreement with the expected Kerr constants shown in Figure 3.5.

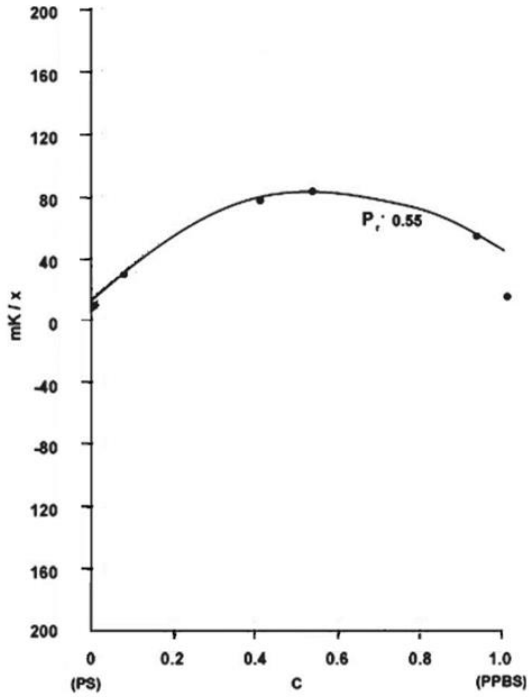

Figure 3.5 Comparison of $_m$Ks (×10−1 cm7 SC−2 mol−1) observed and calculated for atactic S/pBr copolymers made by bromination of a-PS.[6] x, c, and Pr are the number of repeat units (200) and the fractional contents of p-BrS units and racemic or r-diads, respectively.

Thus, it appears the Kerr effect can distinguish between samples with polymer chains that all have the same microstructures from those with a heterogeneous distribution of microstructures, but with the same overall sample average local microstructures, which of course cannot be distinguished by NMR or other spectroscopies with short-range sensitivity to microstructures.

3.4.2 Kerr Effects and Macrostructures of Additional Polymers

Can the interactions/associations between polymers be detected by the Kerr effect? Kerr constants were measured for separate and combined solutions of i- and s-PMMAs in solvents where they do (tetrahydrofuran (THF)) and do not (Dioxane) form 2:1 s-PMMA:i-PMMA complexes.[11] In the complexing solvent, the Kerr constant observed for a 2:1 s-PMMA:i-PMMA mixture was very different from a 2:1 weighting of the Kerr constants observed for neat s- and i-PMMAs. On the other hand, in a noncomplexing solvent the Kerr constant observed for a 2:1 s-PMMA: i-PMMA mixture was very similar to a 2:1 weighting of their neat Kerr constants observed in this solvent. This provides a clear demonstration of the sensitivity of the Kerr effect to strongly interacting/complexing polymers in solution.[11]

Recently, Lee and Bates[9] synthesized random and alternating multiblock copolymers of styrene and butadiene (S/B) that are illustrated in Figure 3.6. Aside from their overall compositions, NMR was unable to differentiate between their random and alternating block sequences. Their Kerr constant measured in dilute dioxane solutions were observed to be distinct, as can be seen in Figure 3.6. So while NMR does not distinguish between samples

with random and with regularly alternating multiblock sequences, the Kerr effect is clearly able to.

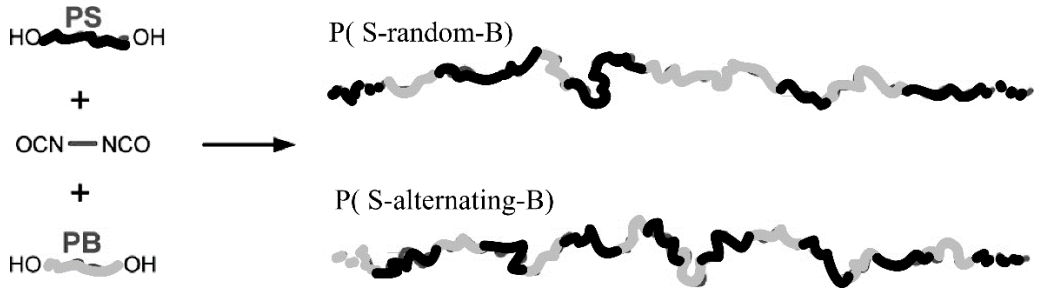

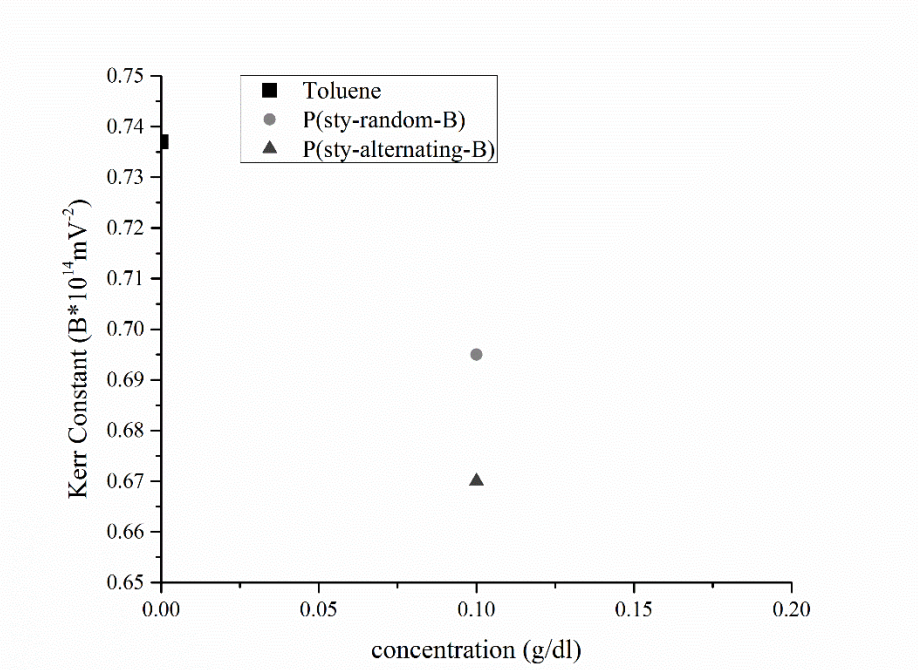

Figure 3.6 Structures and Kerr constants of 0.1 g/dL toluene solutions of styrene/butadiene multiblock copolymers with random and regularly alternating blocks[9].

"Precision linear vinyl acetate/ethylene (VAE) copolymers containing acetoxy groups on precisely every eighth backbone carbon were synthesized by ring-opening metathesis polymerization (ROMP) of racemic 3-acetoxycyclooctene (3AcCOE) and subsequent hydrogenation. The use of enantiomerically pure 3AcCOE resulted in an optically active polyalkenamer that afforded isotactic precision VAE materials after hydrogenation. In contrast, analogous linear VAE copolymers derived from ROMP−hydrogenation of racemic 4- or 5-acetoxy cyclooctenes were regioirregular."[10] Kerr constants were measured for the precise and random VAE copolymers that are atactic and precise VAE copolymers that are atactic or isotactic, all having the same comonomer composition. As seen in Figure 3.7, atactic precise regioregular and atactic random regioirregular VAE samples have the same Kerr constants, while for the regioregular samples the precise isotactic sample has a Kerr constants of opposite sign, with a magnitude nearly 10-fold greater than the atactic precise sample.[10] This large difference is not likely due to the optical activity of the precise isotactic sample, which has a nearly 0° (E = 0 volts) optical rotation.

Thus, though NMR or optical activity observations cannot, Kerr effect observations can easily distinguish the isotactic and atactic regioregular precise VAE samples of Hillmyer and coworkers.[10] Once again this emphasizes that the sensitivity of the Kerr effects is sufficient to readily identify longer range polymer microstructures and their locations along the chain to delineate complete polymer macrostructures.

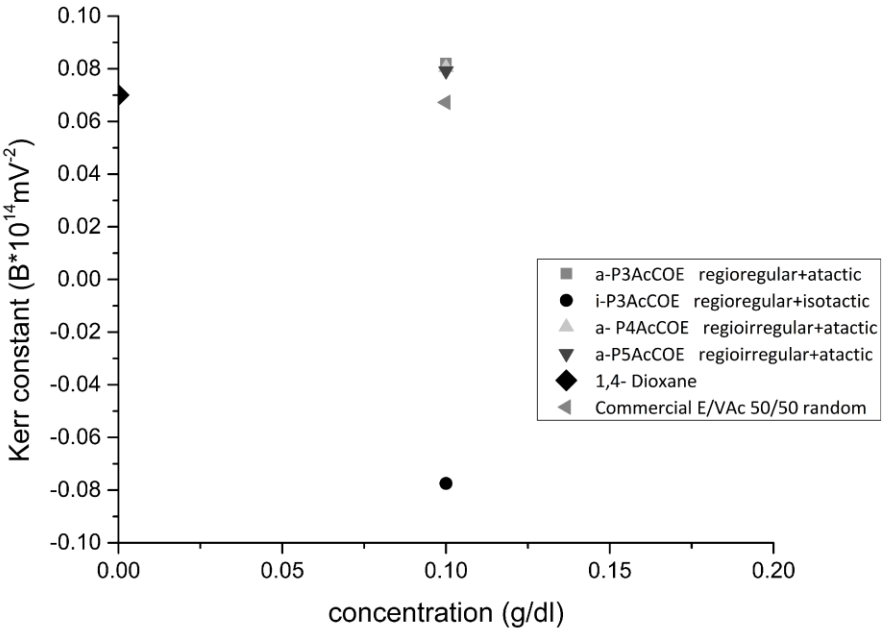

Figure 3.7 Kerr constants of 0.1 g/dL dioxane solutions of E/VAc samples.[10]

In each of the above instances, measured Kerr constants were able to distinguish between and help identify the distinct macrostructures of and interactions between these co- and homo-polymers.

Finally, to increase the practicality of characterizing synthetic polymer macrostructures, we suggest[30] coupling of NMR spectroscopy[1, 2] with Kerr effect observations. Although not for the S/*p-BrS* copolymers discussed here, NMR can usually reveal the types and amounts of short-range microstructures present in synthetic polymers. Kerr effect observations can then be used to locate the NMR-derived microstructures along the polymer chains. This is achieved by comparison of observed molar Kerr constants to those calculated for different distributions/locations of constituent microstructures identified by NMR. The

distribution of microstructures used to calculate an $_{m}\mathbf{K}$ in agreement with the observed value is then identified as its likely macrostructure.

Not using the ^{13}C-NMR-Kerr effect combined approach would require the calculation of Kerr constants for all possible macrostructures and comparing them to the value observed. Because the numbers of distinct synthetic polymer macrostructures are astronomically large, this approach is not practical.

We must instead reduce the potential macrostructures to a manageable number, and ^{13}C-NMR can help us achieve this by identifying and quantifying the constituent short-range microstructures that are present. With this information in hand, we then move them around to locate them at different positions along the polymer chain. The Kerr constants expected for each of this much more manageable number of polymer macrostructures are calculated, compared with the observed value, and, when they agree, are identified as the (those) most likely macrostructure(s).

3.5 Conclusions

In summary, we have called attention to the importance of recognizing that the macrostructures of synthetic polymers are critical to understanding their behaviors, and so their characterization is important. Only a probe that is similarly dependent on the complete macrostructures of polymers can be used to characterize them. It appears that Kerr effects measured in dilute polymer solutions may be sufficiently sensitive to not only determine the types and quantities of microstructures that are present but also to locate their positions along their macromolecular backbones, thereby allowing a more complete description of their

macrostructures. In light of the many recent developments[31] in polymerizations that purportedly produce polymers with elaborate and precise architectures, the ability to experimentally determine and verify their expected macrostructures becomes even more urgent.For example, a recent paper "How Far Can We Push Polymer Architectures"[32] describes the *tour de force* synthesis of the "bottle brush" polymer shown in Figure 3.8.

The authors state "With this study the frontiers in polymer synthesis, molecular analysis, and three-dimensional architectures of polymers are pushed forward, while at the same time the limitations in this endeavor are made clear.

Although all analytical results are in agreement with the structures assigned to structures 4 and 5 (See Fig. 3.8), it should be noted that their syntheses is approaching the limits of today's polymer synthesis and analysis techniques. Hence, deviations in end groups by transfer processes and the presence of small amounts of homo- and co-polymers cannot be excluded, while complete assignment of the NMR spectra of our brush polymers is impossible as well." This means that the tacticities of their constituent block copolymers, numbers, lengths, and distributions of grafted *n*-butyl acrylate brush bristles, and the degree and distribution of functionalized protected 2-(trimethylsiloxy)ethyl methacrylate units in the bottle brush tail, which upon UV exposure permits intramolecular hydrogen-bonding and self-assembly, remain uncharacterized. In other words, the macrostructure of this *tour de force* example of macromolecular architecture remains incompletely characterized, because of the limitations of conventional analytical techniques. Kerr effect examination of the intermediate products of their syntheses would aid in their characterization and possibly lead to characterization of the complete macrostructure of the final bottle brush polymer product.

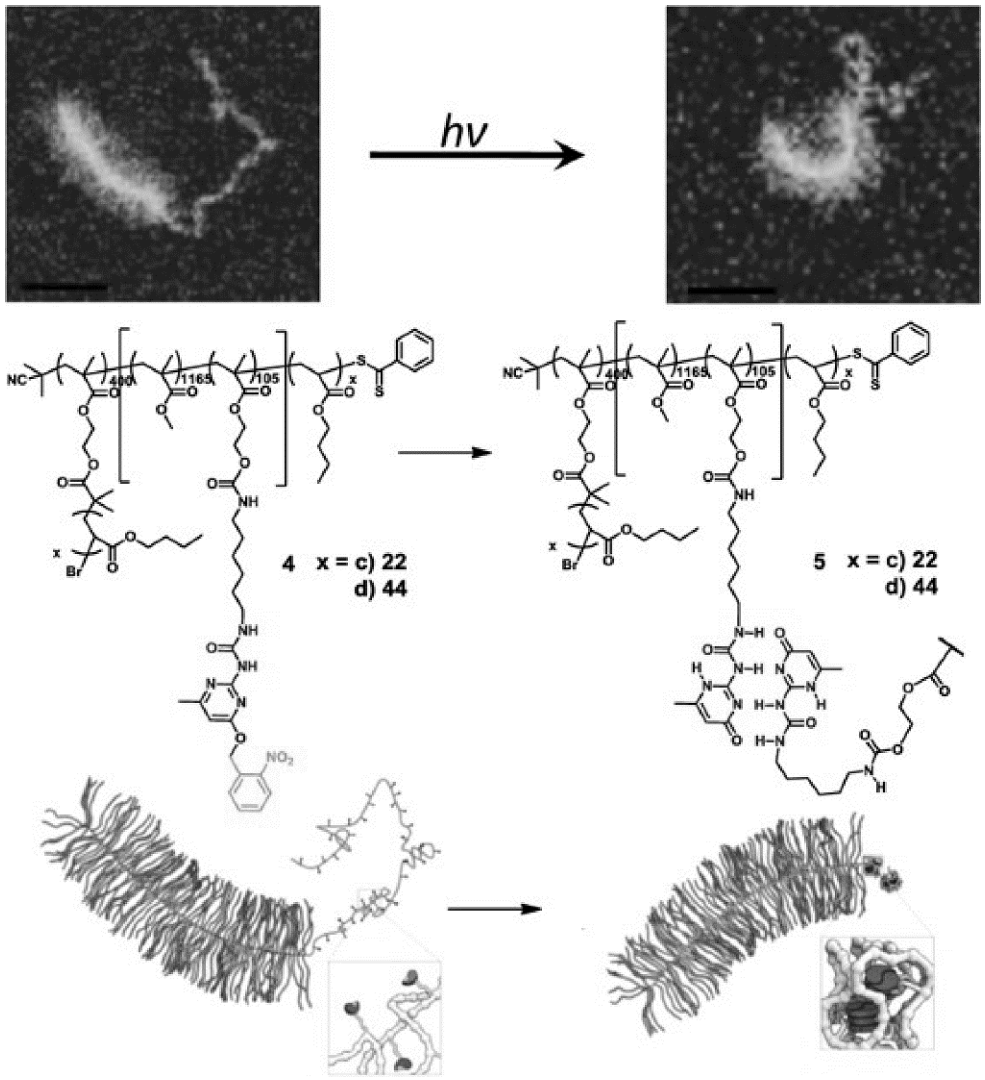

Figure 3.8 Polymer structures 4(c,d) and 5(c,d) including representative AFM height micrographs of 4d (top left) and 5d (top right) (scale bar = 50 nm). Schematic representation of the polymer structures on the mica surface (bottom) (From P. J. M. Stals et al., J Am Chem Soc, 2013, 135, 11421–11424, with permission from the American Chemical Society).

3.6 Experimental

3.6.1 Materials

Styrene (Aldrich, 99%) and 4-bromostyrene (Aldrich, 98%) were passed through a column of basic alumina before use. 2,2′-Azobis(isobutyronitrile) (AIBN) (Aldrich, 98%) was recrystallized from ethanol. 2-(1-Carboxy methylethylsulfanyl-thio-carbonylsulfanyl)−2-methylpropionic acid (CMP) and 2-dodecylsulfanylthio-carbonyl-2-methylproprionic acid (DMP) chain transfer agents (CTAs) were prepared as previously reported. 1,3,5-Trioxane (Acros, 99.5%), *N*,*N*-dimethylformamide (DMF) (Aldrich, 99.9%), THF (Malinckrodt, 99%), anisole (Aldrich, 99%), and methanol (Aldrich, 99%) were used as received.

3.6.2 Instrumentation and Analyses

3.6.2.1 Nuclear Magnetic Resonance

Proton nuclear magnetic resonance spectroscopy (^{1}H NMR) was used to evaluate polymerization reaction kinetics and to confirm the chemical composition of the resulting copolymers. The spectra were obtained with a Bruker Advance 400 Spectrometer operating at 400 MHz; the analyses were performed in $CDCl_3$. Inverse gated decoupling ^{13}C NMR spectroscopy was used to characterize the chemical composition of the copolymers. The spectra were obtained with a JEOL Spectrometer operating at 500 MHz; the analyses were performed from concentrated solutions of the compounds in $CDCl_3$.

3.6.2.2 Elemental Analysis

Elemental analysis (EA) was employed as a measure of chemical composition for the copolymers synthesized. Elemental analyses were performed by Atlantic Microlab, Atlanta, GA.

3.6.2.3 Size Exclusion Chromatography

Size exclusion chromatography (SEC) was used to characterize the molecular weights of the S/*p-BrS* copolymers. The instrument was equipped with a Waters 2695 separations module, a light scattering detector (MiniDawn, Wyatt Technology Co.) and a differential refractive index detector (Optilab Rex, Wyatt Technology Co.), and used a Styrogel HR 4 column. Conventional calibration was done using nine PS standards from Fluka. Samples were filtered through 0.2-μm PTFE syringe filters. THF was used as an eluent solvent at the flow rate of 0.3 mL min^{-1} at room temperature. The results are reported as number average molecular weight (M_n) and polydispersity (M_w/M_n).

3.6.2.4 Kerr Effect Measurements and Calculations

A schematic diagram of the components essential for Kerr effect measurements is presented in the figure below. A state-of-the-art Kerr effect instrument has recently been constructed in our laboratory. We purchased a custom built Kerr effect instrument from Hinds Instruments (Hillsboro, OR). The light source is a 5 mW He—Ne laser, which passes through a polarizer and photoelastic modulator and the polarizer is oriented 45° relative to the photoelectric modulator or PEM. The detection system, explained in detail elsewhere, [38] consists of two Si

photodetectors behind either a −45 or 0° polarizer to measure the magnitude and orientation of the retardation in the sample.

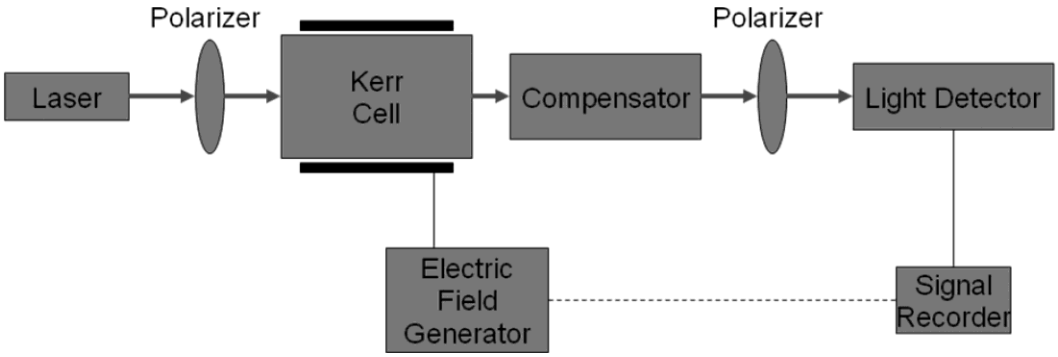

The sample cell consists of two parallel, stainless steel electrodes 15 cm in length, with a cell gap of 2.5 mm maintained by Teflon spacers. The cell windows are made of low-birefringence glass supplied by Hinds Instruments. The instrument contains a high voltage source with an analog control system to obtain the high electric field strengths. Raw data is recorded on a computer through a custom control program supplied by Hinds Instruments, and, for a given sample, data points are collected every 100 ms. The pertinent data recorded for Kerr constant calculations are the retardation (Δn) and voltage.

The Kerr effect of a given copolymer sample was measured at a series of different weight fractions in solution (e.g., C = 0.5, 1.0, and 2.0 w/w %). The Kerr constant of the solution, B, is calculated from the relationship $\Delta n = \lambda B E^2$, where $\lambda = 633$ nm and was averaged over the values observed for applied voltages of 10–12 kV.

Because the triblock and gradient/random S/p-BrS samples under consideration here have similar compositions, we expect refractive index, density, and dielectric constant to remain approximately constant between sample pairs. As such, the ratio of mKs for a sample pair depends on the ratio of slopes of their B versus C plots.

In addition, a refractometer operating at the same wavelength as the Kerr-Effect instrument and a dielectric meter are also necessary components for measuring refractive indices and dielectric constants of the dilute polymer solutions. These are necessary to evaluate their absolute molar Kerr constants and have been obtained to accompany our Kerr effect instrument. Measurements of the Kerr effect were made on polymer solutions (0.5–3% w/w) in 1,4-dioxane (>99% purity from Sigma-Aldrich), THF (>99% purity from Sigma-Aldrich), or Toluene (>99% purity from Sigma-Aldrich) at 293 K.

In a few cases where the Kerr effect of the same sample in Table 3.1 was repeatedly measured, the Kerr constants derived from them varied no more than ~10%.

In the calculation of molar Kerr constants, we considered S/p-BrS copolymers with 300 total comonomer units. For each distinct comonomer composition, comonomer sequence, and tacticity or stereosequence a sample of at least 50 copolymer chains were generated using a commercial random number generator and our own FORTRAN algorithms. Each copolymer chain was built one comonomer unit at a time, with account taken of both the type of comonomer added and with which stereosequence (m or r diad, relative to the previous unit added). Further details of the mK calculations for S/p-BrS copolymers can be found in refs. 3, 4, 6, 7, and 13.

3.6.3 Polymer Syntheses

3.6.3.1 PS-b-p-BrS-b-PS Triblocks

An example synthesis of the triblock copolymers by RAFT polymerization of styrene (S) and *p*-bromostyrene (*p-BrS*) with CMP was conduced as follows. S (4.09 g, 39.3 mmol), CMP (55.5 mg, 0.196 mmol), AIBN (13 mg, 0.079 mmol), trioxane (110 mg, internal NMR standard), and DMF (1.0 mL) were placed in a sealed 20 mL glass vial equipped with a magnetic stir bar. The air space above the reaction solution was purged with nitrogen for 10 min, and the solution was then sparged with nitrogen for an additional 15 min. The vial was placed in a preheated reaction block at 75 °C. Kinetic samples were removed periodically via a nitrogen-purged syringe. Monomer conversion was determined by ^{1}H NMR spectroscopy and terminated at 16 h, at 57% conversion. The polymer was diluted in THF and precipitated in cold MeOH (×2), filtered, and vacuum dried at 40 °C (2.13 g). Molecular weight was determined by SEC (M_n = 12,700 g/mol, M_w/M_n = 1.06): PSty$_{\mathbf{59}}$-*b*-PSty$_{\mathbf{59}}$.

An example RAFT copolymerization of a PS macroCTA with *p-BrS* was performed as follows. PS macroCTA (0.48 g, 0.038 mmol), *p-BrS* (2.80 g, 15.3 mmol), AIBN (2.5 mg, 0.015 mmol; 0.45 mL of 5.5 mg/mL AIBN/DMF stock), trioxane (85 mg, internal NMR standard), and DMF (2.0 mL) were placed in a sealed 20 mL glass vial equipped with a magnetic stir bar. The air space above the reaction solution was purged with nitrogen for 10 min, and then the solution was sparged with nitrogen for an additional 15 min. The vial was placed in a preheated reaction block at 75 °C for 16 h. The polymerization solution was quenched in an ice bath. To isolate the copolymer, the reaction solution was diluted with THF, precipitated in cold MeOH, filtered, and vacuum dried at 40 °C (1.61 g). Molecular weight of

the isolated/dried polymer was determined by SEC (M_n = 45,400 g/mol, M_w/M_n = 1.2): S_{59}-*b*-*p*-*BrS*$_{79}$-*b*-*p*-*BrS*$_{79}$-*b*-S_{59}.

3.6.3.2 P(S-stat-p-BrS) Copolymers—Conventional

An example conventional (uncontrolled) statistical copolymerization (stat) of S and *p*-*BrS* was performed as follows. S (1.36 g, 13.1 mmol), *p*-*BrS* (2.40 g, 13.0 mmol), AIBN (8.7 mg, 0.053 mmol), and trioxane (98.2 mg, internal NMR standard) were placed in a 20 mL glass vial equipped with a magnetic stir bar. The air space above the reaction solution was purged with nitrogen for 10 min, and the solution was then sparged with nitrogen for an additional 15 min. The solution was placed in a preheated reaction block at 75 °C and proceeded for 2 h. To isolate the copolymer, the reaction solution was diluted with THF, precipitated into cold MeOH (×2), filtered, and vacuum dried at 40 °C (1.21 g). Molecular weight of the isolated polymer was determined by SEC ((M_n = 47,920 g/mol,M_w/M_n = 1.7).

3.6.3.3 P(S-stat-p-BrS) Copolymers—RAFT

An example RAFT statistical copolymerization of S and *p*-*BrS* was performed as follows. S (1.36 g, 13.1 mmol), *p*-*BrS* (2.40 g, 13.0 mmol), AIBN (8.6 mg, 0.052 mmol), DMP (47.8 mg, 0.131 mmol), trioxane (99 mg, internal NMR standard), and DMF (1 mL) were placed in a 20 mL glass vial equipped with a magnetic stir bar. The air space above the reaction solution was purged with nitrogen for 10 min, and then the solution was sparged with nitrogen for an additional 15 min.

The solution was placed in a preheated reaction block at 75 °C. Kinetic samples were removed periodically via a nitrogen-purged syringe. Monomer conversion was determined by ^{1}H NMR spectroscopy, comparing the area of the anisole and trioxane signals to the vinyl protons of the residual monomer (8 h, 64%). To isolate the copolymer, the reaction solution was diluted with THF, precipitated into cold MeOH (×2), filtered, and vacuum dried at 40 °C (0.76 g). Molecular weight of the isolated polymer was determined by SEC (M_n = 9296 g/mol, M_w/M_n = 1.1).

3.6.3.4 P(S-grad-p-BrS) Copolymers—RAFT

Gradient copolymerization of S and *p-BrS* were synthesized via RAFT with varying ratios of *p-BrS* (Table 3.1) using either a free-syringe (hand syringe) (**G-48-I**, **G-47**, **G-35**) or a syringe pump (**G-48-II**, **G-32**) method. The polymerizations were conducted as follows. A stock solution of *p-BrS* was purged with nitrogen for 30 min before the reaction. S (1.37 g, 13.1 mmol), AIBN (4.4 mg, 0.027 mmol), DMP (24.1 mg, 0.066 mmol), trioxane (85.9 mg, internal NMR standard), and DMF (1.0 mL) were placed in a sealed 20 mL glass vial equipped with a magnetic stir bar. The air space above the reaction solution was purged with nitrogen for 10 min, and then the solution was sparged with nitrogen for an additional 15 min. The vial was placed in a preheated reaction block at 75 °C. The *p-BrS* was then either drawn into a purged 1 mL syringe, inserted into the septum of the reaction vial for the free-syringe method or a purged syringe of *p-BrS* was secured on a syringe pump with a 22-gauge needle inserted into the septum of the vial for the syringe pump method. *p-BrS* was then added at various rates over a period of 2 h and stirred for an additional 3 h after addition was complete. To isolate

the copolymer, the reaction solution was diluted with THF, precipitated into cold MeOH (×2), filtered, and vacuum dried at 40 °C (1.14 g). Molecular weight of the isolated polymer was determined by SEC (**G-48-I** M_n = 12,850 g/mol, M_w/M_n = 1.2, **G-47** $\boldsymbol{M_n}$ **= 13,020 g/mol**, $\boldsymbol{M_w/M_n}$ **= 1.2**, **G-35** $\boldsymbol{M_n}$ **= 27,202 g/mol**, $\boldsymbol{M_w/M_n}$ **= 1.13**) or a syringe pump (**G-48-II** $\boldsymbol{M_n}$ **= 7057 g/mol,** $\boldsymbol{M_w/M_n}$ **= 1.1**, **G-32** $\boldsymbol{M_n}$ **= 8074 g/mol,** $\boldsymbol{M_w/M_n}$ **= 1.2**).

3.6.3.5 P(S-random-p-BrS) Copolymers—ATRP

S (>99%, Aldrich) was passed through basic alumina column and *p-BrS* (>99%, Aldrich) was distilled (b.p. = 88 °C at 15 mmHg) before use. Phenylethyl bromide, 1-PEBr (>99%, Aldrich), Cu(I)Br (>99%, Aldrich), *N*,*N*,*N*′,*N*″,*N*″-pentamethyldiethylenetriamine, PMDETA, (>99%, Aldrich), and diphenyl ether (≥99%, Aldrich) were used as received.

A typical procedure of ATRP was performed for Random copolymerization of S and *p-BrS*.[33, 34] Cu(I)Br (62.5 mg, 0.435 mmol) was placed in a 25-mL Shlenk flask equipped with a magnetic stir bar under ambient conditions. PMDETA (0.435 mmol, 90 µL), monomers S (21.75 mmol, 2.25 mg), and*p-BrS* (21.75 mmol, 3.9 mg) were added sequentially and the mixture was stirred for 5 min at 25 °C under N_2. Initiator, 1-PEBr (0.87 mmol, 12 µL) was added. The mixture was degassed by three freeze-pump-thaw cycles. The flask was placed in a preheated (100 °C) oil bath. ([Monomer]:[1-PeBr]:[Cu(I)Br]:[PMDETA] = 100:0.2:1:1)

After 24 h, the polymerization reaction was stopped by exposing the reaction mixture to the air. The polymer was dissolved in THF and was introduced to 250 mL Erlenmeyer flask filled with basic alumina in order to remove metal catalyst, Cu(I)Br. The beaker was placed in orbital shaker for 1 day. Polymer was filtered, the excess amount of THF was removed by

rotary evaporation then the polymer was precipitated into cold MeOH (×10), filtered, and vacuum dried at 25 °C. Precipitation was repeated until a white polymer powder was produced. Molecular weight of the isolated polymer was determined by SEC (M_n = 159,773 g/mol, M_w/M_n = 1.25).

3.6.3.6 Synthesis of Poly ("gradient"-S/p-BrS)—ATRP

Gradient copolymers were prepared via a semi-batch copolymerization using ATRP, as described by Matyjaszewski et al.[35] Cu(I)Br (62.5 mg, 0.435 mmol) was placed into a 25-mL Shlenk flask equipped with a magnetic stir bar. PMDETA (0.435 mmol, 90 µL), solvent diphenyl ether[36] (2.5 mL, $V_{solvent}/V_{styrene}$ = 1/1), and S (21.75 mmol, 2.25 mg) were added, respectively, and then the mixture was stirred for 5 min under N_2.[37] Initiator 1-PEBr (0.87 mmol, 12 µL) was added. The mixture was degassed by three freeze-pump-thaw cycles then sealed. The flask was placed in a preheated (100 °C) oil bath.
([Monomer]:[1-PeBr]:[Cu(I)Br]:[PMDETA] = 100:0.2:1:1)

Simultaneously, *p-BrS* was introduced into a 25 mL reaction tube and degassed by three freeze-pump-thaw cycles. Then, *p-BrS* was transferred into an airtight syringe and fixed to a syringe pump. The syringe pump was programmed to deliver 2.80 mL at a rate of 2 µL/min. The reaction was stirred for 24 h after the *p-BrS* addition was completed. The total reaction time was 46 h and 30 min. The polymerization reaction was stopped by exposing the reaction mixture to air. The polymer was diluted with THF and was introduced into a 250 mL Erlenmeyer flask filled with basic alumina in order to remove the metal catalyst, Cu (I) Br. The beaker was placed in an orbital shaker for one day. Polymer solution was filtered, the

excess amount of solvent was removed by rotary evaporation, then the polymer was precipitated into cold MeOH (×10), filtered, and vacuum dried at 25 °C. Precipitation was repeated until a white polymer powder was produced. Molecular weight of the isolated polymer was determined by SEC (M_n = 253,330 g/mol,M_w/M_n = 1.03).

3.6.4 Film Dewetting

Dewetting studies of thin S/p-BrS copolymers films were performed on single-side-polished, 300-μm thick, small pieces (1 × 1 cm^2) of silicon wafers which were covered with an ~1 nm self-assembled monolayer (SAM) of 1H,1H,2H,2H-perfluoro-decyltrichlorosilane. Decoration of the SAMs on silicon wafers was performed as described previously.[7, 39] Slicon wafers were placed into an ultraviolet/ozone cleaner for 30 min in order to produce -OH groups on the surface. A small drop of perfluoromethyldecalin was placed on the bottom of a Petri dish and the silicon wafer was placed above the perfuoro source. The Petri dish was closed and kept at room conditions for 20 min. The wafer was taken out of the Petri dish, washed with ethanol and dried with nitrogen.[39] The SAM decorated silicon sample thicknesses were measured by ellipsometry before spin-casting the S/pBr copolymer films onto them in order to be sure that the sample surfaces were decorated with the SAM.Copolymer films were placed on the silicon wafers decorated with SAM as described previously.[7]

Thin S/p-BrS copolymer films were spun-cast on glass substrates. They were then floated onto the surface of a deionized water bath, and placed onto the SAM decorated silicon wafers. After drying overnight, the sample thicknesses (~35 nm) were measured by ellipsometry and

annealed under a nitrogen atmosphere at $T - Tg = 35$ °C–150 °C.[15] Dewetting of the S/p-BrS copolymer films was monitored by optical microscopy.

ACKNOWLEDGMENTS

We are grateful to the National Science Foundation for financial support [(A. E. Tonelli), DMR-0966478], to the Army Research Office for a DURIP equipment grant [(J. Genzer and A. E. Tonelli) #53583 CH-RIP] to build a Kerr effect instrument, and to the Hinds Instrument Co., Hillsboro, OR for constructing our Kerr effect instrument. We are indebted to Marc Hillmyer for providing several regioregular and irregular atactic and isotactic VAE copolymer samples, with random or precise comonomer sequences. We also thank Frank Bates for providing us with samples of random and regularly alternating S/B multiblock copolymers.

REFERENCES

1. A. E. Tonelli, *NMR Spectroscopy and Polymer Microstructure: The Conformational Connection*; VCH: New York, **1989**.

2. F. A. Bovey, P. A. Mirau, *NMR of Polymers*; Academic Press: New York, **1996**.

3. A. E. Tonelli, *Macromolecules* **2009**, 42, 3830–3840.

4. S. N. Hardrict, R. Gurarslan, C. J. Galvin, H. Gracz, D. Roy, B. S. Sumerlin, J. Genzer, A. E. Tonelli, *J. Polym. Sci. Part B: Polym. Phys*. **2013**, 51, 735–741.

5. S. B. Bulgarevicha, T. V. Burdastykha, Russ. *J. Gen. Chem*. **2008**, 78, 1069–1082.

6. G. Khanarian, R. E. Cais, J. M. Kometani, A. E. Tonelli, *Macromolecules* **1982**, 15, 866–869.

7. J. J. Semler, Y. K. Jhon, A. Tonelli, M. Beevers, R. Krishnamoorti, J. Genzer, *Adv. Mater*. **2007**, 19, 2877–2883.

8. D. Y. Yoon, P. R. Sundararajan, P. J. Flory, *Macromolecules* **1975**, 8, 776–783.

9. I. Lee, F. S. Bates, *Macromolecules*, **2013**, 46, 4529–4539.

10. J. Zhang, M. E. Matta, H. Martinez, M. A. Hillmyer, *Macromolecules* **2013**, 46, 2535–2543.

11. J. Spevacek, B. Schneider, *Adv. Colloid Interface Sci.* **1987**, 27, 81–150, and references therein.

12. (a) J. Kerr, *Philos. Mag.* **1875**, 50, 416; (b) J. Kerr, *Philos. Mag.* **1879**, 8, 229; (c) J. Kerr, *Philos. Mag.* **1880**, 9, 157; (d) J. Kerr, *Philos. Mag*. **1882**, 13, 248; (e) J. Kerr, *Philos. Mag*. **1894**, 37, 380; (f) J. Kerr, *Philos. Mag*. **1894**, 38, 1144.

13. E. Riande, E. Saiz, *Dipole Moments and Birefringence of Polymers*; Prentice Hall: Englewood Cliffs, NJ, **1992**; Chapter 7.

14. C. G. LeFevre, R. J. W. LeFevre, *Rev*. *Pure Appl. Chem*. **1955**, 5, 261–318.

15. C. G. LeFevre, R. J. W. LeFevre, *In Techniques of Organic Chemistry; A.* Weissberger, Ed.; Interscience: New York, **1960**; Vol. I, Chapter XXXVI.

16. K. Nagai, T. Ishikawa, *J. Chem*. *Phys*. **1965**, 43, 4508–4515.

17. P. J. Flory, R. L. Jernigan, *J. Chem*. *Phys*. **1968**, 48, 3823–3824.

18. P. J. Flory, *Statistical Mechanics of Chain Molecules*; Wiley Inter-Science: New York, **1969**; Chapter IX.

19. (a) H. Sato, Y. Tanaka, K. Hatada, *Makromol. Chem*. *Rapid Commun*. **1982**, 3, 175–179; (b) H. Sato, Y. Tanaka, K. Hatada, *J. Polym*. *Sci. Polym*. *Phys. Ed*. **1983**, 21, 1667–1674.

20. D. L. Trumbo, H. J. Harwood, *Polym*. *Bull.* **1987**, 18, 27–32.

21. A. E. Tonelli, *Macromolecules* **1983**, 16, 604–607.

22. T. Kawamura, N. Toshima, *Makromol. Chem*. *Rapid Commun*.**1994**, 15, 479–486.

23. T. Ko, H. J. Harwood, *Makromol. Chem*. *Rapid Commun*.**1983**, 4, 463–470.

24. N. Cherifi, A. Issoulie, A. Khoukh, A. Benaboura, M. Save, C. Derail, L. Billon, *Polym. Chem*. **2011**, 2, 1769–1777

25. J.-F. Lutz, *Polym. Chem*. **2010**, 1, 55–62.

26. K. Ishitake, K. Satoh, M. Kamigaito, Y. Okamoto, *Polym.Chem*. **2012**, 3, 1750–1757.

27. K. Matyjaszewski, *Macromolecules* **2012**, 45, 4015–4039.

28. J.-F. Lutz, D. Neugebauer, K. Matyjaszewski, J. *Am. Chem.Soc*. **2003**, 125, 6986–6993.

29. Y. Sugiyama, K. Satoh, M. Kamigaito, Y. Okamoto, *J. Polym. Sci. Part A: Polym. Chem*. **2006**, 44, 2086–2098.

30. a) A. E. Tonelli, In *Amer. Chem. Soc. Polymer Chemistry Division Graphical Abstracts*, April 10, **2013**; p 529, Dallas; (b) A. E. Tonelli, In APME 2013 Conference, Durham, UK, August 18–22, 2013.

31. K. Matyjaszewski, *Controlled/Living Radical Polymerization: From Synthesis to Materials;* American Chemical Society, Distributed by Oxford University Press: Washington, DC, **2006**; Chapter 9.

32. P. J. M. Stals, Y. Li, J. Burdynska, R. Nicolay, A. Nese, A. R. A. Palmans, E. W. Meijer, K. Matyjaszewski, S. S. Sheiko, *J.Am. Chem. Soc*. **2013**, 135, 11421–11424.

33. J. Wang, K. Matyjaszewski, *Macromolecules* **1995**, 28, 7901–7910.

34. Available at: http://www.cmu.edu/maty/atrp-how/monomers/styrene.html#styrene. Last accessed on September 17, 2014.

35. K. Matyjaszewski, M. J. Ziegler, S. V. Arehart, D. Gresztab, T. J. Pakula, *Phys. Org. Chem*. **2000**, 13, 775–786.

36. J. Qiu, K. Matyjaszewski, *Macromolecules* **1997**, 30,5643-5648.

37. Y. Zhou, Z. Luo, *Polym*. *Chem*. **2013**, 4, 76–84.

38. B. Wang, T. C. Oakberg, *Rev*. *Sci. Instrum*. **1999**, 70, 3847–3854.

39. J. Genzer, K. Efimenko, D. A. Fischer, *Langmuir* **2002**, 18, 9307–9311.

CHAPTER 4

Characterizing Polymers with Heterogeneous Micro- and Macrostructures

4.1 Abstract

We demonstrate the potentially extreme heterogeneity of polymer micro- and macrostructures and suggest a means for characterizing them. To ensure that all possible microstructures, such as diad stereosequences in vinyl homopolymers and monomer sequences in copolymers, including their locations along polymer chains, i.e. all macrostructures, are represented, it becomes necessary to generate samples with huge quantities (many many tons) of constituent polymer chains. This suggests a practical need for distinguishing between polymer samples with chains that have homogeneous and heterogeneous populations of micro- and macrostructures. We suggest that a combination of high resolution ^{13}C-NMR to determine the types and amounts of constituent short-range microstructures, and dilute solution electrical birefringence or Kerr effect measurements to locate them along the polymer chains, may be able to achieve this distinction. This combination of techniques is required to reduce the innumerably large numbers of different possible polymer macrostructures whose Kerr constants would have to be calculated, for comparison to the observed values. The ability to determine polymer macrostructures is critical to the development of relevant, more meaningful, and therefore improved structure-property relations for polymer materials.

Published online in *J. Polym. Sci., Part B: Polym. Phys*. 2014. DOI: 10.1002/polb.23645

4.2 Introduction

In a 50:50 vinyl copolymer with **X** repeat units made from M1 and M2 comonomers, there potentially exist [**X!/(X/2)!(X/2)!**] chains with distinct comonomer sequences, like M1-

M2-M2-M1-M2-M1-M1-M1-M2-…-M1-M2. Suppose each copolymer chain contains **X** = 100 repeat units, for a grand total of **100!/(50!50!) ~ 10^{29}** structurally distinct copolymer chains, or (10^{29})/ (6.023x10^{23}) ~ 1.66x10^{5}moles of copolymers each with different structures. If M1 = ethylene (E) and M2 = propylene (P), then each mole of the E-P copolymer weighs 50x (28 + 42) = 3,500g. We would therefore need to synthesize (1.66x10^{5}moles)x (3,500g/mole) = 6x10^{8}g or 1,245,000lbs or **623tons** of this E-P copolymer to be certain that all possible complete chain comonomer sequences or macrostructures are represented in the sample. A similar large number of vinyl homopolymer chains, such as polypropylene (PP), would have to be generated to contain all potential distinct sequences of meso (*m*) and racemic (*r*) diads.

The example presented above to illustrate the almost limitless number of copolymer chains possessing distinct full-chain comonomer sequences, is in facta gross underestimate if one or both of the comonomer units contains a side-chain, as does the propylene monomer P. This is because the modes of attachment of neighboring side-chains, or stereosequence, is an additional microstructural element that must be considered.

For example, in a copolymer sample made from propylene and vinyl chloride, containing two pseudo-asymmetrically substituted monomer units, with CH_3 and Cl side-chains, respectively, the number of distinct copolymers ***N(n)*** containing ***n*** total comonomer units is given by[1] $\boldsymbol{N(n) = 2^{2(n-1)} + 2^{n-1}}$, which for long chains is $\sim 2^{2n}$. Remember that ***N(n)*** accounts for both comonomer and stereosequences. For ***n*** = 100 unit chains, there are $\boldsymbol{N(n) \sim 2^{200} \sim 10^{60}}$ different macrostructures for this copolymer of only very modest length.

If PP stereosequences were accounted for in the case of the E-P copolymers described above, then the number of distinct E-P copolymers of 100 repeat units would lie between **10^{29} and 10^{60}**. This would make necessary the synthesis of a quantity approaching or possibly even exceeding the total mass of the Earth (**~6x10^{27}g**)[2] to ensure that E-P copolymers with all possible microstructures (comonomer- and stereosequences) located at all possible positions along the E-P chains, *i.e.*, their complete macrostructures, were represented.

Rather mind boggling isn't it !

Currently high resolution ^{13}C-NMR observation of polymer solutions is the best method for determining their microstructures[3,4]. However, due to the relatively short-range local sensitivity of NMR, and other spectroscopic probes, the microstructures identified by them cannot be located along the polymer backbone. Nor can they reveal if all chains in the observed polymer sample the same microstructural types, amounts, and locations, or if they are distributed non-uniformly, *i.e.*, heterogeneously, along or among the polymer chains in the sample.

Of course the reason we want to determine the complete macrostructures of polymers, through identification, quantification, and location of their constituent microstructures, is because it is the macrostructures of polymers that dictate their overall behaviors. Structure-property relations developed for polymer materials that are truly useful and relevant must be based on their complete macrostructures, and not, as is currently done, simply upon identification of the types and quantities of short-range microstructural elements they possess. Just as the tertiary and quaternary structures and biological functions of proteins are determined by the sequences of their amino acids, *i.e.*, their primary structures or macrostructures, so too are the behaviors and properties of synthetic polymers critically dependent on their macrostructures.

Is there an available experimental means that can identify and count or quantify local microstructures, and that can also locate them along or among polymer chains? If there is, unlike short-range spectroscopic probes, the technique must necessarily be sensitive to and therefore probe the complete structures or molecular architectures of macromolecular chains. We have recently demonstrated[5-7] that the contributions made by polymer solutes to the electrical birefringence observed for their dilute solutions when subjected to strong electric fields, or their Kerr effects, may be such an experimental means. Not only does the Kerr effect probe the microstructures of polymer chains, but it also appears, as well, to be sensitive enough to locate them along the polymer chains and so distinguish among their macrostructures[5-7].
As an example, the styrene/*p*-bromostyrene (S/*p*-BrS) triblock copolymers shown in Figure 4.1 differ only in the locations of their S and *p*-BrS blocks. They cannot be distinguished by short-range experimental probes, even ^{13}C-NMR[6]. However, their Kerr constants measured in

dilute dioxane solutions, though of similar magnitude, are positive for triblock (II) and negative for triblock (I) [6].

The distinct Kerr effects shown by the S/*p*-BrS triblocks is a consequence of two factors: 1. The Kerr effects of polymers observed in solutions are sensitive to their complete macrostructures[6,7], *i.e.*, the types, quantities, and locations of their constituent short-range microstructures, and 2.

The molar Kerr constants observed for small molecules[8], ~ the size of monomers, range over nearly five-orders of magnitude and may be either positive or negative in sign. Thus, polymers with comparable types and quantities of short-range microstructures, but which are located differently along or among their chains, may produce distinct Kerr effects [5-7].

Here we measure and compare the Kerr effects observed for an atactic 50:50 S/*p*-BrS copolymer and a 50:50 by weight mixture of atactic 80:20 and 20:80 S/*p*-BrS copolymers, all three having random comonomer sequences (See Figure 4.2). We seek to learn if the Kerr effect can distinguish between samples with polymer chains that all have the same microstructures from those with a heterogeneous distribution of microstructures, but with the same overall sample average of local microstructures. Such samples cannot of course be distinguished by NMR or other spectroscopies, because they are limited by their short-range sensitivities to polymer microstructures.

4.3 Polymer Kerr Effects

The Kerr effect[8] is the birefringence produced in materials through application of a strong electric field **E**. John Kerr showed that $\mathbf{\Delta n = (B/\lambda)E^2}$, where $\mathbf{\Delta n = n_{\parallel} - n_{\perp}}$, *i.e.*, the difference in refractive indices along and perpendicular to the direction of **E**, $\mathbf{\lambda}$ is the wavelength of light used to measure the birefringence $\mathbf{\Delta n}$, and **B** has become known as the Kerr constant. Riande and Saiz[9] have summarized the experimental observation of Kerr constants, and from them, the derivation of molar Kerr constants, $\mathbf{{}_mK}$s. They are obtained experimentally at infinite dilution and may be evaluated from the following relation[10,11]:

$$\mathbf{{}_mK = (6N_A\lambda nB)/[\rho(n + 2)^2(\varepsilon + 2)^2]},$$

where **n**, **B**, **ρ**, and **ε** are the refractive index, Kerr constant, density, and dielectric constant of the solution, respectively, all extrapolated to infinite dilution.

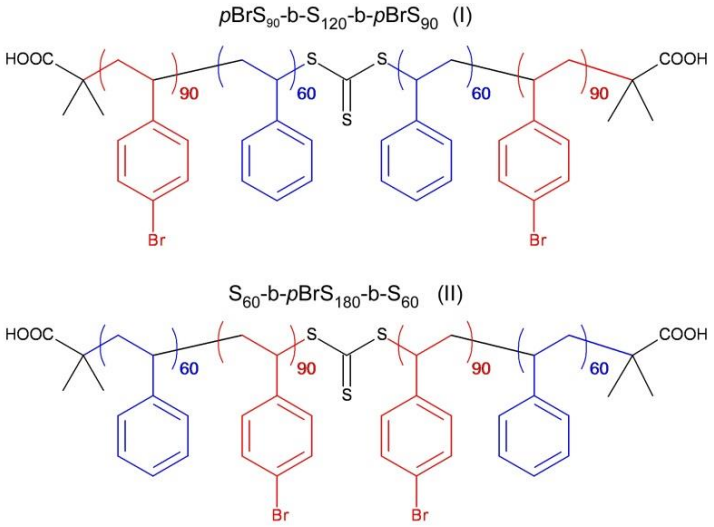

Figure 4.1 Structures of the p-BrS$_{90}$-S$_{120}$-p-BrS$_{90}$ (I) and S$_{60}$-p-BrS$_{180}$-S$_{60}$ (II) tri-block copolymers synthesized by reversible addition-fragmentation chain transfer (RAFT) controlled free-radical polymerization[6,7].

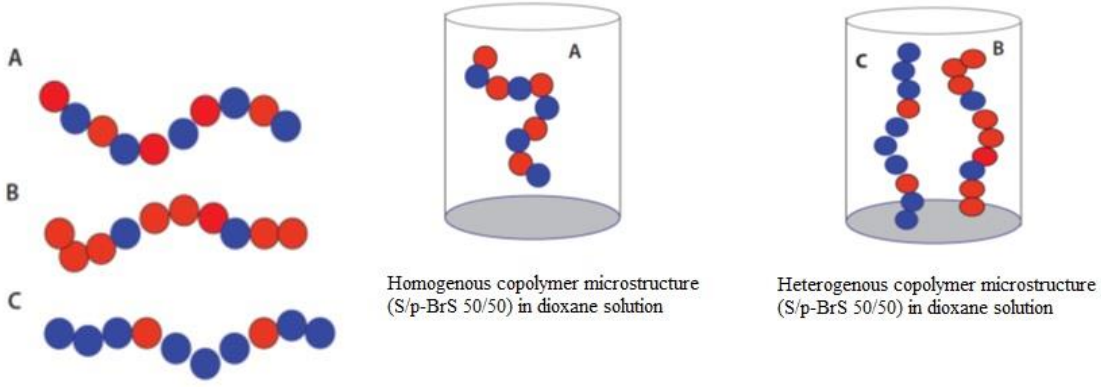

Figure 4.2 Schematic illustration of homogeneous and heterogeneous copolymer samples.

Kerr effects are characteristic of the magnitudes and directions of their resultant overall polarizability tensors, $\boldsymbol{\alpha}$, and dipole moments, $\boldsymbol{\mu}$. Nagai and Ishikawa[12] have shown that the molar Kerr constant is given molecularly by,

$$_{m}\mathbf{K} = (2\pi N_A/135)[(<\boldsymbol{\mu}^T\boldsymbol{\alpha}\boldsymbol{\mu}>)/k^2T^2 + (<\boldsymbol{\alpha}^R\acute{\boldsymbol{\alpha}}^C>)/kT],$$

where < > indicates an average over all conformations of the molecule. This is particularly important for flexible macromolecules, which can assume a myriad of conformations. Provided a reliable description of a polymer's conformational characteristics is available, Flory and Jernigan[13,14] showed how matrix multiplication techniques can accomplish the appropriate conformational averaging.

Like its mean-square end-to-end distance ($<r^2>$) or radius of gyration ($<s^2>$) and dipole moment $(<\mu^2>)^{1/2}$, the molar Kerr constant of a polymer is a macroscopic property characteristic of the entire chain, Unlike their dimensions ($<r^2>$,$<s^2>$) or dipole moments $(<\mu^2>)^{1/2}$, however, which may be altered by factors of ~2-5 due to different macrostructures, as mentioned previously, the $_{m}\mathbf{Ks}$ of small molecules[5] (*e.g.* monomers) range over more than four orders of magnitude, and may be either positive or negative.

A microstructural alteration anywhere along a polymer chain may potentially be evident in its NMR spectrum. However, because of its inherent short-range sensitivity, the spectral consequence of such a microstructural alteration, *i.e.*, shifting of its resonance frequencies[3,4], are not sensitive to nor reflect its position or location along the chain. On the other hand, identical or similar microstructural features located at different positions along the macromolecular chain backbone may produce substantially different overall $_{m}\mathbf{Ks}$.

As in the case of the S/p-BrS triblocks discussed above, their different $_{m}\mathbf{Ks}$ can be used to distinguish and locate their microstructures (blocks), because the molar Kerr constants of polymers depend on the magnitudes and relative orientations of their overall macroscopic dipole moment vectors and anisotropic polarizability tensors. However, their macrostructures, *i.e.*, types, amounts, and locations of their contributing microstructures, can be interpreted or identified only by the successful comparison of their observed $_{m}\mathbf{Ks}$ to those calculated for the corresponding assumed macrostructural features.

4.4 Kerr Effect Examination of Polymer Samples with Heterogeneous Macrostructures

By employing uncontrolled free radical polymerization, we have synthesized atactic 50:50, 20:80, and 80:20 S/*p*-BrS copolymers ($P_r \sim 0.5$), as determined by ^{13}C-NMR, each with random comonomer sequences. The Kerr constants for their neat dioxane solutions were measured, as was that of a 50:50 by weight mixture of the 20:80 and 80:20 S: *p*-BrS copolymers. This was done to learn if the 50:50 and the equal mixture of 20:80, and 80:20 random atactic S/*p*-BrS copolymers exhibit distinct Kerr constants, as the data shown in Figure 4.3 suggest they should. As seen there, the molar Kerr constants, $_{m}\mathbf{Ks}$, calculated and observed for S/*p*-BrS copolymers[15] produced through the bromination of atactic PS[16,17] show a near maximum value for the 50:50 copolymer, with reduced $_{m}\mathbf{Ks}$ for the 20:80 and 80:20 copolymers.

As seen in Table 4.1 and in Figures 4.3 and 4.4, the 50:50 copolymer showed a Kerr constant/repeat unit ~10% larger than that of an equal mixture of the 20:80 and 80:20 copolymers. The expected difference between the Kerr constants from Figure 4.3 is ~30%. At least some of this disparity is due to the differences between assumed or calculated (20:80, 50:50, and 80:20) and actual or experimental (27:73, 54:46, and 81:19) S: *p*-BrS comonomer compositions. On the other hand, both the measured and calculated differences in the Kerr constants between the neat 80:20 and 20:80 S/p-BrS copolymers is ~25%.

Thus, the Kerr effect appears to be able to distinguish between samples whose polymer chains all have the same macrostructures from those with a heterogeneous distribution, but with the same overall sample average of local microstructures. Of course this distinction cannot be made by NMR or other spectroscopies whose sensitivities are limited to short-range microstructures.

It should be noted that the average of Kerr constants measured for the neat 20:80 and 80:20 S:*p*-BrS copolymers (50% of each neat Kerr constant) is 0.110, and that measured for their 50:50 mixture is also a nearly identical 0.111. Several repeat Kerr effect measurements support the Kerr constants given in Table 4.1, so we are confident that in their 50:50 combined solution the 20:80 and 80:20 S/*p*-BrS copolymers are independently aligning in the electric

field. If they were not, then we should have observed a difference between the Kerr constants of their 50:50 common solution and the 50:50 average of their neat solutions, as was observed previously for the stereocomplex formed between syndiotactic (s) and isotactic (i) poly(methyl-methacrylate)s (PPMAs)[7].

Table 4.1 Kerr constants (10^{-14} V m^{-2}) measured in dioxane on 2% w/w solutions of S/p-BrS copolymers.

Copolymer microstructure	Mole fractions S/*p*-BrS	Kerr constant/ repeat unit	%Std
Homogenous	20/80	**0.123**	**0.02**
Homogenous	50/50	**0.122**	**0.03**
Heterogeneous	50/50	**0.111**	**0.03**
Homogenous	80/20	**0.097**	**0.02**

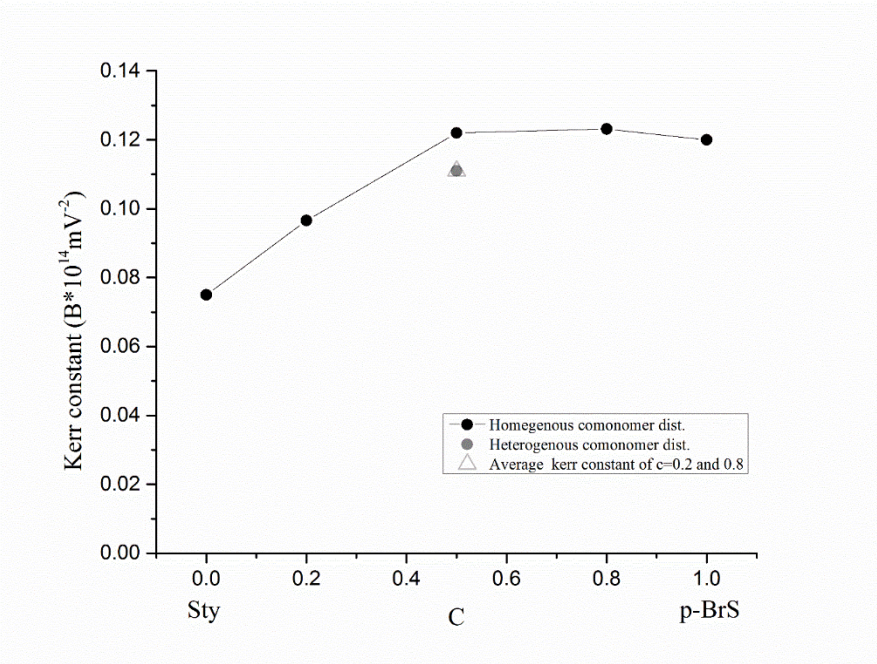

Figure 4.3 Comparison of Kerr constants B (x10^{-14} Vm^{-2})/repeat unit observed for S/p-BrS copolymers in 2 wt% dioxane solutions at room temperature. c is mole fractional content of p-BrS units.

In solvents that do and do not cause s- and i-PMMAs to form a 2:1 s-:i-PMMA complex, we observed different and the same Kerr constants, respectively, for their 67:33 s-:i-PMMA common solution and the 67:33 average of their neat s- and i-PMMA solutions. This provides strong evidence that the Kerr effect can potentially distinguish/characterize polymers that interact in solution from those that do not. This is because in strong electric fields interacting polymers in solution align together, while non-interacting polymers align independently, resulting in distinct Kerr effects. The sensitivity of polymer Kerr effects to strong molecular interactions may, as well, possibly be extended to the study of polymer-solvent interactions.

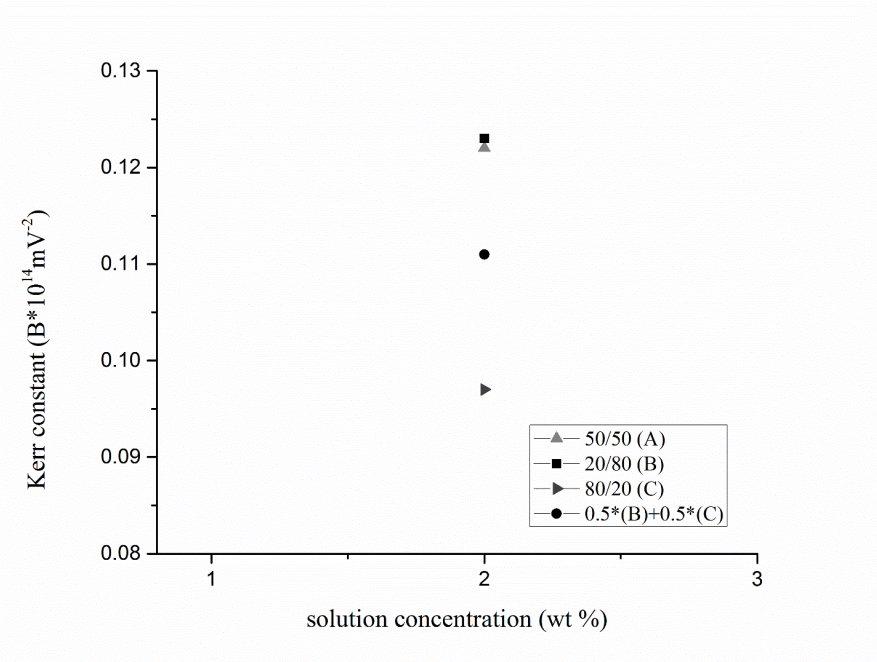

Figure 4.4 Kerr constants (B)/repeat unit measured on 2 wt% dioxane solutions of 50:50, 20:80, 80:20, and a 50:50 mixture of the latter two S/p-BrS copolymers.

In Table 4.2 we present the glass-transition temperatures, T_gs, observed for each of these three neat S/*p*-BrS copolymers, and that of the 50:50 solid mixture of the 20:80 and 80:20

copolymers. There it is apparent that the 20:80 and 80:20 copolymers are not miscible, because their 50:50 solid mixture show distinct T_gs. The 50:50 mixture was obtained by casting from dioxane and vacuum drying. The two T_gs observed suggest that possibly in dioxane solutions the 20:80 and 80:20 copolymers may not be homogeneously dissolved, *i.e*, separated into regions with different concentration of the 20:80 and 80:20 copolymers. If this were the case, then we might expect the Kerr constant of the 50:50 S/p-BrS copolymer solution and the average of the equally weighted Kerr constants of the 20:80 and 80:20 S/*p*-BrS solutions to be different. Since they are not, we can conclude that either all of their dioxane solutions are single phase, or, if the 50:50 mixture of the 20:80 and 80:20 copolymers is phase separated, with regions containing mostly the 20:80 copolymer or mostly the 80:20 copolymer, this does not interfere with the independent alignment of the 20:80 and 80:20 copolymers when the electric field is applied.

Table 4.2 DSC Observed T_gs of Atactic Random S/p-BrS Copolymers

S/ BrS (moles)	T_{g1}	T_{g2}
80/20	113.9	
50/50	126.26	
20/80	154.28	
50/50 soln. mix. of 20/80 and 80/20	**130.88**	**140.4**

Finally, to make the characterization of synthetic polymer macrostructures using the Kerr effect practical, we suggest[7] coupling of ^{13}C-NMR spectroscopy with Kerr effect observations. Though not for the S/*p*-BrS copolymers treated and discussed here[6,7,16], NMR can usually reveal the types and amounts of short-range microstructures present in synthetic polymers. Kerr effect observations can then be used to locate them along the polymer chains.

This is achieved by comparison of observed molar Kerr constants to those calculated for different distributions/locations **of** the constituent microstructure identified by ^{13}C-NMR. The distributions/locations of microstructures employed to calculate an $_{m}$K in agreement with the value observed for the polymer is then identified as its likely macrostructure. Without coupling the Kerr effect with ^{13}C-NMR, the molar Kerr constants of all polymer macrostructures have to be considered, calculated, and compared with the observed values. This includes all potential types and all possible amounts of short-range microstructures, as well as all of their potential locations along the polymer backbone. As noted in the **Introduction**, the potential number of distinct polymer macrostructures is virtually insurmountable and certainly impractically large.

The S/*p*-BrS copolymers treated and discussed here have known macro- structures, *i.e.*, atactic stereosequences and random comonomer sequences. So in this case, the ability (actually failure) of ^{13}C-NMR to determine the types and amounts of constituent microstructures in S/*p*-BrS copolymers [6,7,17] is not necessary to connect their observed Kerr effects with their contributing macro-structures.

4.5 Experimental

4.5.1 Materials

Styrene, S (> 99%, Aldrich) was passed through a basic alumina column and *p*-bromostyrene, *p*-BrS (> 99%, Aldrich) was distilled (b.p. = 88° C at 15mm Hg) prior to use. 2,2'-Azobis(isobutyronitrile) (AIBN > 98%, Aldrich) initiator was used as received.

4.5.2 Synthesis of Random S/p-BrS Copolymers

Conventional (uncontrolled) copolymerizations of S and *p*-BrS with a 50:50 monomer ratio was performed as follows. S (1.4 g, 13.5 mmol), *p*-BrS (2.47g, 13.5 mmol), AIBN (15mg, 0.09 mmol) were placed in a 25 ml Schlenk flask equipped with a magnetic stir bar. The mixture was degassed *via* three freeze-pump-thaw cycles. The flask was then placed in a preheated (65° C) oil bath. ([Monomer]: [AIBN] = 100:0.3) After 8h, the reaction was stopped

by exposing the reaction mixture to air. To isolate the copolymer, the reaction solution was diluted with THF, precipitated into cold MeOH (x3), filtered, and vacuum dried at 25° C.

The other two copolymers containing 20:80 and 80:20 S:*p*-BrS mole fractions were synthesized in a similar way.

4.5.3 Gel Permeation Chromatography (GPC)

The GPC instrument was equipped with a Waters 2695 separations module, a light scattering detector (MiniDawn, Wyatt Technology Co.) and a differential refractive index detector (Optilab Rex, Wyatt Technology Co.), and used a Styrogel HR 4 column. Conventional calibration was done using nine polystyrene standards from Fluka. Samples were filtered through 0.2 μm PTFE syringe filters. THF was used as the eluent solvent at a flow rate of 0.3mL min^{-1} at room temperature. The results are reported as number average molecular weights (M_n) and polydispersities (M_w/M_n). Molecular weights of the S/*p*-BrS copolymers are as follows:

S:*p*-BrS = 20:80 M_n = 52,000 g/mol, M_w/M_n = 1.65

S:*p*-BrS = 50:50 M_n = 70,000 g/mol, M_w/M_n = 1.57

S:*p*-BrS = 80:20 M_n = 38,000 g/mol, M_w/M_n = 1.73

4.5.4 NMR

The NMR samples were prepared by dissolving ~60 mg copolymer in 0.6 ml of $CDCl_3$ and transferring the solutions to a 5-mm NMR tube for analysis. ^{13}C NMR data were obtained using a Bruker AVANCE 500 MHz spectrometer and processed with Bruker TOPSPIN 3.0 software. According to the ^{13}C-NMR spectra of the 50:50, 20:80, and 80: 20 S: p-BrS presented in supplementary information, the aromatic ring carbon portion of the ^{13}C-NMR spectra of the 50:50, 20:80, and 80:20 S:p-BrS copolymers. The *p*-carbons of the S and *p*-BrS phenyl rings at ~ 126 and ~ 119ppm, respectively, are well separated and easily integrated to obtain the molar S:*p*-BrS compositions, which were found to be S:*p*-BrS = 27:73, 54:46,

and 81:19, which compare favorably to the starting comonomer compositions (20:80, 50:50, and 80:20) used in their syntheses.

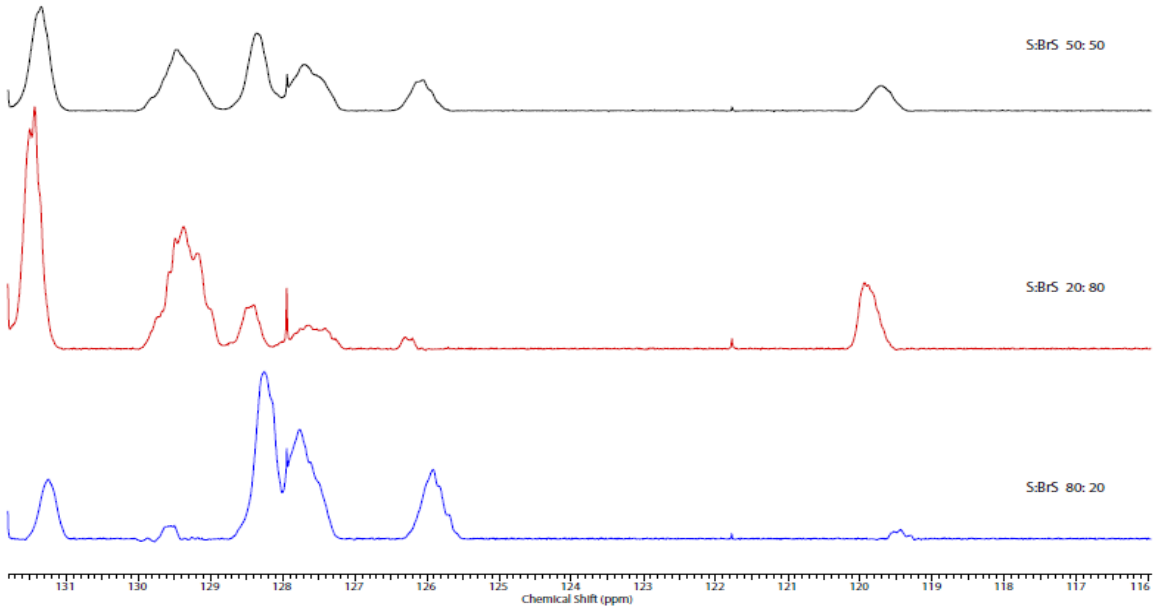

Figure 4.5 Aromatic carbon region of the 125 MHz ^{13}C-NMR spectra of the 50:50, 20:80, and 80: 20 S: p-BrS (From top to bottom). The resonances at ~119 and ~126ppm belong to the p-carbons of p-BrS and S, respectively, so their integration provides a measure of the copolymer composition.

4.5.5 DSC

A Perkin-Elmer DSC-7 differential scanning calorimeter was used to measure S/p-BrS copolymer glass-transition temperatures. DSC analysis of a sample was repeated at least 3 times with different scanning rates starting from 10° C/min to 30° C/min until a smooth thermograph were obtained. Represented results were analyzed at the second heating at a rate

of 30° C/ min under a nitrogen atmosphere and over a temperature range of 25 to 160° C. The T_gs reported here correspond to the midpoint of the heat capacity transition observed in the first heating scans.

4.5.6 Kerr Effects

S/*p*-BrS polymers were dissolved in anhydrous dioxane (99.8%, Alfa Aesar) by stirring for 1 day at room temperature. The solutions were then passed through 0.2 μm PTFE filters, and were optically clear. Measurements were made on (2%w/w) solutions with a λ= 632nm laser. 10 -12kV cell voltages were applied and the birefringence results they produced were averaged. Kerr constant measurements were repeated three times on the same solution. (For more experimental details see refs. 6 and 7)

REFERENCES

1. Frisch, K. L., Mallows, C. L., Bovey, F. A., 1966, *J. Chem. Phys., 45*, 1565.

2. "Solar System Exploration: Earth: Facts & Figures". *NASA*. 13 Dec 2012. Retrieved 2012-01-22, *Wikipedia,http://en.wikipedia.org/ wiki/Earth_mass*

3. Tonelli, A. E., "NMR Spectroscopy and Polymer Microstructure: The Conformational Connection" **1989**; VCH: New York.

4. Bovey, F. A.; Mirau, P. A. "NMR of Polymers" **1996**; Academic Press: NewYork.

5. Tonelli, A. E., *Macromolecules* **2009**, *42*, 3830.

6. Hardrict, S. N.; Gurarslan, R.; Galvin, C. J.; Gracz, H.; Roy, D.; Sumerlin, B. S.; Genzer, J.; Tonelli, A. E. ; *J. Polym. Sci., Polym. Phys.* **2013,** *51*, 735.

7. Gurarslan, R.; Hardrict, S. N.; Roy, D.; Galvin, C.; Hill, M. R.; Gracz, H.; Roy, D.; Sumerlin, B. S.; Genzer, J.; Tonelli, A. E. ; *J. Polym. Sci., Polym. Phys.* **2014**, 52, xxxx.

8. Kerr, J. Philos. Mag. **1875**, 50 (337), 416; **1879**, 8 (85), 229; **1880**, 9,157; **1882**, 13 (153), 248; **1894**, 37, 380; **1894**, 38, 1144.

9. Riande, E.; Saiz, E. "Dipole Moments and Birefringence of Polymers" **1992**; Prentice Hall: Englewood Cliffs, NJ, Chapter 7.

10. LeFevre, C. G.; LeFevre, R. J. W. *Rev. Pure Appl. Chem.* **1955**, *5*, 26.

11. LeFevre, C. G.; LeFevre, R. J. W. In "Techniques of Organic Chemistry" **1960**; Weissberger, A., Ed.; Interscience: New York, Vol. I, Ch 36.

12. Nagai, K.,Ishikawa, T., *J. Chem. Phys.***1965**, *43*, 4508.

13. Flory, P. J.; Jernigan, R. L. *J. Chem. Phys.* **1968**, *48*, 3823.

14. Flory, P. J. "Statistical Mechanics of Chain Molecules" **1969**; Wiley Inter-Science: New York; Chapter IX.

15. Khanarian, G.; Cais, R. E.; Kometani, J. M.; Tonelli, A. E., *Macromolecules 1982, 15*, 866.

16. R. J. Kambour, R. Bendler, R. Bopp, *Macromolecules* **1983**, *16*, 753.

17. Semler, J. J.; Jhon, Y. K.; Tonelli, A.; Beevers, M.; Krishnamoorti, R.; Genzer, J. *Adv. Mater.* **2007**, *19*, 2877.

18. Yoon, D. Y.; Sundararajan, P. R.; Flory, P. J. *Macromolecules* **1975**, *8*, 77.

CHAPTER 5

Conclusion

The importance of the analysis of polymer macrostructures, the complete full scale structure or detailed architecture of a polymer including the types, amounts of short-range microstructures and their locations or positions along the polymer chain, has recently caught the attention of polymer scientists after development of novel syntheses[1,2] and particularly the recent emergence of the field of sequencing synthetic copolymers [3,4]

It is very surprising that while advance techniques for sequence distribution analysis of very complex biopolymers are available, the analytical tools currently used for macrostructural characterization of a lot less complex synthetic macromolecules are not equally developed. Indeed, whereas full mapping of the human genome was reported in 2001[5], studies on macrostructural characterization of synthetic copolymers are still limited[3,6].

Synthetic copolymers have been mainly characterized by high resolution solution ^{1}H and ^{13}C NMR spectroscopy. However, classical NMR measurements cannot determine the macrostructures of copolymers with complex structures. Due to its local sensitivity ·it is incapable to identify positions of constituent short range microstructures along the polymer backbone, in other words, their complete architectures[7-9]. 'Single molecule tracking techniques'[10] arise among the latest developments on exploring the conformation and physics

of individual polymer chains. However, they do not seem feasible for evaluating/characterizing polydisperse polymer samples where all chains have the potentially extreme heterogeneity of micro- and macrostructures[11].

The primary goal of this Ph.D. study was to contribute to the recent advances in macromolecular analyses of synthetic copolymers. We demonstrated the ability of the coupling of NMR spectroscopy with the Kerr Effect technique to reveal not only constituent microstructures, but also their locations and positions along the polymer back bone.

The molar Kerr constant, as a macroscopic property of copolymers was used as a probe to investigate macrostructural properties of our model triblock, statistical/random and gradient S/p-BrS copolymers; multi- block S/Butadiene copolymers with random and regularly alternating block sequences; precise and random ethylene/vinyl acetate copolymers with different stereosequences.

We also showed that RAFT copolymerization yields an unexpected additional stereogradient along with gradient in monomer sequence of S/p-BrS copolymers. Further evidence on the proposed associated stereosequence gradient was provided via annealing studies. Distinct dewetting behaviors of S-stat/ran-p-BrS copolymers made by RAFT and uncontrolled free radical copolymerization were related to the increased racemic (r) p-BrS-p-BrS diad population in random S/p-BrS made by RAFT. We concluded that not only composition and sequence, but also stereosequence- or complete arrangement of copolymers in the polymer chain affects their thin film behaviors. Moreover, this study proved the ability of Kerr effect measurements to elucidate specific characteristics of polymerization

mechanisms. We were able to establish both the interrelations between synthesis methods/conditions and copolymer macrostructure and their physical properties.

The Kerr effect showed a unique sensitivity to not only stereosequence and comonomer sequence of the above S/p-BrS copolymers, but also intermolecular interaction between i- and s- PMMA molecules in dilute solutions with solvents known to form soluble complexes, and served as a sensitive probe to distinguish S/*p*-BrS copolymer samples with homogenous and heterogeneous macrostructures.

We therefore conclude that our approach combining Kerr effect and ^{13}C-NMR observations has the potential to provide a strong contribution to advancement in the characterization of modern synthetic polymers with complex structures.

REFERENCES

1. Elsen, A. M., Li, Y., Li, Q., Sheiko, S. S., & Matyjaszewski, K. Macromolecular rapid communications **2014**, 35(2), 133-140.

2. Ouchi et. al. Nature Chemistry,**2011**, 3- 917-924

3. Lutz, J.F.; Mutlu, H. *Angew. Chem. Int. Ed.* **2014**, 53, 2- 12.

4. Lutz, J. F., Ouchi, M.,Liu, D., Sawamoto, M. *Science* **2013**, 341, 1238149.

5. International Human Genome Sequencing Consortium, Nature **2001**, 409, 860 – 921.

6. Tonelli, A. E., Macromolecules **2009**, 42, 3830–3840.

7. Tonelli A. E., NMR Spectroscopy and Polymer Microstructure: The Conformational Connection; VCH: New York, **1989**.

8. Bovey F. A., Mirau P. A., NMR of Polymers; Academic Press: New York, **1996**.

9. Mirau, P. A. *A Practical Guide to Understanding the NMR of Polymers*. Hoboken, NJ: Wiley-Interscience, **2005**.

10. Vacha, M.; Habuchi, S. Conformation and physics of polymer chains: A single-molecule perspective. *NPG Asia Mater.* **2010**, *2*, 134–142.

11. Gurarslan, R.; Gurarslan, A.; Tonelli, A. Characterizing Polymers with Heterogeneous Micro- and Macrostructures, J. Polym. Sci., Polym. Phys. 2014, DOI: 10.1002/polb.23645